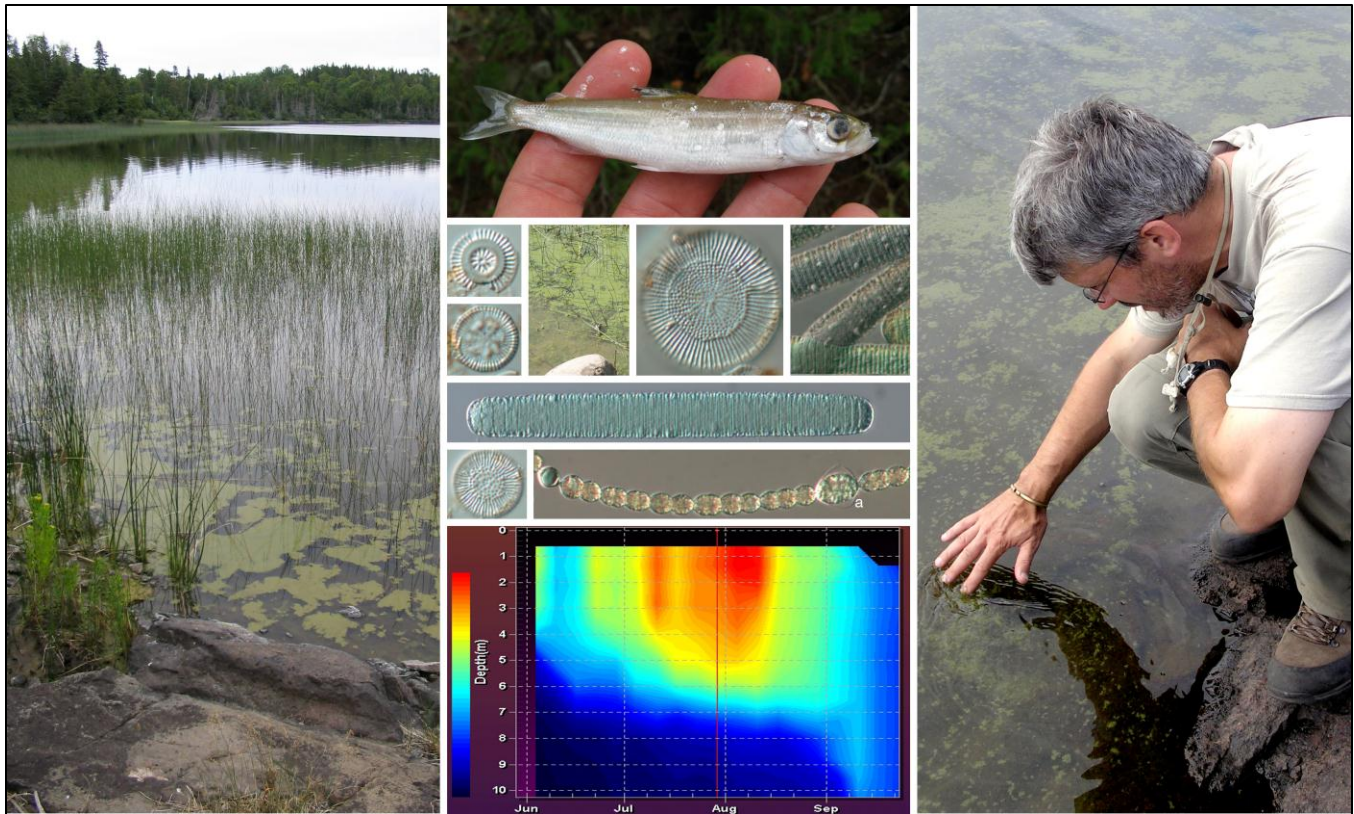




# Modeling the Effects of Past Climate Change on Lakes in Isle Royale and Voyageurs National Parks

Natural Resource Technical Report NPS/GLKN/NRTR—2014/909



### **ON THE COVER**

Indicators of climate affecting lakes in the Great Lakes Network include (left-to-right and top-to-bottom) unprecedented cyanobacterial blooms in Lake Richie (Isle Royale National Park; ISRO), stressed and dead lake herring (*Coregonus artedii*) from Lake Desor (ISRO), diatom and cyanobacterial species whose abundances have changed in recent decades, and a May-to-September thermal profile of Lake Richie (ISRO). Photo credits: Mark Edlund (Science Museum of Minnesota), Rick Damstra (NPS, GLKN), and Joan Elias (NPS, GLKN).

---

# Modeling the Effects of Past Climate Change on Lakes in Isle Royale and Voyageurs National Parks

Natural Resource Technical Report NPS/GLKN/NRTR—2014/909

Mark B. Edlund<sup>1\*</sup>, James E. Almendinger<sup>1</sup>, Daniel R. Engstrom<sup>1</sup>, Xing Fang<sup>2</sup>, Joan Elias<sup>3</sup>, and Ulf Gafvert<sup>3</sup>

<sup>1</sup> St. Croix Watershed Research Station

Science Museum of Minnesota

16910 152nd St N

Marine on St. Croix, MN 55047

\* Primary contact: [mbedlund@smm.org](mailto:mbedlund@smm.org)

<sup>2</sup> Department of Civil Engineering

Auburn University

Auburn, Alabama 36849-5337

<sup>3</sup> National Park Service

Great Lakes Inventory and Monitoring Network

2800 Lake Shore Drive East

Ashland, WI 54806

September 2014

U.S. Department of the Interior

National Park Service

Natural Resource Stewardship and Science

Fort Collins, Colorado

The National Park Service, Natural Resource Stewardship and Science office in Fort Collins, Colorado, publishes a range of reports that address natural resource topics. These reports are of interest and applicability to a broad audience in the National Park Service and others in natural resource management, including scientists, conservation and environmental constituencies, and the public.

The Natural Resource Technical Report Series is used to disseminate results of scientific studies in the physical, biological, and social sciences for both the advancement of science and the achievement of the National Park Service mission. The series provides contributors with a forum for displaying comprehensive data that are often deleted from journals because of page limitations.

All manuscripts in the series receive the appropriate level of peer review to ensure that the information is scientifically credible, technically accurate, appropriately written for the intended audience, and designed and published in a professional manner.

This report received informal peer review by subject-matter experts who were not directly involved in the collection, analysis, or reporting of the data.

Views, statements, findings, conclusions, recommendations, and data in this report do not necessarily reflect views and policies of the National Park Service, U.S. Department of the Interior. Mention of trade names or commercial products does not constitute endorsement or recommendation for use by the U.S. Government.

This report is available in digital format from the Great Lakes Inventory and Monitoring website (<http://science.nature.nps.gov/im/units/glkn/publications.cfm>), and the Natural Resource Publications Management website (<http://www.nature.nps.gov/publications/nrpm/>). To receive this report in a format optimized for screen readers, please email [irma@nps.gov](mailto:irma@nps.gov).

Please cite this publication as:

Edlund, M. B., J. E. Almendinger, D. R. Engstrom, X. Fang, J. Elias, and U. Gafvert. 2014. Modeling the effects of past climate change on lakes in Isle Royale and Voyageurs national parks. Natural Resource Technical Report NPS/GLKN/NRTR—2014/909. National Park Service, Fort Collins, Colorado.

# Contents

	Page
Figures.....	v
Tables.....	vii
Executive Summary.....	ix
Acknowledgments.....	xi
Introduction.....	1
Hypotheses.....	2
Methods.....	5
Study Sites.....	5
Thermal Modeling.....	6
Model Mechanics.....	6
Input Variables: Lakes.....	8
Input Variables: Weather.....	10
Input Variables: Model Goodness-of-Fit Statistics.....	12
Model Runs and Post-Processing.....	13
Lake-Sediment Coring and Analyses.....	13
Coring.....	13
Isotopic Dating and Geochemistry.....	14
Diatom Analysis.....	14
Statistical Approach.....	15
Results and Discussion.....	17
Thermal Modeling.....	17
Model Fits.....	17
Selection of Output Variables.....	20
Model Runs.....	22
Paleolimnological Records.....	25
Diatom Species Response.....	26
Diatom Community Turnover.....	35
Biogenic Silica.....	35

## Contents (continued)

	Page
Summary and Recommendations.....	37
Literature Cited .....	41
Appendix A.....	47

# Figures

	Page
<b>Figure 1.</b> Locations of study lakes within Voyageurs National Park.....	5
<b>Figure 2.</b> Locations of study lakes within Isle Royale National Park.....	6
<b>Figure 3.</b> Data from Peary Lake as an example of observed versus simulated temperatures (T), showing regression line (red) through the cloud of observed values and the 1:1 line (blue).....	12
<b>Figure 4.</b> Regression plots of observed versus modeled temperatures (T) for lakes at Voyageurs National Park.....	19
<b>Figure 5.</b> Regression plots of observed versus modeled temperatures (T) for lakes at Isle Royale National Park.....	20
<b>Figure 6.</b> Sediment core record from Ek Lake, Voyageurs National Park, 1960–2010.....	27
<b>Figure 7.</b> Sediment core record from Peary Lake, Voyageurs National Park, 1960–2010.....	28
<b>Figure 8.</b> Sediment core record from Cruiser Lake, Voyageurs National Park, 1960–2010.....	29
<b>Figure 9.</b> Sediment core record from Little Trout Lake, Voyageurs National Park, 1960–2010.....	30
<b>Figure 10.</b> Sediment core record from Ahmik Lake, Isle Royale National Park, 1960–2010.....	32
<b>Figure 11.</b> Sediment core record from Lake Harvey, Isle Royale National Park, 1960–2010.....	33
<b>Figure 12.</b> Sediment core record from Siskiwit Lake, Isle Royale National Park, 1960–2010.....	34
<b>Figure 13.</b> Sediment core record from Lake Richie, Isle Royale National Park, 1960–2010.....	36



# Tables

	Page
<b>Table 1.</b> Study lake locations and assembled background data.....	7
<b>Table 2.</b> Definitions of general lake categories based on maximum depth, area, and secchi disk depth. ....	8
<b>Table 3.</b> Study lake categories based on size, trophic status, and stratification potential. ....	9
<b>Table 4.</b> MINLAKE-specific parameters for study lakes.....	11
<b>Table 5.</b> Model goodness-of-fit statistics relative to lake depths and range of observed temperatures. ....	18
<b>Table 6.</b> Significance of differences between output from first half (1962–1986) and second half (1987–2011) of MINLAKE runs for selected variables. ....	23



## Executive Summary

Climate change has the potential to severely disrupt aquatic ecosystems directly through changes in temperature and precipitation, indirectly through watershed effects, and in concert with other man-made stressors such as nutrient pollution, invasive species, and land-use change. We currently have only a limited scientific grasp of how these forces will interact or how lakes will respond, yet predicting these effects will be critical to both resource management and public understanding of changes. Recent studies have documented a series of possible climate-induced changes in boreal-region lakes, including a longer ice-free season, stronger thermal stratification, increased inputs of dissolved organic carbon, shifts in algal communities, and an increased frequency of cyanobacterial blooms.

To better understand recent changes in wilderness boreal lakes, we combined retrospective thermal modeling of temperature-depth relationships in lakes and compared model output with historical biological and physical changes in lakes as interpreted from dated sediment cores. Eight lakes that spanned a range of lake types were studied and included four lakes in Voyageurs National Park (Cruiser, Ek, Little Trout, and Peary lakes) and four lakes in Isle Royale National Park (Ahmik, Harvey, Richie, and Siskiwit lakes).

The model MINLAKE2012 describes change in temperature over discrete time intervals (e.g., one day) for discrete layers in a lake (e.g., one meter increments), and a model was developed for each lake spanning the time period of 1960–2011. The instrumental climate record for the last 50–100 years can be translated into a physical response of the lake thermal structure, which may in turn provide a more direct relation to the biological change interpreted in the lake-sediment record. Input data for the model included meteorological data from International Falls, Minnesota, for use on Voyageurs National Park lakes and Duluth, Minnesota, for Isle Royale National Park lakes. The model also required optical, physical, chemical, and biological characteristics of each lake, which were provided by the National Park Service or inferred from measured data.

Thermal model output was compared across multiple dates to actual thermal profiles taken in the course of regular monitoring programs in the National Park lakes. The Nash-Sutcliffe coefficient of efficiency was used as the measure of model fit and showed that, in general, the model fits were quite good for the deeper lakes (Cruiser and Little Trout in Voyageurs and Richie and Siskiwit in Isle Royale), with a wide range of temperatures and thermoclines situated at about the correct depth and the overall shapes of the profiles similar between simulated and observed values. The model had more trouble with the shallower lakes, particularly for the Isle Royale lakes, Ahmik and Harvey. Although other thermal models do exist for lakes, we feel MINLAKE2012 performed well, is appropriate and well suited for the GLKN lakes, and could be applied to other lakes and for forecasting future lake responses.

Model output was also post-processed to analyze trends in shallow and deep water temperatures, and the behavior and timing of temperature gradients between two 25-year time periods (1962–1986, 1987–2011). The most common significant trend was the increase in summer shallow-water temperatures, which held true for all eight lakes. The next most common significant trend was, for

the deep lakes, an increase in the frequency and duration of thermal gradients equaling or exceeding 2°C or 3°C per meter. These trends appear to be the most likely candidates for how thermal structure may have impacted lake biology during the simulation period.

Sediment cores were previously recovered from deep central depositional basins of each lake and subjected to <sup>210</sup>Pb dating, loss-on-ignition, biogenic silica, and diatom microfossil analysis for sediments dated ca. 1850–2010. Parameters analyzed in sediment cores included diatom communities, community turnover, and biogenic silica as a proxy for past algal productivity.

Sediment core data were reported in a comparable fashion to thermal model output using downcore data from 1960–2010. Across the eight lakes, changes in predominant diatom species between 1960 and 2010 are well differentiated between the shallower and deeper lakes but also differ between the two park units. In general diatom communities in shallow lakes appear to be responding to mixing events, and as shown with thermal modeling, the overall trend of shallow water warming that affect the distribution and abundance of benthic (bottom-dwelling) and/or tychoplanktonic (species that periodically are entrained by mixing into the water column) diatom species. Indirect effects from watershed inputs may also be a factor as shallow lakes in Voyageurs are inferred to be rising in pH. Changes in deep lake diatom communities are most often evident in members of the deep chlorophyll layer such as *Cyclotella* and *Discostella* species, which thrive along the thermal, density, and nutrient gradients at the thermocline, and secondarily by diatoms that respond to nutrient inputs and/or length of spring mixing.

Community turnover, as estimated using ordination axis scores, shows that diatom communities in the deep lakes have generally changed more than in shallow lakes between 1960–2010, providing support that the community changes and modeled thermal changes that are accentuated in structuring the deeper lakes are likely linked. In contrast, there is little consistency among lake response in historical diatom productivity beyond temporal consistency; in those lakes where biogenic silica flux shows changes between 1960–2010, flux generally began increasing between samples deposited in the 1970s and 1980s with rates continuing to climb upcore. But, lakes with increased biogenic silica flux span the range of lake types used in this study.

## **Acknowledgments**

We thank the National Park Service Great Lakes Inventory and Monitoring Network for providing funding under Cooperative Agreement H6000C02000. We thank Joy Ramstack Hobbs and Will Hobbs for statistical analyses, Norman Andresen for diatom analysis, Jasmine Saros and Kristin Strock (University of Maine) for access to Siskiwit Lake core material and data, Erin Mortenson, Erin Mittag, Alaina Fedie, and Jill Coleman Wasik for geochemistry and dating analysis, Rick Damstra and Mark Hart for providing supporting data, and David VanderMeulen for coordinating this effort. Reviewers, including Paul Brown, Ryan Maki, and Brenda Moraska Lafrancois, provided valuable comments that significantly improved the project.



# Introduction

Ecological changes, including increases in cyanobacteria (blue-green algae), are occurring in our remote northern lakes. These changes do not fit the traditional paradigm of nutrient loading and eutrophication and may be the result of recent climate warming. Climate change has the potential to severely disrupt aquatic ecosystems directly through changes in temperature and precipitation, indirectly through watershed effects, and in concert with other man-made stressors such as nutrient pollution, invasive species, and land-use change. We currently have only a limited scientific grasp of how these forces will interact or how lakes will respond, yet predicting these effects will be critical to both resource management and public understanding of changes that have already begun.

Recent studies have documented a series of possible climate-induced changes in boreal-region lakes, including a longer ice-free season (Jensen et al. 2007, Johnson and Stefan 2006), stronger thermal stratification, increased inputs of dissolved organic carbon (Monteith et al. 2007), shifts in algal communities (Rühland et al. 2008), and an increased frequency of cyanobacterial blooms (Edlund et al. 2010). These changes have been noted in remote lakes far removed from direct human disturbance, with the strongest evidence coming from analysis of dated sediment cores that record the recent history of the lakes. However, the scientific picture is currently very incomplete: the observed changes vary considerably among lakes, the physical and biological controls are poorly understood, and the consequences for higher food-chain organisms are virtually unknown.

Because of year-to-year variability, long-term records are needed to decipher trends in lake biological responses to climate change. Where lake monitoring data are missing, lake-sediment cores can fill the gap by providing a long-term record of algal response. Possible climate effects on lakes have already been noted in sediment-core studies from arctic and boreal regions (Rühland et al. 2008, Smol et al. 2005) and more locally in our recent work at Isle Royale National Park (ISRO) and Voyageurs National Park (VOYA) (Edlund et al. 2011, Serreyssol et al. 2009). These studies document in some lakes a systematic replacement of heavily silicified diatoms (e.g., *Aulacoseira* spp.) by small centric species (e.g., *Cyclotella* spp.), a change that has been attributed to differences in sinking rates with increased stability of thermal stratification (Rühland et al. 2008). Increases in cyanobacterial blooms, reconstructed from algal pigments preserved in sediment cores, may likewise be related to lake thermal structure through direct effects of higher surface temperatures, longer and more intense stratification, and increased internal nutrient loads (Wagner and Adrian 2009).

To understand the mechanism behind climate-driven biological change in lakes, we need a better understanding of how climate drives physical and chemical changes in lakes. Just as lake-monitoring records of algal communities are generally sparse and short-term, so are monitoring records of lake temperature and chemistry. Sediment records have been used with questionable success in reconstructing past temperatures (Anderson 2000), but the results (mean summer water temperatures) are very general and lack important details that could be critical in determining algal response, such as duration of ice cover and duration of thermocline formation that could lead to hypolimnetic oxygen depletion and internal loading of nutrients (Adrian et al. 2009, Wagner and Adrian 2009).

Physically based computer models of lake thermal structure provide an alternative way to extend the record back in time to allow comparison with biological change recorded in lake sediments. Computer modeling of the thermal structure of lakes in Minnesota began over 30 years ago with the MINLAKE modeling framework (Ford and Stefan 1980, Riley and Stefan 1988). Improved algorithms relating to regional water temperatures (Hondzo and Stefan 1993), dissolved oxygen (Stefan and Fang 1994), and ice and snow dynamics (Gu and Stefan 1990) led to the development of MINLAKE96 (Fang and Stefan 1996, 1997), which allowed for continuous, multiyear simulation of water temperature and ice formation. Subsequently, the model was adjusted to allow for deep oligotrophic lakes and renamed MINLAKE2010 (Fang et al. 2010). Most recently the model has been updated to MINLAKE2012 with enhanced usability via an MS Excel interface for pre- and post-processing (Xing Fang and Zhongshun Li, Auburn University, personal communication, 2012). With such a model, the instrumental climate record for the last 50–100 years can be translated into a physical response of the lake thermal structure, which may in turn provide a more direct relation to the biological change interpreted in the lake-sediment record.

In this study we combine thermal lake modeling with traditional paleolimnology to retrospectively consider potential climate impacts on the thermal structure and biology of wilderness lakes. Thermal models were developed for eight lakes, four in Voyageurs National Park and four in Isle Royale National Park, which represented a range of typical lake types in the boreal region from small and shallow to large and deep. Model outputs covered a 50-year window from 1962–2011 and were compared to paleoecological records from the same time period of biological change including predominant diatom species, community turnover, and biogenic silica, a proxy for historical diatom algae productivity.

## **Hypotheses**

The basic premise of this study is that remote lakes in the Great Lakes Network (GLKN) parks are showing ecological change that may be related to climate warming or other broad regional stressors. These changes, which are occurring in algal communities at the base of the aquatic food chain, have been clearly documented from lake sediment cores spanning the last century. It is our working hypothesis that these ecological shifts are tied to changes in thermal structure of the lakes including stability and depth of stratification, length of the ice-free season, surface and bottom water temperatures, and hypolimnetic oxygen conditions. These physical factors in turn affect algal communities by influencing in-lake nutrient cycling, light regime, or possibly turbulence and cell sinking rates. The study is designed to test this hypothesis by answering the following questions:

*(1) How have thermal conditions in these lakes changed over a 50-year (1962–2011) period; how does the timing and magnitude of these changes vary among lakes of differing morphometry (depth) and surface area?*

*(2) What is the relationship between the ecological and thermal histories of these lakes and how does that relationship vary with respect to lake size and depth?*

The study is thus an historic experiment in which the hypothesized changes have already occurred and will be evaluated by environmental reconstruction and correlation. We know from previous studies that both the thermal structure and ecological state of these lakes have likely changed (Edlund et al. 2011, Saros et al. 2012). The question is whether these changes are related in a cause/effect manner and how lake morphometry influences sensitivity to climate forcing. These results should shed light on the likely mechanisms by which thermal structure affects algal communities (e.g., nutrients, light, and turbulence). The ultimate aim is to provide a means of predicting from simple morphometric parameters the likely sensitivity of different lake types to future climate forcing.



# Methods

## Study Sites

Eight lakes located in two National Park units were identified for thermal modeling and paleoecological reconstruction. Four lakes are in VOYA: Cruiser, Ek, Little Trout, and Peary (Figure 1). On ISRO, study sites were Ahmik, Harvey, Richie, and Siskiwit lakes (Figure 2). The lakes were chosen to capture a gradient of lake types across the boreal ecoregion and included lakes ranging from small and shallow to large and deep and also represented a spectrum of lake productivity (Table 1).

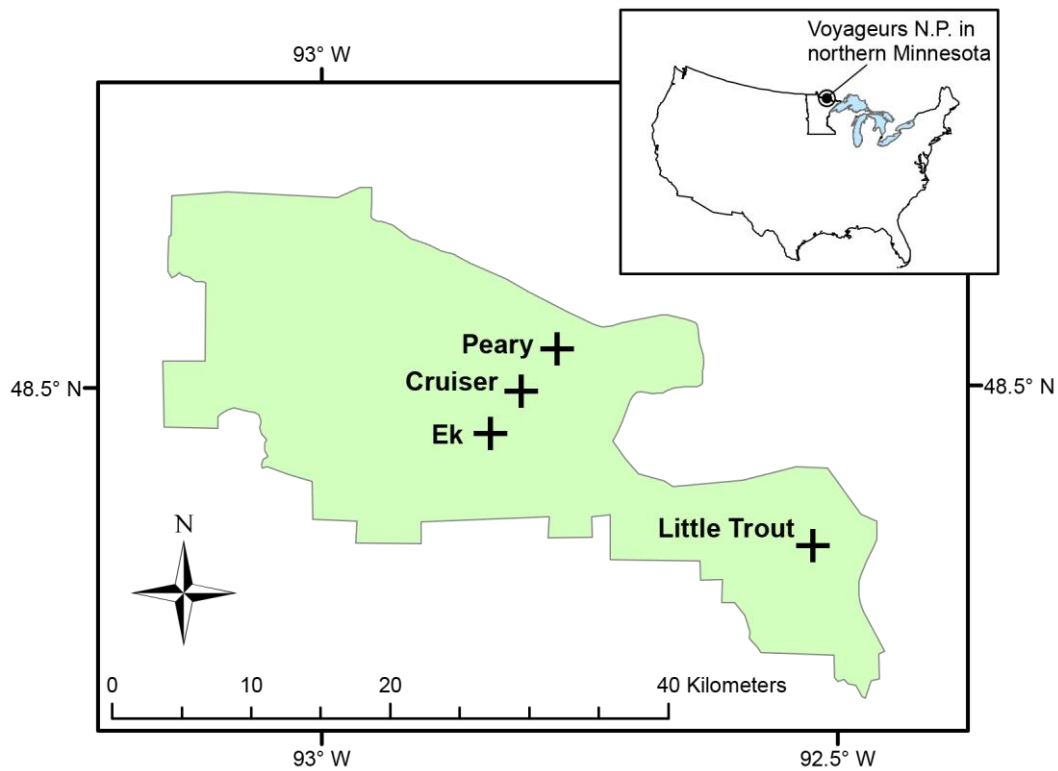


**Figure 1.** Locations of study lakes within Voyageurs National Park.

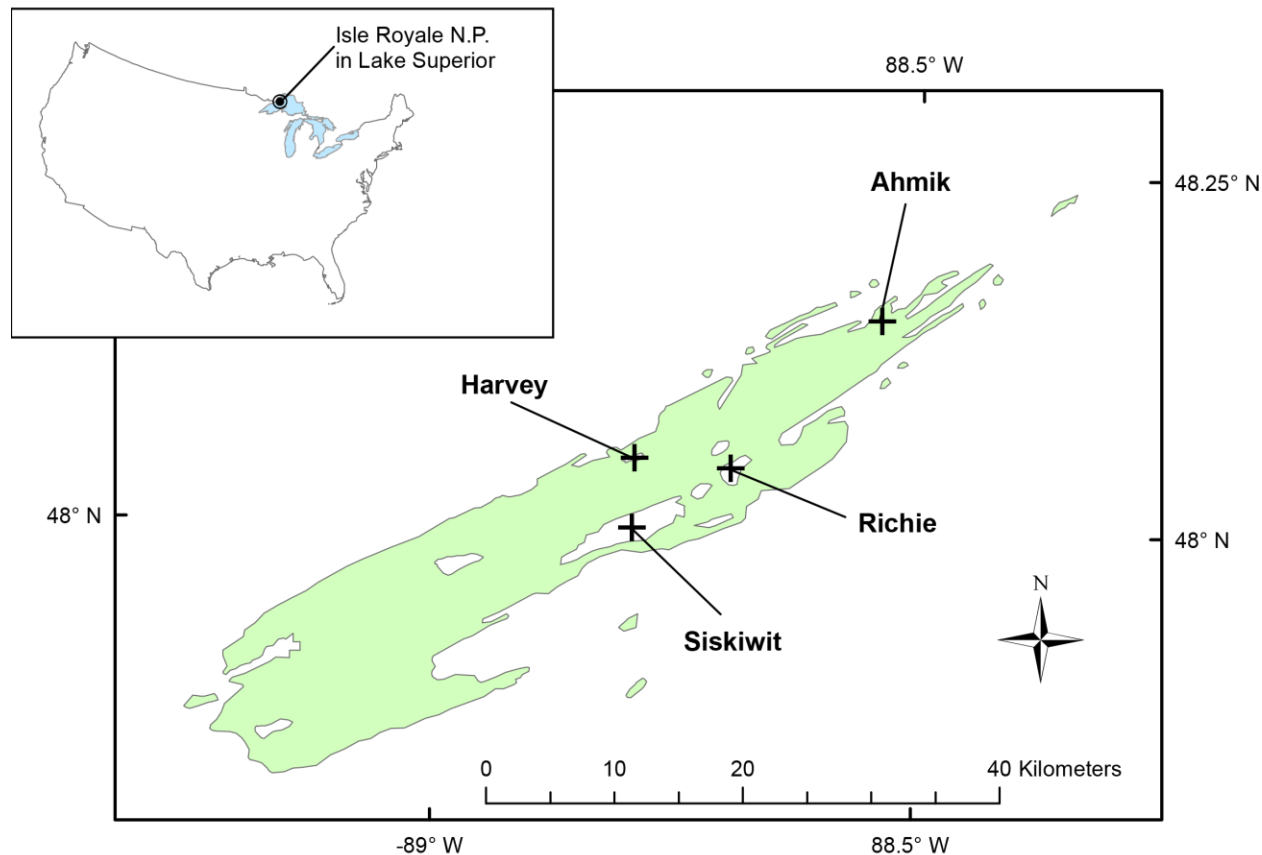


**Figure 2.** Locations of study lakes within Isle Royale National Park.

## Thermal Modeling

### *Model Mechanics*

The MINLAKE models (beginning with MINLAKE96) solve the one-dimensional, unsteady differential equation describing heat transfer with depth in a lake, i.e., the change in temperature over time for each depth in a lake (Fang et al. 2010). The equation is solved numerically with a finite-difference scheme, thereby describing change in temperature over discrete time intervals (e.g., one day) for discrete layers in a lake (e.g., one meter increments). Heat transfer related to atmospheric exchanges (precipitation, evaporation, conduction) is applied to the top-most layer, whereas solar radiation is applied as a heat source to all layers down to the effective depth of light penetration. Submodels handle the details of ice formation and heat transfer across the sediment/water interface. The upper meter of the lake is finely divided into at least eight layers (depths of 2.5, 5, 10, 20, 40, 60, 80, and 100 cm) to allow for the dynamics of ice formation and melt. Including the sediment heat capacity adds an important storage component that can smooth seasonal water temperatures, especially for shallow lakes (Fang et al. 2010).

**Table 1.** Study lake locations and assembled background data.

<i>Park Unit–Lake</i>	<i>Lat</i>	<i>Lon</i>	<i>Alt (m ASL)</i>	<i>Area (ha)</i>	<i>Aws (ha)</i>	<i>Inlets</i>	<i>Outlets</i>	<i>Zmax (m)</i>	<i>Zseci (m)</i>	<i>TP (ug/L)</i>	<i>Chl-a (ug/L)</i>	<i>DOC (mg/L)</i>
<i>VOYA</i> Cruiser	48.498	-92.805	380	47.3	118	1	1	28.8	7.72	3.8	0.9	4.2
Ek	48.470	-92.836	346	36.3	250	3	1	6.2	2.01	18.5	6.8	13.2
Little Trout	48.397	-92.523	349	104.0	236	0	1	30.0	6.40	4.4	1.1	5.0
Peary	48.525	-92.771	343	44.8	976	3	1	5.2	2.51	17.5	5.6	10.1
<i>ISRO</i> Ahmik	48.150	-88.539	190	10.3	36	1	1	2.9	2.17	20.1	2.5	17.8
Harvey	48.050	-88.800	233	51.4	341	6	1	5.1	3.39	14.8	2.1	10.1
Richie	48.043	-88.693	190	200.0	1956	4	1	11.1	1.80	26.1	6.4	9.9
Siskiwit	48.000	-88.800	197	1619.1	7239	10	1	45.3	7.36	4.2	0.9	5.2

NOTES: Latitude (Lat) and longitude (Lon) for lake center estimated from Google Earth. Altitude for Voyageurs National Park (VOYA) lakes from National Park Service (NPS) bathymetry data; altitude for Isle Royale National Park (ISRO) lakes estimated from Google Earth. Lake area, watershed area (Aws), inlets, and outlets from Ulf Gafvert (NPS, personal communication, 2012). Maximum lake depth (Zmax), secchi-disk depth (Zseci), TP (total phosphorus), Chl-a (chlorophyll-a), and dissolved organic carbon (DOC) from Joan Elias (NPS, personal communication, 2012), based partly on Great Lakes Network (GLKN) lake monitoring. VOYA lakes were sampled 2006–2011, and ISRO lakes 2007–2011. TP and Chl-a were sampled three times each year (ice-free season); DOC sampled three times in the first year and once per year (mid-summer) thereafter. Chlorophyll-a values are based on fluorometric readings. Earlier values from spectrophotometer analyses were adjusted to be consistent with fluorometric readings. For each variable, values in the table above are the multi-year average of each year's average value.

7

The current MINLAKE model also solves the one-dimensional, unsteady transport equation for changes in dissolved oxygen (DO) concentration with depth. As with the temperature calculations, the equation is solved numerically resulting in the change in DO concentration over discrete time and depth intervals (Fang et al. 2010). We did not use the DO capabilities of MINLAKE2012 in this pilot project. However, we recognize that changes in DO may be a primary driver of ecological change in lakes with altered thermal structure due to climate warming. This important consideration warrants continued research.

***Input Variables: Lakes***

MINLAKE requires data on the geometric, optical, and thermal properties for each lake, as well as the time series of weather data used to drive the model. Fortunately, based on interrelations among the parameters developed in prior studies, many values may be estimated from relatively simple measurements of a few fundamental parameters (see Ch. 7 in Fang et al. 2010). Lake and watershed areas were determined by National Park Service (NPS) personnel from available spatial data sets (Ulf Gafvert, NPS, personal communication, 2012). The lakes have been sampled about three times each year by NPS personnel since 2006 (VOYA) or 2007 (ISRO) (Joan Elias, NPS, personal communication, 2012). Average values for secchi disk depth, total phosphorus, chlorophyll-*a*, and dissolved organic carbon are given in Table 1. Following work by Stefan et al. (1996) and Heiskary and Wilson (1988) in Minnesota, lakes may be simply categorized according to area and depth (Table 2). The eight study lakes then range from small and shallow (Ahmik in ISRO) to large and deep (Siskiwit in ISRO), with the other six lakes being medium in area, depth, or both (Table 3).

**Table 2.** Definitions of general lake categories based on maximum depth, area, and secchi disk depth.

Parameter	Category	Minimum	Maximum	Typical
Maximum Depth, $Z_{max}$ (m)	Shallow	0	4	4
	Medium	4	20	13
	Deep	20	45	24
Lake Area, $A$ (km <sup>2</sup> )	Small	0	0.4	0.2
	Medium	0.4	5	1.7
	Large	5	40	10
Secchi-Disk Depth, $Z_{seci}$ (m)	Eutrophic	0	1.8	1.2
	Mesotrophic	1.8	4.5	2.5
	Oligotrophic	4.5	7	4.5

NOTES: Based on Table 2 in Stefan et al. (1996) and on Heiskary and Wilson (1988).

**Table 3.** Study lake categories based on size, trophic status, and stratification potential.

<i>Park Unit</i> – <i>Lake</i>	<i>by Area</i>	<i>by Depth</i>	<b>Trophic Status</b>						<b>Stratification</b>		
			<i>Secchi</i>		<i>TP</i>		<i>Chl-a</i>		<i>Geom Ratio</i>	<i>Class</i>	
			<i>TSI</i>	<i>Class</i>	<i>TSI</i>	<i>Class</i>	<i>TSI</i>	<i>Class</i>			
VOYA	Cruiser	Medium	Deep	31	O	23	O	30	O	0.9	Strong
	Ek	Small	Medium	50	M	46	M	49	M	4.0	Medium
	Little Trout	Medium	Deep	33	O	26	O	32	O	1.1	Strong
	Peary	Medium	Medium	47	M	45	M	47	M	5.0	Medium
ISRO	Ahmik	Small	Shallow	49	M	47	M	39	M	6.2	Weak
	Harvey	Medium	Medium	42	M	43	M	38	O	5.3	Weak
	Richie	Medium	Medium	52	E	51	M	49	M	3.4	Medium
	Siskiwit	Large	Deep	31	O	25	O	29	O	1.4	Strong

NOTES: Lake categorization for Voyageurs National Park (VOYA) and Isle Royale National Park (ISRO) lakes. See Table 2 for definitions of lake category based on area and depth, based on Stefan et al. (1996) and Heiskary and Wilson (1988). Trophic status index (TSI) based on Carlson (1977), where “O” is oligotrophic, “M” is mesotrophic, and “E” is eutrophic. Breakpoints between O, M, and E from Heiskary and Wilson (1988). Geometric ratio (GR) defining stratification potential from Gorham and Boyce (1989), where GR<3 is “Strong,” 3<GR<5 is “Medium,” and GR>5 is “Weak.”

Area and depth influence light interception, wind fetch, and lake volume and are thus critical in determining the likelihood of thermal stratification. For a large set of Minnesota lakes, Gorham and Boyce (1989) determined the likelihood of stratification according to a geometric ratio (GR) defined as the following:  $GR = A^{0.25} / Z_{max}$ , where A is lake area in square meters and  $Z_{max}$  is maximum lake depth in meters. Based on ranges of GR values, the study lakes range from shallow and small lakes with a weak likelihood of stratification to deep and large lakes with a strong likelihood of stratification (Table 3).

Trophic status may be inferred from the Secchi depth, total phosphorus (TP), and chlorophyll-*a* measurements (Carlson 1977, Heiskary and Wilson 1988). About half the study lakes were oligotrophic, and about half mesotrophic, depending on the parameter (Table 3). Only Lake Richie reached the eutrophic category, based on Secchi depth. However, these categories can vary from year to year, with Richie demonstrating the potential for excessive algal productivity.

The optical, physical, chemical, and biological characteristics of each lake required by the model were inferred from the measured data discussed above (Fang et al. 2010). Based on the total light attenuation determined by Secchi depth and light attenuation due to chlorophyll content, light attenuation due to the water matrix was determined by taking the difference of the two (Table 4). This water-matrix attenuation is generally proportional to DOC, as expected (compare with Table 1). The wind-sheltering coefficient was estimated from lake area, although it can vary substantially based on the stature of vegetation and topography surrounding the lake. Diffusion coefficients for the metalimnion and hypolimnion were inferred from lake size based on empirical relations given by Fang et al. (2010). A number of parameter values required for modeling dissolved oxygen concentration were also estimated and were included in Table 4, although they were not used for this project.

#### ***Input Variables: Weather***

Weather data needed by the model include daily values for air temperature, dew point temperature, wind speed, solar radiation, sunshine percentage, and precipitation as rain or snow (Fang et al. 2010). Most of these data are available from National Weather Service (NWS) first class weather stations, of which there are six in Minnesota, including Duluth and International Falls. However, no station has a complete record, and compiling model-ready data sets is a significant task. Fortunately, Fang and colleagues at Auburn University have compiled climate data for Minnesota for the period 1961–2011 (Xing Fang, Alam Shoeb, and Zhongshun Li, Auburn University, personal communication, 2013). Weather data for International Falls were used for modeling the VOYA lakes, and data for Duluth were used for modeling the ISRO lakes. While lakes within VOYA are relatively close (about 20–30 miles) to International Falls, lakes in ISRO are fairly far away (about 150–200 miles) from Duluth. Nonetheless, good model results for the ISRO lakes indicate that weather data from Duluth are adequate for modeling thermal structure, suggesting that the principal drivers (temperature and wind, presumably) are reasonably similar between ISRO and Duluth. Stations closer to ISRO (Thunder Bay, e.g.) may give better results but were not explored at this stage.

**Table 4.** MINLAKE-specific parameters for study lakes.

<i>Park Unit-Lake</i>	Light Attenuation Parameters (per m)			Wind Sheltering coeff (Wstr)	SOD (Sb20)	BOD (mg/L) (BOD)	Metalimnion diffusion coefficient (EMCOE(1))	SOD multiplier (EMCOE(2))	Hypolimnion diffusion coefficient (EMCOE(4))	Lower Chl-a multiplier (EMCOE(5))
	Total, from Zseci	Algal, from Chl-a	Water, by diff (XK1)							
<i>VOYA</i>										
Cruiser	0.24	0.02	0.22	0.17	0.2	0.50	0.5	5.0	1.0	1.5
Ek	0.91	0.14	0.78	0.13	0.8	0.75	1.0	2.3	1.0	1.0
Little Trout	0.29	0.02	0.27	0.33	0.2	0.50	0.5	5.0	1.0	1.5
Peary	0.73	0.11	0.62	0.16	0.8	0.75	1.0	2.3	1.0	1.0
<i>ISRO</i>										
Ahmik	0.85	0.05	0.80	0.04	1.0	0.75	1.0	1.9	1.0	1.0
Harvey	0.54	0.04	0.50	0.18	0.4	0.50	1.0	3.0	1.0	1.5
Richie	1.02	0.13	0.89	0.54	0.8	0.75	1.0	2.3	1.0	1.0
Siskiwit	0.25	0.02	0.23	1.00	0.2	0.50	0.5	5.0	1.0	1.5

NOTES: Lake parameters for Voyageurs National Park (VOYA) and Isle Royale National Park (ISRO) lakes. All values based on Fang et al. (2010), which cites Hondzo and Stefan (1992) for total light attenuation, Megard et al. (1979) for chlorophyll-a (chl-a) light attenuation, and Hondzo and Stefan (1993) for wind sheltering coefficient (Wstr). Sb20, sediment oxygen demand (SOD) at 20 deg C per unit area of sediment per day. BOD, biochemical oxygen demand. EMCOE(1) (empirical coefficient 1), multiplier for diffusion coefficient in the metalimnion. EMCOE(2), multiplier for SOD below the mixed layer. EMCOE(4), multiplier for diffusion coefficient in the hypolimnion. EMCOE(5), multiplier for chlorophyll a below the mixed layer. Sb20, BOD, EMCOE(2), and EMCOE(5) affect only DO calculations and hence were not critical for this report.

### ***Input Variables: Model Goodness-of-Fit Statistics***

Model goodness of fit refers to how closely modeled values are matched by observed values. The observed data set comprised temperature profile data collected by NPS personnel several times per year on each lake, from 2006–2010 for VOYA lakes and from 2007–2010 for ISRO lakes. Multiple measurements taken within 0.1-m-depth on the same day were considered duplicates and replaced with their averaged depth and temperature. The modeled data set comprised simulated temperatures for the same day and depth as the observed data. Modeled temperatures at the observed depth were calculated as the linearly interpolated temperature value between the depth midpoints of the adjacent model layers. Model goodness of fit may be qualitatively assessed by visual comparison of observed temperature profiles with simulated profiles (see Appendix A, first set of figures for each lake).

Quantitative assessment of model goodness of fit is based on selected statistics that aggregate and summarize the deviations between each observed value and its corresponding simulated value. A commonly used statistic is the coefficient of determination, or R-squared ( $R^2$ ; range 0 to 1), which quantifies the fraction of variance explained by a linear model. In ordinary least-squares linear regression,  $R^2$  is the equivalent of the square of the Pearson correlation coefficient ( $r$ ; range -1 to +1).

$$R^2 = SS_{reg}/SS_{tot} = (SS_{tot} - SS_{res})/SS_{tot} = 1 - SS_{res}/SS_{tot} \quad (\text{equation 1})$$

Where  $SS_{tot}$  is the sum of squared deviations from the mean,  $SS_{reg}$  is the sum of squared deviations explained by the regression model (found by difference), and  $SS_{res}$  is the sum of squared residuals. In Figure 3, the regression line is shown in red, and the residuals are the differences between the observed data points and this red line. In lake thermal modeling, there is some justification for forcing the regression line through the origin, because 0°C just happens to be the temperature of ice formation and melting, and thermal models should be constrained to match this temperature very well. However, the regression in Figure 3 was left unconstrained to better identify the differences between the observed and modeled values within the range of observed temperatures.

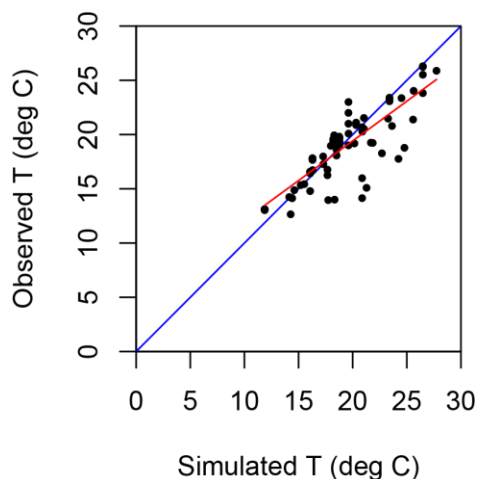


**Figure 3.** Data from Peary Lake as an example of observed versus simulated temperatures (T), showing regression line (red) through the cloud of observed values and the 1:1 line (blue).

The Nash-Sutcliffe coefficient of efficiency (NSE; range negative infinity to 1) is another common measure of model goodness of fit. It is similar to  $R^2$  in that it attempts to quantify the fraction of variance explained by a model.

$$NSE = SS_{mod}/SS_{tot} = (SS_{tot} - SS_{dev})/SS_{tot} = 1 - SS_{dev}/SS_{tot} \quad (\text{equation 2})$$

Where  $SS_{tot}$  is the same as before (sum of squared deviations from the mean),  $SS_{mod}$  is the sum of squares explained by the model (obtained by difference), and  $SS_{dev}$  is the sum of squared deviations from the model, in this case shown by the blue 1:1 line in Figure 3. That is, for any model value on the x-axis, the model would predict that the observations (y-axis) should fall exactly on the 1:1 if the model were perfect. The model is not perfect, of course, and the mismatch is measured by  $SS_{dev}$ , in the same way that the mismatch in linear regression is measured by  $SS_{res}$ . The difference is that in linear regression, the regression line is optimally placed to minimize  $SS_{res}$  and thus maximize  $R^2$ , whereas in the NSE calculation there is no such optimization.  $SS_{dev}$  can be quite large, and if it exceeds  $SS_{tot}$ , then NSE becomes negative, indicating that a simple mean does a better job explaining the variance than does the model (the blue 1:1 line).  $R^2$  is the upper limit to NSE, and the closer the regression intercept and slope are to 0 and 1 respectively (i.e., the closer the red regression line is to the blue 1:1 line), then the closer NSE will be to  $R^2$ .

### ***Model Runs and Post-Processing***

MINLAKE was run for a 51-year period, from mid-April 1961 through 2011. The model was begun in mid-April when the lakes are approximately isothermal, which provided uniform initial conditions for all lakes and reduced concerns about thermal inertia. Output from the first calendar year (1961) was discarded to allow for model equilibration, and all further post-processing was based on the 50 years of output from 1962–2011. While MINLAKE provides useful data summaries for many purposes, significant post-processing was needed to build the variables selected to be compared with the paleoecological proxies. Scripts were written within the R statistical framework (R Core Development Team 2013) to allow the automated reading of MINLAKE output, conversion to selected summarized variables, plotting of annual values, and output of tabular data and statistical test results. Trends during the 50-year runs were assessed by dividing the data output into two halves (1962–1986 and 1987–2011) and determining the significance of their differences with a Mann-Whitney U Test (R Development Core Team 2013, based on Bauer 1972; Hollander and Wolfe 1973). Lowess curves were plotted over time through all outputs using default settings and span of 0.75 (R Development Core Team 2013, based on Cleveland 1979, 1981).

## **Lake-Sediment Coring and Analyses**

### ***Coring***

Sediment cores were previously recovered from central depositional basins from the eight lakes as part of other projects. All cores were retrieved with a 6.5-cm inner diameter polycarbonate tube fitted with a piston and operated from the lake surface from an anchored boat or canoe. Rigid drive rods were used to push the tube into the lake sediments while the piston was held in place by cable

(Wright 1991). Sediment cores were extruded vertically from the coring tube in the field at 1-cm increments to 60–85 cm core depth and placed in polypropylene jars; the remainder of the core was capped. Cores and sectioned material were transported to 4°C laboratory storage for further processing. Cores from Ek, Peary, Cruiser lakes at VOYA and Ahmik, Harvey, and Richie lakes at ISRO were taken as part of GLKN's diatom monitoring program (Ramstack et al. 2008, Edlund et al. 2011), the core from Little Trout Lake (VOYA) was recovered as part of a mercury study (Engstrom et al. 2012), and the Siskiwit Lake (ISRO) core was recovered as part of a study on climate impacts on lake mixing (Saros et al. 2012). Sediment samples were homogenized and subsampled for loss-on-ignition and diatom analyses. Remaining sediments were freeze-dried within the sample jars for  $^{210}\text{Pb}$  dating and geochemical analysis and are archived in scintillation vials at the St. Croix Watershed Research Station (Science Museum of Minnesota).

### ***Isotopic Dating and Geochemistry***

Sediment cores were analyzed for  $^{210}\text{Pb}$  activity to determine age and sediment accumulation rates for the past 150 to 200 years. Lead-210 activity was measured from its daughter product,  $^{210}\text{Po}$ , which is considered to be in secular equilibrium with the parent isotope. Aliquots of freeze-dried sediment were spiked with a known quantity of  $^{209}\text{Po}$  as an internal yield tracer and the isotopes distilled at 550°C after treatment with concentrated HCl. Polonium isotopes were then directly plated onto silver planchets from a 0.5 N HCl solution. Activity was measured for  $1\text{--}3 \times 10^5$  s using an Ortec alpha spectrometry system. Supported  $^{210}\text{Pb}$  was estimated by mean activity in the lowest core samples and subtracted from upcore activity to calculate unsupported  $^{210}\text{Pb}$ . Core dates and sedimentation rates were calculated using the constant rate of supply model (Appleby and Oldfield 1978). Dating and sedimentation errors represented first-order propagation of counting uncertainty (Binford 1990).

Dry-density (dry mass per volume of fresh sediment), water content, organic content, and carbonate content of sediments were determined by standard loss-on-ignition techniques (Dean 1974). In short, weighed sediment subsamples were dried at 105°C for 24 hours to determine water content and dry density, then heated at 550°C and 1000°C to detect organic and carbonate content from post-ignition weight loss, respectively.

The same samples from each long core that were analyzed for diatoms were also examined for biogenic silica (BSi). Weighed subsamples (30 mg) from each primary core were digested for BSi analysis using 40 mL of 1% (w/v)  $\text{Na}_2\text{CO}_3$  solution heated at 85°C in a reciprocating water bath for five hours (DeMaster 1979, 1981; Conley and Schelske 2001). A 0.5 g aliquot of supernatant was removed from each sample at 3, 4, and 5 hrs. After cooling and neutralization with 4.5 g of 0.021N HCl solution, dissolved silica was measured colorimetrically on a Lachat QuikChem 8000 flow injection autoanalyzer as molybdate reactive silica (McKnight 1991).

### ***Diatom Analysis***

Diatoms are a group of microscopic algae that are common in all aquatic habitats and are characterized by having an ornamented cell wall made of biologically produced glass. The cell walls of diatoms are used to identify each species, and they are resistant to decay and often accumulate in lake sediments to provide a snapshot of the historical diatom community and its changes through

time. Diatoms and chrysophyte cysts were prepared by placing approximately 0.25 cm<sup>3</sup> of homogenized sediment in a 50 cm<sup>3</sup> polycarbonate centrifuge tube and adding 2–5 drops of 10% v/v HCl solution to dissolve carbonates. Organic material was subsequently oxidized by adding 10 ml of 30% H<sub>2</sub>O<sub>2</sub> and heating for 3 hours in an 85°C water bath. After cooling, the samples were centrifuged and rinsed 4–6 times with deionized water to remove oxidation byproducts. Aliquots of the remaining material, which contain the diatoms, were dried onto 22x22 mm #1 coverglasses. Coverglasses were permanently attached to microscope slides using Zrax mounting medium (Ramstack et al. 2008, Edlund et al. 2011).

Diatoms were identified along random transects to the lowest taxonomic level under 1250X magnification (full immersion optics of NA>1.3) (Edlund et al. 2011). A minimum of 400 valves was counted in each sample. Identification of diatoms relied on floras and monographs such as Hustedt (1927–1966, 1930), Patrick and Reimer (1966, 1975), Collins and Kalinsky (1977), Camburn et al. (1978, 1984–1986), Krammer and Lange-Bertalot (1986–1991), Cumming et al. (1995), Reavie and Smol (1998), Camburn and Charles (2000), Fallu et al. (2000), and the primary literature (e.g., Koppen 1975). All diatom counts were converted to percentage abundances by taxon; abundances are reported relative to total diatom counts in each sample.

### ***Statistical Approach***

To summarize the timing and degree of change in diatom communities within cores, detrended correspondence analysis (DCA) was used, where DCA axis 1 represents diatom compositional turnover (Hill and Gauch 1980). All diatom species were included in each analysis, with downweighting of rare taxa, detrending by segments, and nonlinear rescaling applied using the software R (Ramstack et al. 2008, R Development Core Team 2013). The DCA axis 1 scores were plotted stratigraphically to show the amount of turnover between samples over time in units of standard deviation (SD). Axis scores were plotted for each lake together with the downcore relative abundance of predominant diatom species (two or more occurrences at >5% relative abundance) and the weight percent and flux of biogenic silica as a proxy of historical algal (diatom) productivity. Presentation of downcore data is truncated at 1960–2010 for consistency with thermal model output.



## Results and Discussion

### Thermal Modeling

Results of all model runs are presented as figures in Appendix A, arranged alphabetically by lake name, to help the reader find the results for each lake. Within the set of figures for each lake, figures are arranged in consistent order showing (a) short-term runs to test goodness of fit between observed and modeled temperature profiles and (b) longer runs (50-year) to look for trends in water temperatures, occurrence, and depth of temperature gradients, and occurrence of ice.

### *Model Fits*

The model fit for each lake may be assessed qualitatively by scanning the depth profiles of simulated versus observed temperatures (Appendix A, Figures A1, A6, A11, A12, A17, A22, A27, A32, A33, and A38). In general, the model fits were quite good for the deeper lakes (Cruiser and Little Trout in VOYA and Richie and Siskiwit in ISRO), with a wide range of temperatures and thermoclines situated at about the correct depth. While the simulated temperatures at any depth might be off by several degrees, the overall shapes of the profiles were similar between simulated and observed values. The model had more trouble with the shallower lakes, particularly for the ISRO lakes, Ahmik and Harvey. The profiles for the shallower lakes in VOYA, Ek and Peary, appeared reasonable but not quite as good as for the deeper lakes.

The quantitative measures of model goodness of fit support these qualitative observations (Table 5). For lakes within both national parks, the measure of model fit, Nash-Sutcliffe coefficient of efficiency (NSE), increases as maximum depth ( $Z_{max}$ ) and range of observed temperatures both increase. NSE values were generally large and just a few points below their effective maximum ( $R^2$ ) in most cases. Commonly an NSE value of 0.5 or greater is considered to be acceptable (Moriassi et al. 2007). The only lake falling below this threshold was Ahmik Lake in ISRO, whose negative NSE indicated that a simple mean was a better predictor of temperature than was the model. The mean error was positive for all lakes (Table 5), indicating that the model systematically overestimated temperatures, with Ahmik again having not only the largest mean error but also the largest root mean squared error (RMSE). These measures of model fit are graphically displayed in Figures 4 and 5, as explained earlier for Figure 3. The clouds of points for the deeper lakes have wide ranges of values, and the regression lines (red) are nearly collinear with the blue 1:1 line. In contrast the shallower lakes have smaller clouds of points with less elongation, and hence the regression line is less constrained to be similar to the 1:1 line. Most points fell just to the right of the blue 1:1 line, demonstrating that the model overestimated temperatures slightly but consistently.

The reason the thermal structure of shallow lakes was not simulated as well as that of deep lakes may be related to less well-constrained factors in the model that have a disproportionate effect on smaller and shallower lakes. Heat loss to sediments and to outflowing water (both surficial outlets and groundwater recharge) would have a greater effect on lakes with small volumes. Lakes shallow enough to have sunlight reach their bottoms would be susceptible to small errors in the solar absorptance of the sediment surface. Lakes with small surface areas are more influenced by the wind sheltering effects of surrounding topography and vegetation, especially the effects of winds from different directions. MINLAKE allows the user to set a constant wind-sheltering coefficient to aid

**Table 5.** Model goodness-of-fit statistics relative to lake depths and range of observed temperatures.

Lake	Statistics				Observations				
	NSE	R <sup>2</sup>	RMSE (°C)	Mean Error (°C)	Zmax (m)	N	Min (°C)	Max (°C)	Range (°C)
VOYA lakes									
Peary	0.58	0.69	2.1	0.4	5.2	85	12.7	26.3	13.7
Ek	0.74	0.78	2.0	0.2	6.2	112	10.0	28.6	18.6
Cruiser	0.92	0.94	1.7	0.7	28.8	363	4.8	24.4	19.5
Little Trout	0.94	0.96	1.6	0.8	30.0	384	3.9	25.3	21.4
ISRO lakes									
Ahmik	-0.25	0.15	2.7	1.1	2.9	41	15.2	24.1	8.8
Harvey	0.42	0.56	2.1	0.5	5.1	57	14.4	25.7	11.3
Richie	0.76	0.76	1.8	0.1	11.1	213	9.1	25.3	16.3
Siskiwit	0.92	0.94	1.3	0.5	45.3	357	6.9	22.8	15.9

NOTES: NSE, Nash-Sutcliffe coefficient of efficiency; R<sup>2</sup>, coefficient of determination, the fraction of variance explained by linear regression; RMSE, root mean square error, essentially the standard deviation of the errors; Zmax, maximum lake depth; N, number of observations compared against simulated values; Min, minimum; Max, maximum; VOYA, Voyageurs National Park; ISRO, Isle Royale National Park.

calibration (see Table 4), but the coefficient is a general term meant to account for average or typical conditions, not for details of different wind speeds from different directions.

Finally, the proximity of the weather station used to drive the model can be important. The model runs for the VOYA lakes used data from the nearby International Falls weather station, and model fits for these four lakes were all quite good, with even the shallowest lake (Peary) having a good NSE value of 0.58. Evidently the weather conditions measured at the station were representative of those occurring at the lake, including windiness. In contrast, the nearest weather station with model-ready data to the ISRO lakes was Duluth, 150 to 200 miles away. Large lakes like Siskiwit may have enough thermal inertia to respond to a smoothed average of weather conditions and so may be reasonably modeled based on a somewhat distant weather station. Smaller lakes with faster responses would be more prone to mismatches due to wind and radiation differences between ISRO and the weather station in Duluth. Small and shallow lakes would have relatively large variations on water temperature and stratification characteristics during the course of each day from early morning to late afternoon. Simulated temperature using MINLAKE2012 with a daily time step is closer to temperature at late afternoon because daily solar radiation is used to heat the lake, whereas observed profiles in these lakes may have taken earlier or later. The mismatch of times for simulated and measured temperature profiles would create larger errors in shallow lakes than in deep lakes.

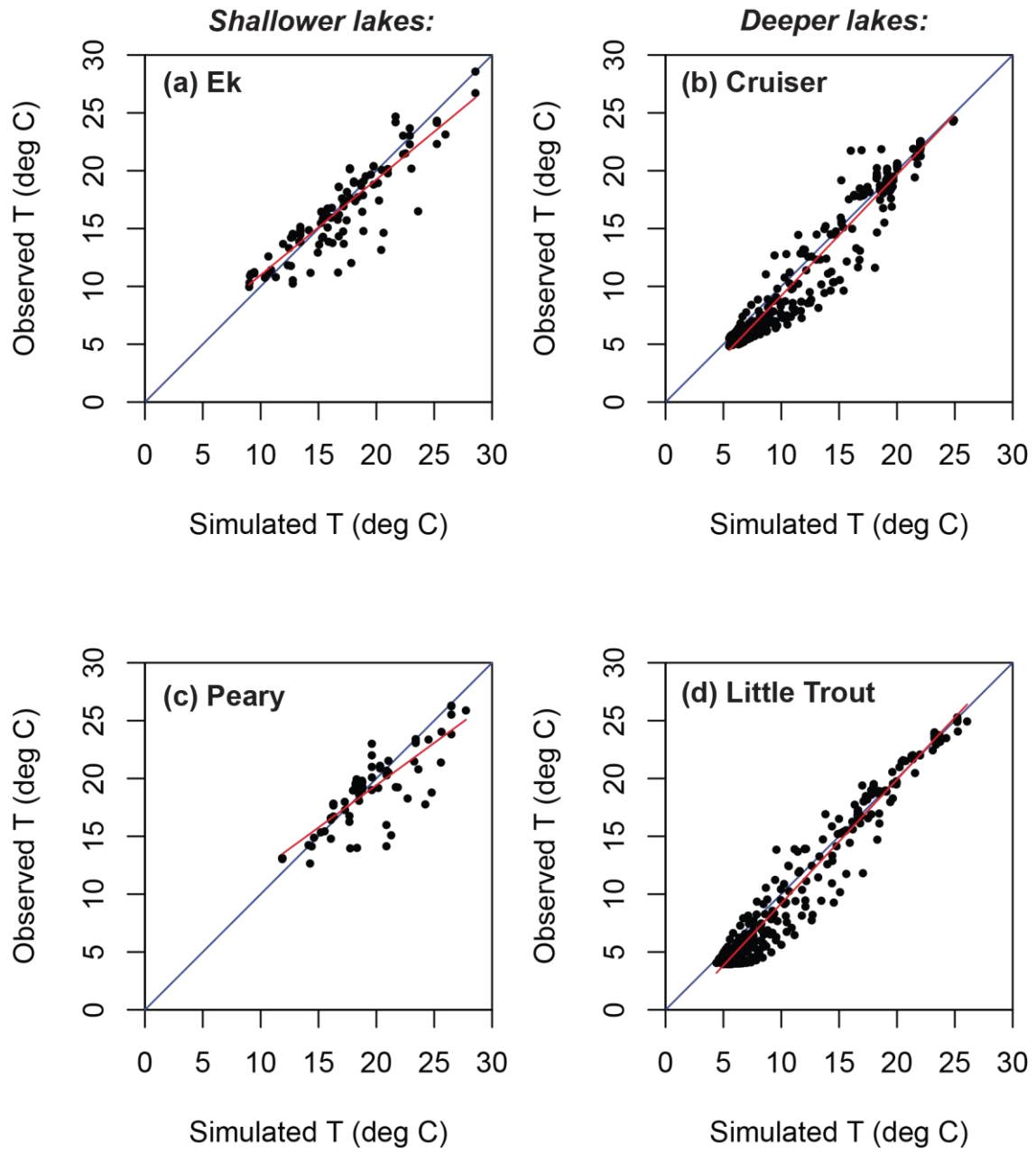


**Figure 4.** Regression plots of observed versus modeled temperatures (T) for lakes at Voyageurs National Park.

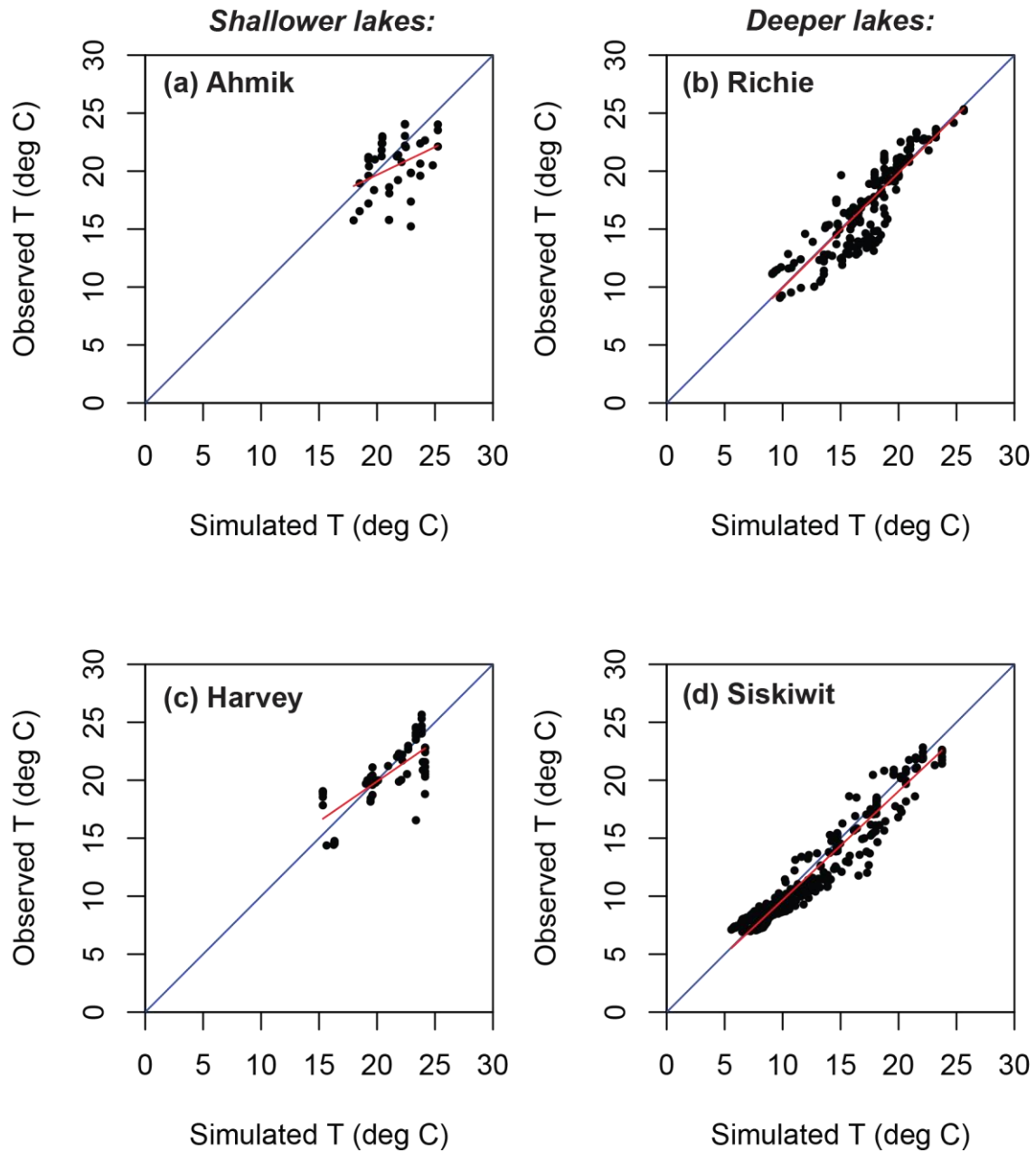


**Figure 5.** Regression plots of observed versus modeled temperatures (T) for lakes at Isle Royale National Park.

### ***Selection of Output Variables***

Model output for the 50-year runs (1962–2011) was summarized for variables that were deemed representative of factors that potentially influence biological activity in lakes. To allow comparison with the paleoecological records from the sediment core analyses, the lake thermal data were summarized as time series of annual values. Water temperatures during the growing season are obviously important in affecting not only biological activity in the upper waters but also microbiological activity at depth. Hence, average summertime (June–July–August: JJA) shallow and

bottom water temperatures were calculated for each year of simulation. The shallow water temperature was taken at the 1-m depth in the model, and the bottom water temperature was taken at a depth corresponding to  $0.9 \cdot Z_{\max}$ , but no closer than 1 m to the bottom to avoid any gradients near the sediment surface. These depths should be representative of epilimnetic and hypolimnetic temperatures for those lakes deep enough to stratify.

The formation of thermal gradients can affect lake mixing and thus the distribution of key nutrients and escalation of redox-sensitive microbiological activity. The depth of steepest gradient and whether it forms earlier, dissipates later, and has greater continuity through the year are potential mechanisms by which climate warming may impact lake biology. We calculated thermal gradients with the central-difference method (i.e., negative  $T_2 - T_1$  divided by  $Z_2 - Z_1$ , applied at the midpoint (average) depth between  $Z_1$  and  $Z_2$ ). The thermocline depth was defined as the depth of the steepest gradient each day (Wetzel 1975), even though under certain conditions the steepest gradient may not be a truly stable thermocline but a shallow transient feature in response to very warm, calm conditions. Output was tested for a variety of gradients, from 1 °C per meter to 4 °C per meter. While a gradient of 1 °C per meter is commonly invoked as defining a thermocline (Wetzel 1975), such gradients formed and dissipated frequently in the model during the spring and fall and thus did not seem representative of features that could strongly isolate top and bottom waters. Hence we focused on steeper gradients in order to identify less-easily formed but more persistent, stable features with a greater potential to isolate top from bottom waters. The steeper the selected gradient, the fewer days each year attained that gradient. Gradients of 4 °C per meter or larger were too infrequent to be considered, and so we settled on gradients of 2 °C and 3 °C per meter. The days with a 3 °C per meter gradient formed a subset of those with a 2 °C per meter (or larger) gradient. For both the 2 °C and 3 °C per meter gradients, for each year of model run, we determined the date the gradient first formed, the total number of days and the longest continuous period the gradient existed, and the date the gradient dissipated. In addition, for those days that achieved the selected gradient or larger, we also calculated the average summertime depth of the steepest daily gradient (i.e., the thermocline depth). We treated all model output equally without regard to lake depth, recording all gradients as they occurred even in shallow lakes. However, we note in the output plots that such gradients have short duration and thus probably limited impact in shallow lakes that are generally well-mixed.

Ice cover is perhaps the most obvious thermally driven feature of a lake in cold regions that could affect lake biology. Although photosynthesis can take place below ice if snow cover is not too deep, algal biomass and productivity are generally small under the ice during winter (Wetzel 1975), indicating that the growing season for aquatic vegetation is largely determined by the length of the ice-free season. All other factors remaining equal, the length of the growing season can directly alter the annual net primary productivity and rates of nutrient cycling. Length of ice cover further affects the eventual redox state of the lake water over the course of winter, which in turn can affect the fish community and nutrient release from the sediments. Consequently, MINLAKE output was processed to extract the dates of first open-water (ice-out) in the spring, last ice in the spring, first ice in autumn, and last open water in autumn to search for trends in how early ice-out occurred in the spring or how late ice-on occurred in the autumn. In addition, the durations of continuous ice cover in the winter and open water in the summer were calculated for each year of the simulations.

### **Model Runs**

Output of the selected variables is given for the eight study lakes, ordered alphabetically, in Appendix A (see Figures A1–A5 for example from Ahmik Lake). For each lake, figures are arranged to show (a) a comparison of observed and modeled lake-temperature profiles, (b) shallow and bottom water temperatures, (c) dates, durations, and depths of selected temperature gradients, and (d) dates and durations of ice cover and open water.

Most output was distilled into a time series of annual values from 50 years of MINLAKE model run, from 1962–2011. As noted earlier, to assess the significance of simple trends during this time period, we split model output into two even halves (1962–1986 and 1987–2011) and used a Mann-Whitney U Test to determine the significance of their differences between these two groups. In Table 6, lakes are arranged by park unit (VOYA and ISRO), and by depth (shallow to deep) within each park unit. Dark gray table cells and bold font indicate trends that are significant at the 0.05 level, and light gray table cells indicate those significant at the 0.1 level. The significance value does not identify the direction of change, only that the two halves of the data output are different. Direction of change may be inferred by inspection of the output plots in Appendix A.

Not surprisingly, the most direct relation found in the lake output to climate warming was in shallow-water temperatures during summer (JJA). Every lake showed an apparent warming at 1-m depth over time (Table 6). The lowess curves (R Development Core Team 2013, based on Cleveland 1979, 1981) indicate that shallow temperatures rose from about 1962–1980, remained steady from 1980–1992, and then continued upward from 1992–2011 (Appendix A, e.g., Appendix Figure A2). Variability appeared greater following about 1985. Trends in JJA bottom-water temperatures were not so uniform. For well-mixed shallow lakes, bottom water temperatures should follow similar trends as for shallow water. While this generalization held true for the shallower ISRO lakes (Ahmik and Harvey) (Figures A2, A18), it did not for the shallower VOYA lakes (Ek and Peary) (Figures A13, A28) because these two lakes had some summer stratifications based on observed profiles (Figures A12 and A27) and the geometry ratio. The deep lakes generally showed no significant bottom-water temperature trends, with the exception of Little Trout, whose temperature appeared to decline. This counterintuitive result may have been caused by greater separation of epilimnetic and hypolimnetic waters resulting from longer periods of time each year with steep thermal gradients.

Trends were assessed for temperature gradients equaling or exceeding 2 °C and 3 °C per meter depth. We focus here on the four deep lakes because short-lived temperature gradients in shallow lakes are less likely to impact aquatic biology. Climate warming might be expected to result in a higher

**Table 6.** Significance of differences between output from first half (1962–1986) and second half (1987–2011) of MINLAKE runs for selected variables.

Physical/Chemical Parameters	Parameter Units	VOYA Lakes				ISRO Lakes			
		Peary	Ek	Cruiser	Little Trout	Ahmik	Harvey	Richie	Siskiwit
Zmax (maximum depth)	(m)	5.18	6.2	28.8	30	2.87	5.1	11.1	45.26
Area	(ha)	44.75	28.56	41.11	90.88	8.53	53.38	204.73	1687.42
Geometric Ratio		5.0	4.0	0.9	1.1	6.2	5.3	3.4	1.4
Zseci (secchi depth)	(m)	2.5	2.0	7.7	6.4	2.2	3.4	1.8	7.4
TP (total phosphorus)	(ug/L)	17	18	4	4	20	15	26	4
DOC (dissolved organic carbon)	(mg/L)	10	13	4	5	18	10	10	5
Aws (watershed area)	(ha)	976	250	118	236	36	341	1956	7239
<b>Temperatures</b>									
Shallow (1 m)		0.03	0.032	0.095	0.084	0.013	0.011	0.013	0.027
Deep (0.9*Zmax)		0.335	0.658	0.969	0.032	0.039	0.016	0.500	0.773
<b>Temperature gradients: &gt;2 °C per m</b>									
First day of year with gradient		0.854	0.698	0.109	0.763	0.793	0.398	0.248	0.052
Last day of year with gradient		0.081	0.114	0.037	0.669	0.393	0.443	0.528	0.052
Total days with gradient		0.892	0.225	0.264	0.061	0.793	0.192	0.024	0.084
Longest continuous duration with gradient		0.861	0.299	0.204	0.009	0.009	0.851	0.058	0.449
Summertime (JJA) depth of gradient (mean)		0.503	0.298	0.112	0.097	0.809	0.834	0.0004	0.001
<b>Temperature gradients: &gt;3 °C per m</b>									
First day of year with gradient		0.756	0.748	0.615	0.547	0.528	0.818	0.151	0.062
Last day of year with gradient		0.467	0.362	0.021	0.461	0.509	0.471	0.915	0.070
Total days with gradient		0.915	0.356	0.065	0.065	0.276	0.927	0.012	0.089
Longest continuous duration with gradient		0.930	0.923	0.115	0.051	0.033	0.665	0.365	0.278
Summertime (JJA) depth of gradient (mean)		0.178	0.441	0.208	0.209	0.487	0.779	0.003	0.028

**Table 6 (continued).** Significance of differences between output from first half (1962–1986) and second half (1987–2011) of MINLAKE runs for selected variables.

Physical/Chemical Parameters	Parameter Units	VOYA Lakes				ISRO Lakes			
		Peary	Ek	Cruiser	Little Trout	Ahmik	Harvey	Richie	Siskiwit
<b>Ice and Water</b>									
First day of open water		0.793	0.808	0.869	1.000	0.272	0.232	0.248	0.372
First day of continuous ice		0.808	0.484	0.256	0.712	0.727	0.580	0.771	0.876
Duration of continuous ice		0.617	0.881	0.912	0.465	0.406	0.307	0.562	0.548
Duration of open-water season		0.892	0.771	0.900	0.655	0.299	0.190	0.210	0.277

NOTES: Mann-Whitney U Test used to determine if early period is significantly different from later period. Dark bold cells are significant at the 0.05 level; shaded cells are significant at the 0.1 level. Summary data for each lake given at top of table, to help search for patterns.

Abbreviations: VOYA, Voyageurs National Park; ISRO, Isle Royale National Park; m, meters; ha, hectares; ug/L, micrograms per liter; mg/L, milligrams per liter.

frequency (total number of days) and continuous duration of these steep gradients, and this appeared to be generally true for all four of the deep lakes (Table 6). In general, these results imply an earlier spring formation and later fall dissipation of these gradients—even though, individually, these dates did not commonly show significant trends, with Cruiser and Siskiwit lakes being the exceptions (Figures A8, A9, A40, A41). Climate warming, especially if accompanied by stronger winds, might also be expected to cause an increase in thermocline depth. Diatom data from Siskiwit Lake is in fact consistent with this hypothesis, suggesting a large increase (a deepening) in thermocline depth (Saros et al. 2012). In Table 6, a change in thermocline depth was significant for both gradients (2 °C and 3 °C per meter) for both of the deeper lakes in ISRO (Richie and Siskiwit), and for the 2°C per meter gradient for Little Trout Lake in VOYA. However, even the direction of these trends is not necessarily evident in the plots of thermocline depth (Appendix A), and the magnitude of change is only in the range of a meter or less.

Under warmer climate, one would expect earlier ice-out in spring, later ice-on in autumn, a shorter duration of continuous ice, and a longer duration of open water, but none of the lakes had significant trends in these variables (Table 6) according to the simple statistical tests chosen here. However, visual inspection of the model output plots (Appendix A) indicates that perhaps some of the lakes have showed a shortening of continuous ice since about 1992. This appears most likely for the two shallower lakes in ISRO (Ahmik and Harvey) (Figures A5, A21), but it was not obvious for most of the lakes. Nonetheless, dates of fall freeze up were not obviously later in most cases. This conclusion is somewhat incongruent with the generally warmer water temperatures during the summer, which should delay ice formation, all other things being equal. As with ice cover, the length of the open-water season did not show an obvious trend over the 50 years of the model study, which again is somewhat surprising given the clear trend toward increasing shallow-water temperatures.

To summarize the trends in lake thermal structure from the 50 years of model runs for the eight study lakes, the most common significant trend was simply an increase in summer shallow-water temperatures, which held true for all eight lakes. The next most common significant trend was, for the deep lakes, an increase in the frequency and duration of thermal gradients equaling or exceeding 2 °C or 3 °C per meter. These trends appear to be the most likely candidates for how thermal structure may have impacted lake biology during the simulation period.

### **Paleolimnological Records**

Although cores were analyzed back to sediment levels that pre-date Euroamerican settlement (ca. 1850–1870) (Edlund et al. 2011, Engstrom et al. 2012, Saros et al. 2012), here we report data in a comparable fashion to thermal model output using downcore data from 1960–2010. In most cores, sampling intervals from 1960–2010 represent an approximate decadal sampling resolution. Relative abundance of predominant species in the cores captures biological changes in community makeup; species autecology is used in interpreting these data. The DCA Axis 1 scores are reported as a measure of community compositional turnover (Hill and Gauch 1980). Although thermal model output treats only the time period 1960–2010, DCA scores were calculated for the entire core record (ca. 1800–2010) (Edlund et al. 2011) but are only reported for 1960–2010. Biogenic silica content and accumulation rates are also plotted for each core as a measure of historical diatom productivity.

### ***Diatom Species Response***

In addition to nutrient levels, pH, and conductivity, the depth of lakes and lake morphometry are strong determinants of diatom communities primarily through physicochemical structuring and habitat availability. As such, the diatom communities and changes between 1960 and 2010 in the eight lakes are well differentiated between the shallower and deeper lakes but also differ between the two park units. The downcore distribution of diatoms that were present at >5% abundance in two or more core depths provides an overview of biological changes that have occurred during the last 50 years in these wilderness lakes.

Shallower lakes of VOYA (Ek, Peary)—Sediment records from the two shallower lakes of VOYA were dominated by similar diatom species, notably the acidophilic taxon *Eunotia zasuminensis* and *Tabellaria flocculosa* (morph IIIp) (Figures 6 and 7). These taxa behaved similarly in both lakes between 1960 and 2010 with *E. zasuminensis* decreasing and *T. flocculosa* IIIp simultaneously increasing in abundance. Additionally, *Staurosirella pinnata* decreased in abundance in Ek Lake and *Discostella stelligera* decreased slightly in Peary Lake. Changes in *E. zasuminensis* and *T. flocculosa* IIIp likely reflect subtle increases in lake pH as noted by Edlund et al. (2011), and the decrease of *D. stelligera* possibly the deepening or weakening of the thermocline in Peary Lake (Saros et al. 2012) although this was not identified as a significant response in our thermal modeling output.

Deeper lakes of VOYA (Cruiser, Little Trout)—The plankton of Cruiser Lake was dominated by few species, including *Discostella stelligera* and *Asterionella formosa* and two morphs of *Cyclotella ocellata* (Figure 8) (Edlund et al. 2011). The two former taxa showed little change in abundance between 1960 and 2010, whereas the two morphs of *C. ocellata* showed opposite trends with the nominate form increasing in abundance in recent decades. In Little Trout Lake, the plankton comprised a more diverse diatom community of several *Cyclotella* species: *D. stelligera*, *Asterionella formosa*, *Aulacoseira subarctica*, and *Tabellaria flocculosa* IV (Figure 9). *Discostella stelligera* had variable abundance, while *C. ocellata* and *C. michiganiana* increased in abundance since the 1980s. In contrast, *Asterionella formosa* and *Aulacoseira subarctica* decreased in abundance in recent decades. The ecologies of these deep lake species have not been completely resolved; however, we generally consider the small *Cyclotella* and *Discostella* species to be members of the deep chlorophyll layer, i.e., associated with the thermocline. Changes in their abundance may reflect changes in thermal structure of the lakes (Saros et al. 2012). *Asterionella formosa* and *Aulacoseira subarctica* are more responsive to increasing nutrients and longer periods of spring turnover. Thermal modeling results show Cruiser Lake to be trending toward longer periods of stability and deepening of the thermocline (Appendix Figure A8), whereas Little Trout Lake had a slight shallowing of the thermocline but extended period of stability in recent decades (Appendix Figure A24).

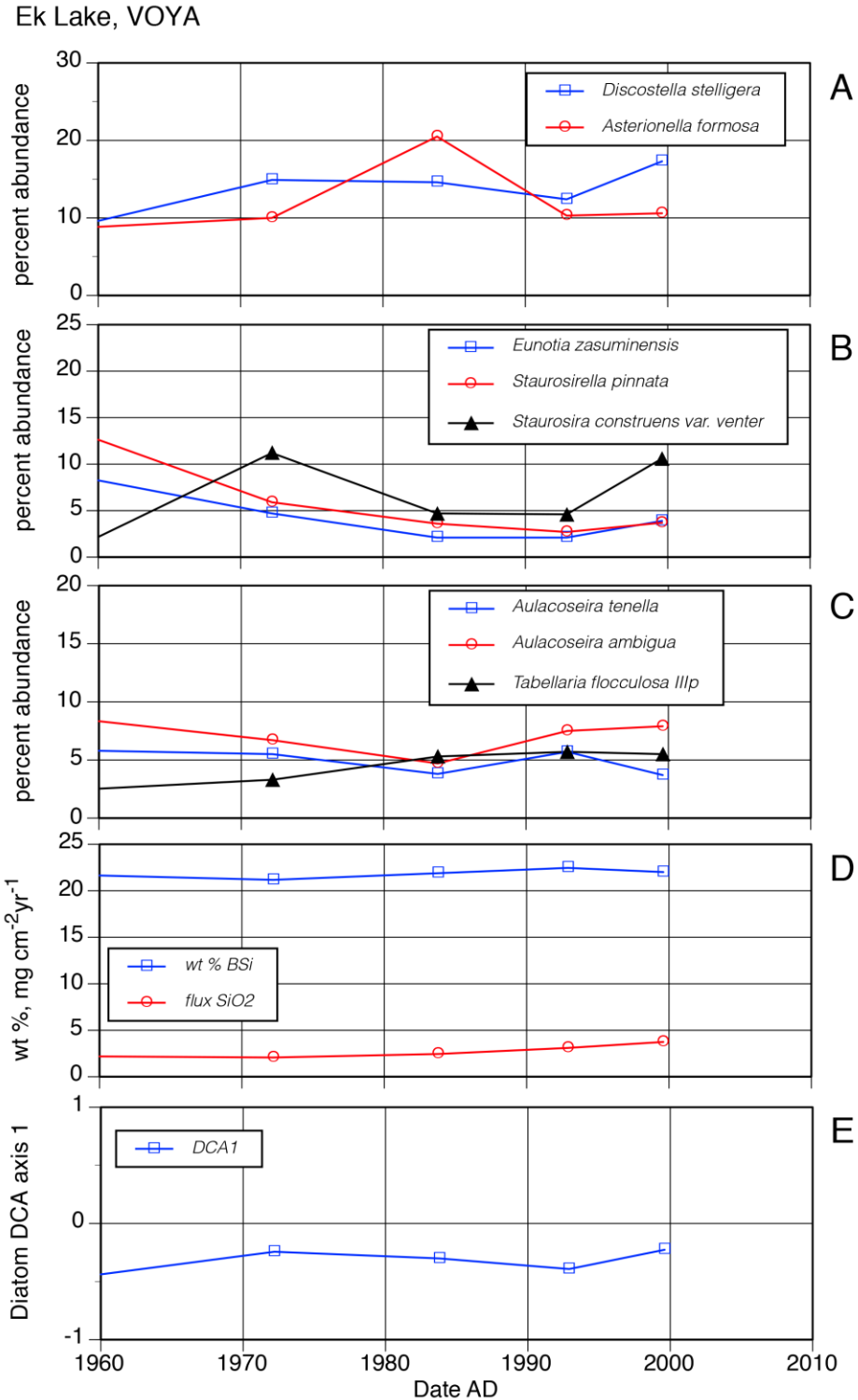


**Figure 6.** Sediment core record from Ek Lake, Voyageurs National Park, 1960–2010. A–C. Predominant diatom species preserved in sediment core. D. Biogenic silica content. Open squares are weight percent, and open circles are accumulation rate or flux ( $\text{mg cm}^{-2}\text{yr}^{-1}$ ). E. Diatom community turnover based on Detrended Correspondence Analysis axis 1 scores.

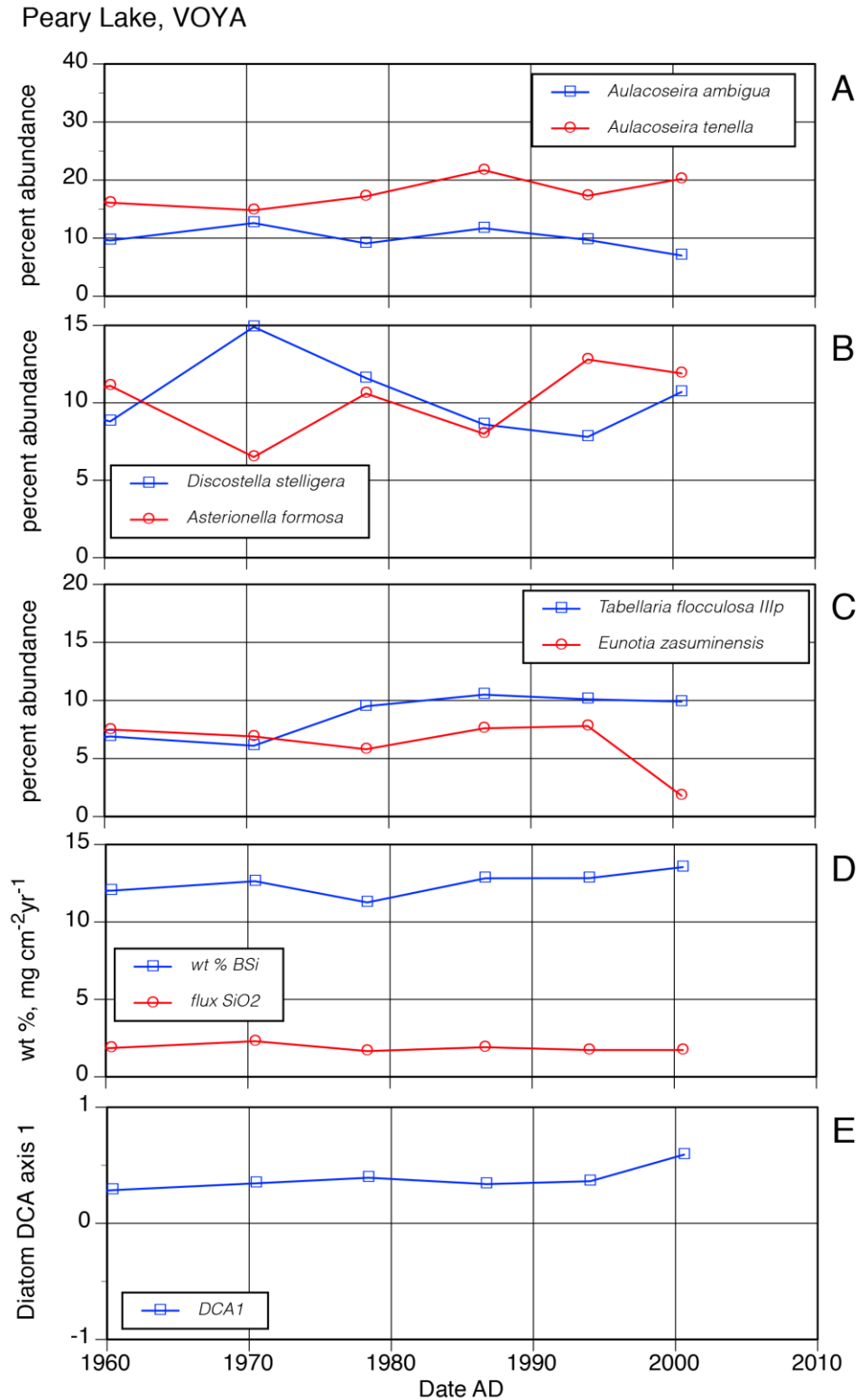


**Figure 7.** Sediment core record from Peary Lake, Voyageurs National Park, 1960–2010. A–C. Predominant diatom species preserved in sediment core. D. Biogenic silica content. Open squares are weight percent, and open circles are accumulation rate or flux ( $\text{mg cm}^{-2}\text{yr}^{-1}$ ). E. Diatom community turnover based on Detrended Correspondence Analysis axis 1 scores.

Cruiser Lake, VOYA

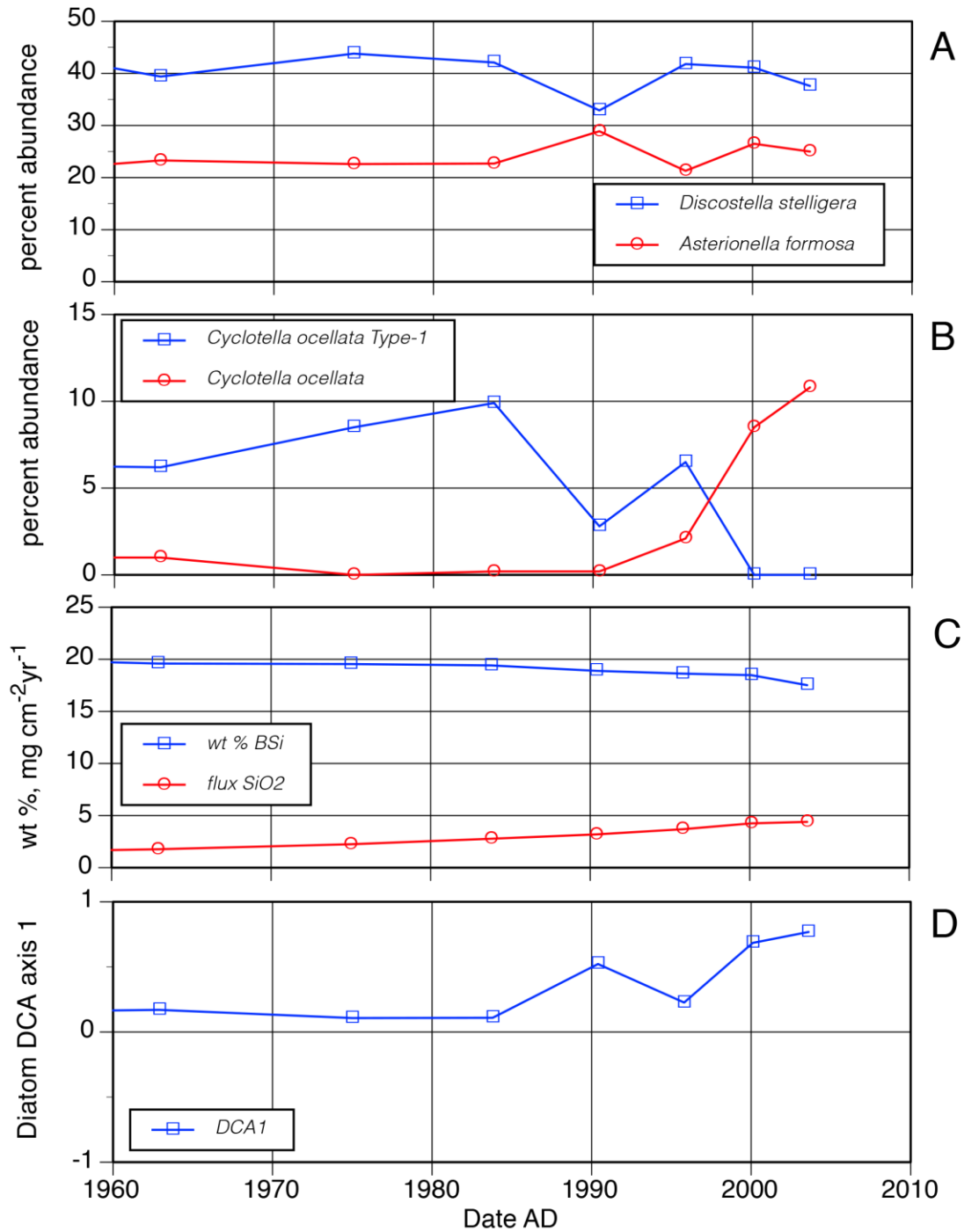


**Figure 8.** Sediment core record from Cruiser Lake, Voyageurs National Park, 1960–2010. A–B. Predominant diatom species preserved in sediment core. C. Biogenic silica content. Open squares are weight percent, and open circles are accumulation rate or flux (mg cm<sup>-2</sup> yr<sup>-1</sup>). D. Diatom community turnover based on Detrended Correspondence Analysis axis 1 scores.

Little Trout Lake, VOYA

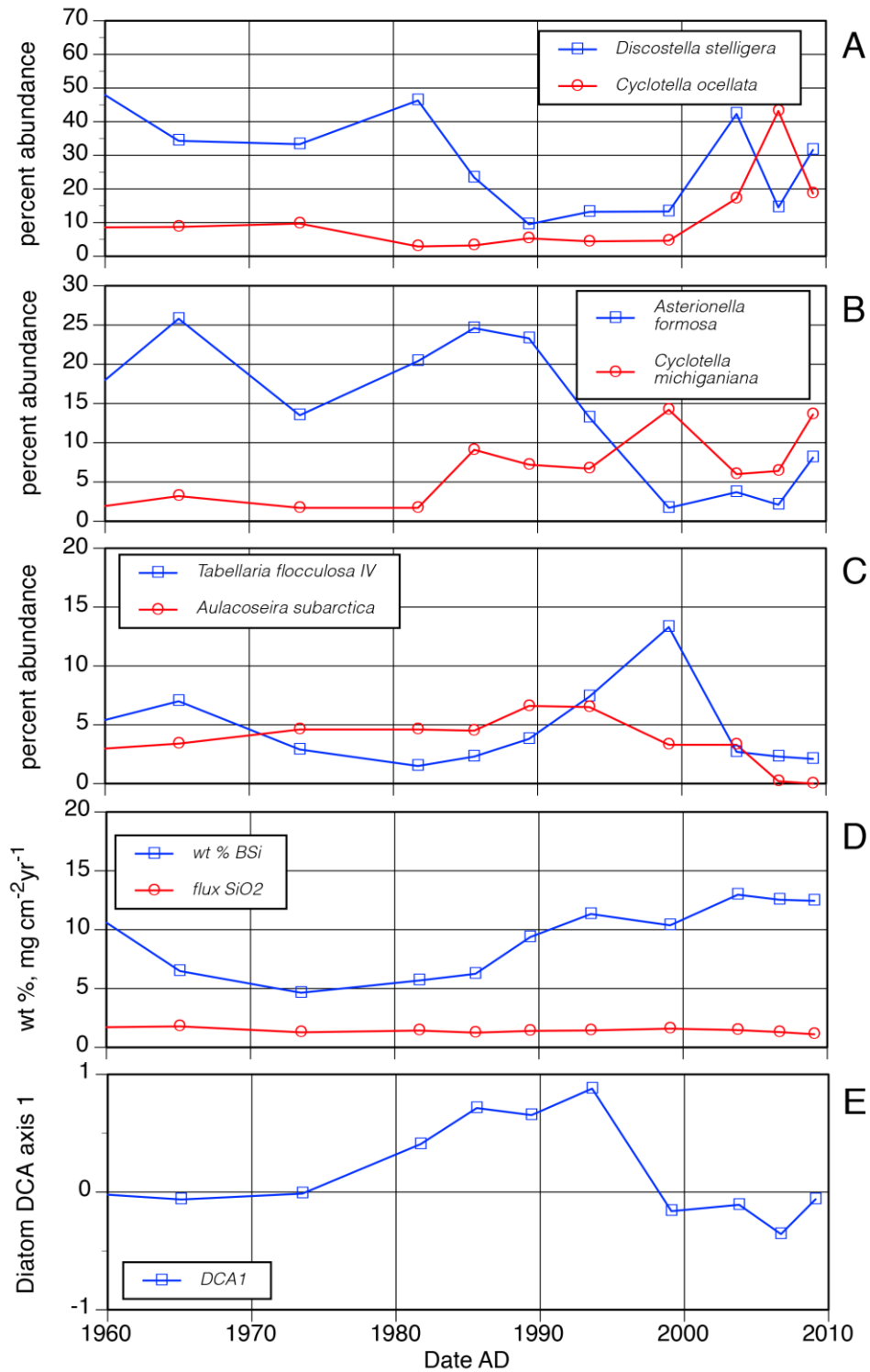


**Figure 9.** Sediment core record from Little Trout Lake, Voyageurs National Park, 1960–2010. A–C. Predominant diatom species preserved in sediment core. D. Biogenic silica content. Open squares are weight percent, and open circles are accumulation rate or flux (mg cm<sup>-2</sup> yr<sup>-1</sup>). E. Diatom community turnover based on Detrended Correspondence Analysis axis 1 scores.

Shallower lakes of ISRO (Ahmik, Harvey)—In contrast to the shallower VOYA lakes, ISRO’s Ahmik and Harvey lakes were dominated by what are known as small fragilarioid diatoms (Figures 10 and 11). These species are considered ecological generalists and can live on benthic surfaces and be entrained in the water column during mixing events as tychoplankton. In Ahmik Lake, *Staurosirella pinnata* and *Staurosira construens* have recently increased in abundance, whereas *Pseudostaurosira brevistriata* decreased in abundance. Lake Harvey saw the increase of *Staurosirella pinnata* and the morph of *Staurosira construens* SWMN#2 simultaneous with decreasing abundance of *S. construens* and *S. elliptica*. Changes in abundance of these small fragilarioid forms likely represent shifts in benthic microhabitat availability and shallow lake mixing events and may be related to the overall trend of shallow water warming shown with thermal modeling (Table 6, Appendix Figures A2 and A18).

Deeper lakes of ISRO (Siskiwit, Richie)—The two deeper lakes sampled at ISRO have strong differences in productivity, watershed area, and morphometry. Lake Richie is mesotrophic to borderline eutrophic, and its deep waters are limited to a south basin. Much of the lake remainder is relatively shallow and in recent years Richie has been experiencing mid- to late-summer cyanobacterial blooms. Siskiwit Lake is much larger and deeper than Richie, is oligotrophic, and has a coldwater lake trout and cisco fishery. The plankton diatom flora of Siskiwit is dominated by cyclotelloid species such as *Cyclotella planktonica*, *C. atomus*, *C. michiganiana*, the *C. comensis*-group, and *Discostella stelligera* (Figure 12). Patterns of change over the last 50 years include increasing abundance of *C. planktonica* and *C. atomus*, and declining abundance of *D. stelligera* and *C. michiganiana*. The abundance of these species is thought to be strongly reflective of thermal structure in the water column. Many of the taxa are found at their greatest abundance in the deep chlorophyll layer. The increased abundance of *C. planktonica* and decreased abundance of *Discostella stelligera* has been used in models to suggest that the thermocline in Siskiwit Lake has deepened significantly in recent decades (Saros et al. 2012), a conclusion that was not well supported by the thermal modeling (Table 6, Appendix Figure A40). While the trend analysis indicates a significant change in thermocline depth (Table 6), the graphical presentation (Appendix Figure A40) suggests only a subtle change that appears to be a shallowing, and not a deepening, of the thermocline. We are not able to readily resolve these conflicting results. It may be a reflection of the meteorological data used for modeling ISRO lakes being from the Duluth (Minnesota) weather station and not accurately capturing conditions on an island in Lake Superior that is over 150 miles (280 km) distant. Nonetheless, the meteorological data were good enough to result in a very good fit of the model to observed values: of all the lakes, Siskiwit had the lowest RMSE and the second highest NSE and R2 values (Table 5).

Lake Ahmik, ISRO

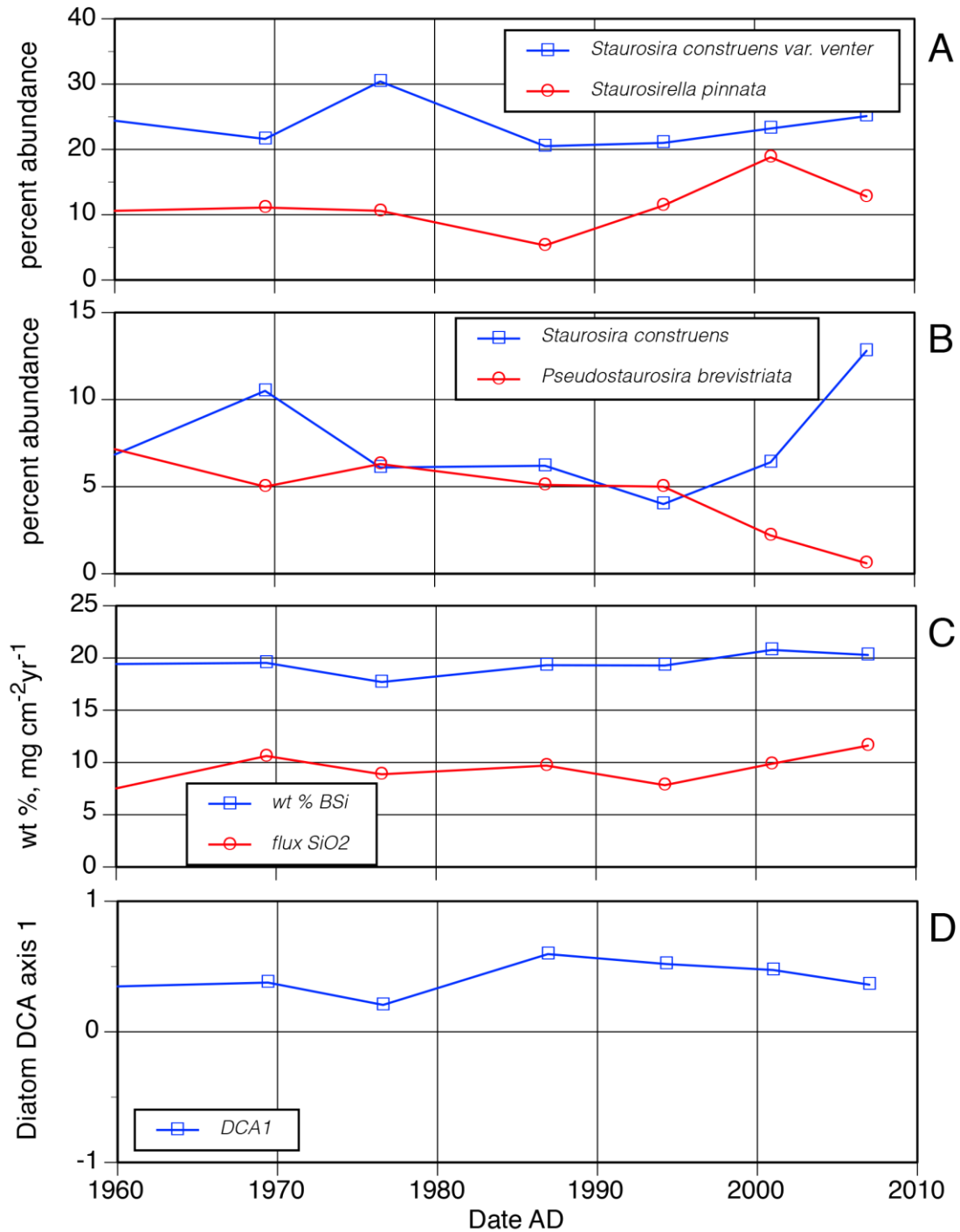


**Figure 10.** Sediment core record from Ahmik Lake, Isle Royale National Park, 1960–2010. A–B. Predominant diatom species preserved in sediment core. C. Biogenic silica content. Open squares are weight percent, and open circles are accumulation rate or flux (mg cm<sup>-2</sup> yr<sup>-1</sup>). D. Diatom community turnover based on Detrended Correspondence Analysis axis 1 scores.

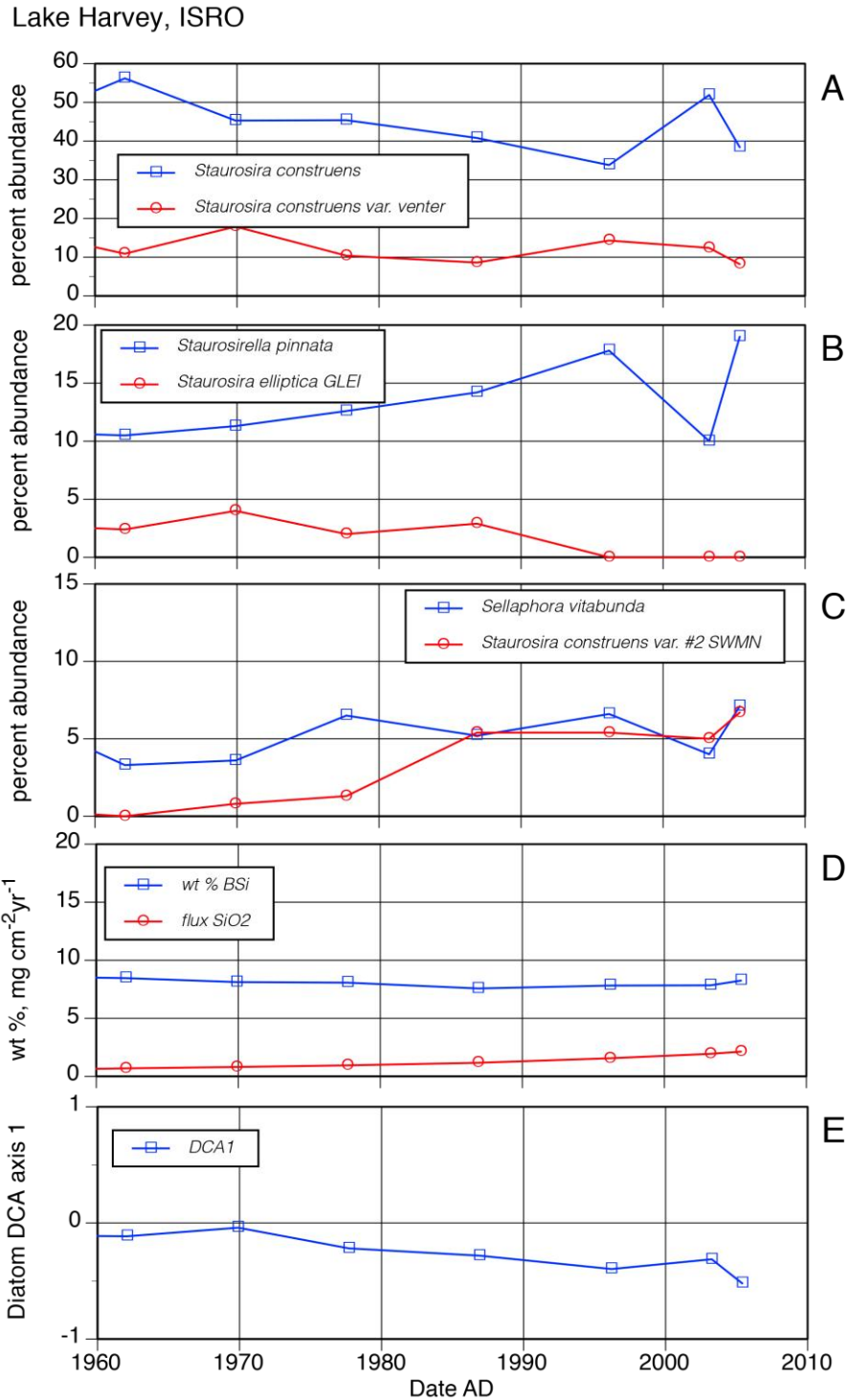


**Figure 11.** Sediment core record from Lake Harvey, Isle Royale National Park, 1960–2010. A–C. Predominant diatom species preserved in sediment core. D. Biogenic silica content. Open squares are weight percent, and open circles are accumulation rate or flux ( $\text{mg cm}^{-2}\text{yr}^{-1}$ ). E. Diatom community turnover based on Detrended Correspondence Analysis axis 1 scores.

Lake Siskiwit, ISRO

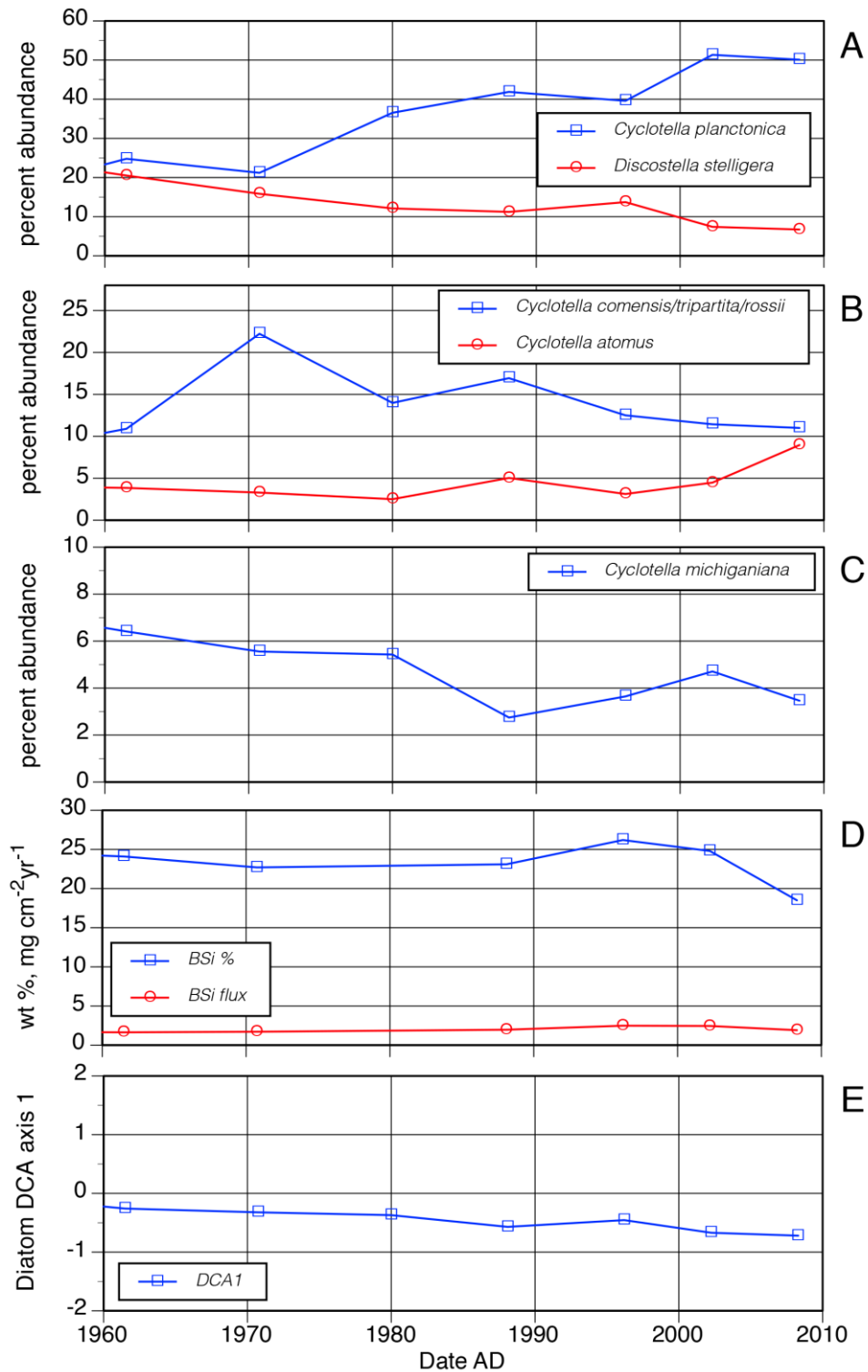


**Figure 12.** Sediment core record from Siskiwit Lake, Isle Royale National Park, 1960–2010. A–C. Predominant diatom species preserved in sediment core. D. Biogenic silica content. Open squares are weight percent, and open circles are accumulation rate or flux (mg cm<sup>-2</sup> yr<sup>-1</sup>). E. Diatom community turnover based on Detrended Correspondence Analysis axis 1 scores.

Alternatively, the mixing depth model used by Saros et al. (2012) is based on observations and experimental data from Rocky Mountain lakes and may be limited in its applicability to Siskiwit Lake. Detailed species-level ecological data on the dominant diatom plankters are needed to fully resolve the conflicting interpretations. In contrast to Siskiwit, the plankton flora preserved in the core from Lake Richie comprises a meso- to eutrophic flora of *Aulacoseira* species, *Fragilaria crotonensis*, *Asterionella formosa*, and *Tabellaria flocculosa* IIIp (Figure 13). The last fifty years have seen decreased abundances of *Aulacoseira subarctica*, *A. granulata*, and *T. flocculosa* IIIp. The period of time since the 1980s has been characterized by rapid increased abundance of *F. crotonensis* and *Asterionella formosa*. These trends have continued in repeat sediment samples taken in 2012 and suggest a combination of changes in the mixing and nutrient environment (greater availability) of Lake Richie are at play in driving recent unprecedented change in this lake (Appendix Figure A35) (Edlund et al. 2013).

### **Diatom Community Turnover**

Community turnover among diatoms based on DCA axis 1 scores varied among the eight lakes. In general, shallower lakes had lower species turnover compared to deeper lakes. For example, Ek and Peary lakes at VOYA showed only 0.22 and 0.31 SD units of turnover, respectively, between 1960 and 2010 (Figures 6 and 7). Cruiser and Little Trout lakes had DCA axis score that ranged over 0.60 and 1.04 SD units during the same time period (Figures 8 and 9). Of note is the rapid turnover in diatom communities in Little Trout Lake between the mid-1970s and mid-1990s (Figure 9). At ISRO, a similar pattern emerged with somewhat lower turnover in the shallower lakes, Harvey and Ahmik, with community turnover of 0.48 and 0.025 units, respectively (Figures 10 and 11). The larger and deeper lakes of ISRO, Siskiwit and Richie, had turnover of 0.46 and 1.14 SD units (Figures 12 and 13). Lake Richie in particular had the highest community turnover rates among the eight lakes (Figure 13), and of course this wilderness lake has been noted to have periodic cyanobacteria blooms since 2007 (Edlund et al. 2010).

### **Biogenic Silica**

Biogenic silica is reported both as a weight percent and as a flux or accumulation rate to the sediments. The latter quantity better reflects historical diatom productivity in lakes. Among the eight lakes, two patterns in biogenic silica accumulation were evident, either no change in flux or slightly increasing flux rates. Little Trout and Peary lakes at VOYA and Siskiwit and Ahmik lakes at ISRO showed no change in BSi flux between 1960 and 2010 (Figures 7, 9, 10, and 12). In contrast, Cruiser and Ek lakes at VOYA and Richie and Harvey lakes at ISRO showed modest increases in BSi accumulation rates from 1960–2010 (Figures 6, 8, 11, and 13). Although downcore sampling resolution is approximately decadal, the lakes that showed increased flux of BSi generally began increasing between samples deposited in the 1970s and 1980s with rates continuing to climb upcore. There is little consistency among lake response in historical diatom productivity beyond temporal consistency; lakes with increased BSi flux span the gamut of lake types used in this study.

Lake Richie, ISRO

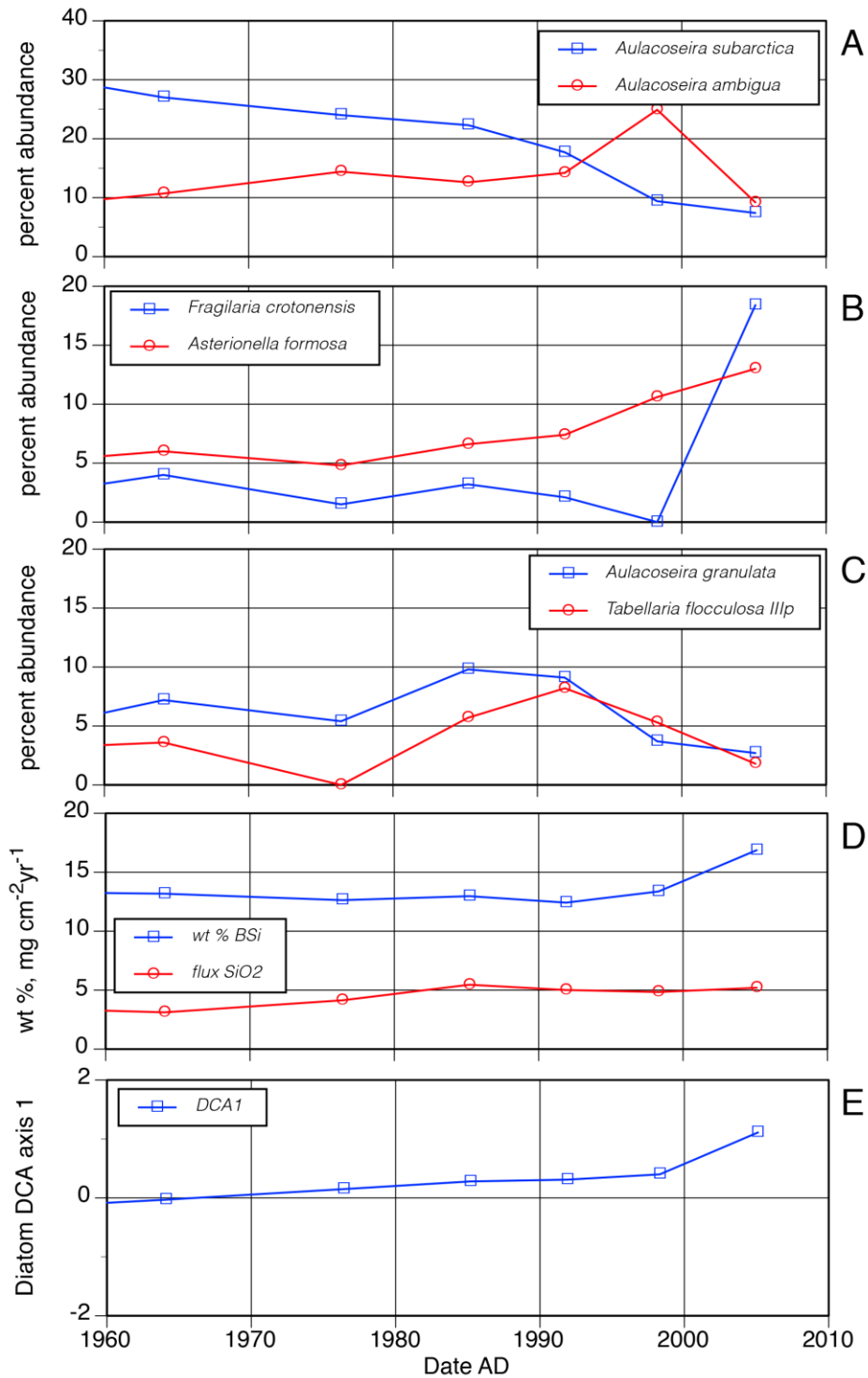


**Figure 13.** Sediment core record from Lake Richie, Isle Royale National Park, 1960–2010. A–C. Predominant diatom species preserved in sediment core. D. Biogenic silica content. Open squares are weight percent, and open circles are accumulation rate or flux (mg cm<sup>-2</sup> yr<sup>-1</sup>). E. Diatom community turnover based on Detrended Correspondence Analysis axis 1 scores.

## Summary and Recommendations

Recent climate change impacts lakes through the direct and indirect effects of shifting energy and mass inputs to lakes (Leavitt et al. 2009). Direct effects include transfer of energy to lakes by heat, radiant energy, and wind, and inputs of mass (e.g., precipitation, nutrients) directly to the lake. Indirect effects of climate are mediated through the watershed, for example by changes in transfer of energy to the lake by shading or post glacial terrestrial development or by inputs of mass from the watershed (nutrients, DOC, and mineral matter, both particulate and dissolved). In many lake-rich regions, human activities in the lake or watershed may mask changes driven by climate. Here we focus on changes in wilderness lakes where lake use by humans is minimal and watershed disturbances are primarily limited to natural forces. To explore potential climate impacts on wilderness boreal lakes, we paired paleolimnological analysis of sediment cores with thermal modeling of eight lakes in ISRO and VOYA to link historical lake thermal structure with biological response.

For each lake the program MINLAKE2012 was used to develop depth-temperature profiles and ice cover at daily time steps for the time period 1962–2011. Meteorological data were used from International Falls, Minnesota, for Voyageurs National Park lakes and from Duluth, Minnesota, for Isle Royale National Park lakes. Model output was extracted and post-processed with an MS Excel interface to compare modeled thermal profiles with observed thermal profiles based on GLKN monitoring data collected variously from 2006/2007–2011. Nash-Sutcliffe coefficient of efficiency (NSE) values demonstrated good agreement between modeled and monitored depth-temperature profiles, with greater discordance in shallow lake results. Although other thermal models do exist for lakes (Hadley et al. 2013), we feel MINLAKE2012 is appropriate and well-suited for the GLKN lakes and could be applied to other lakes and for forecasting future lake responses. The ultimate aim is to provide a means of predicting from simple morphometric parameters the likely sensitivity of different lake types to future climate forcing, and to enable managers to better target their management and monitoring efforts. We did not use the DO capabilities of MINLAKE2012 in this pilot project. However, we recognize that changes in DO may be a primary driver of ecological change in lakes with altered thermal structure due to climate warming. This important consideration warrants continued research.

Specific MINLAKE2012 model results were extracted and further analyzed with scripts written in the R statistical framework to determine trends in shallow and deep water temperatures and the behavior and timing of water column gradients over two time periods (1962–1986, 1987–2011). The most common significant trend was increased summer shallow-water temperatures for all eight lakes. The next significant trend was, for the deep lakes, an increase in the frequency and duration of thermal gradients equaling or exceeding 2 °C or 3 °C per meter. These trends are likely key for understanding how changes in thermal structure may have impacted lake biology during the simulation period and are similar to other temperate lake thermal model results (Hadley et al. 2013). Surprisingly, there were no significant trends identified among the lakes in timing or duration of ice cover.

Biological changes in the lakes between 1960 and 2010 differed among the shallow and deep lakes and also between the two park units; the latter difference most likely reflects differences in lake type and water chemistry between the parks. Regardless, many taxa shifted in abundance, especially after the 1980s. Shallow lakes showed a combination of primary shifts in benthic or tychoplanktonic taxa and secondary shifts in planktonic species. In VOYA shallow lakes, the enigmatic taxon *Eunotia zasuminensis* declined in abundance supporting previous reports of slight increases in shallow lake pH, while shifts in other species indicated that mixing and habitat availability may be shifting in concert in recent years. At ISRO, the small benthic and tychoplanktonic fragilarioid diatoms were the main responders in Ahmik and Harvey lakes; this may reflect the modeled change in number of days with stratification, i.e., the lakes are more well-mixed, possibly in relation to increased wind over Lake Superior (Desai et al. 2009).

Diatom shifts in the deep lakes appear to track changes in thermal structure as evidenced by shifts in the cyclotelloid species from the genera *Cyclotella* and *Discostella*. These diatoms are often found in the deep chlorophyll layer and reside near the thermocline. Other diatom species shown to change in the deep lakes are more likely responding to length of mixing time and nutrient supplies. In Cruiser, Little Trout, and Siskiwit lakes, it is the cyclotelloid diatoms that have shifted and we also note that these lakes are identified with significant changes in the thermal-depth gradient in the last 30 years of modeled results. Lake Richie at ISRO showed changes in many diatom species that suggest increased nutrient availability and possibly changes in spring mixing.

Diatom community turnover is accentuated in the deeper lakes compared to the shallow lake sediment records of VOYA and ISRO. The greatest turnover is noted in ISRO's Lake Richie, where noxious cyanobacterial blooms have been commonplace since the mid-2000s. The less productive deep lakes (Cruiser, Siskiwit, Little Trout) also show higher community turnover rates than most of the shallower lakes. Subtle shifts in accumulation rates of biogenic silica, a proxy for diatom productivity, hint that some lakes may be becoming more productive in the last few decades (Cruiser, Ek, Richie, Harvey). There is no apparent pattern among this set of lakes as they represent a crosscut of all lake types we see in these two park units.

Based on this preliminary thermal modeling exercise on GLKN lakes, we offer the following recommendations for further application and improvements of lake thermal models and paleoecological analysis for determining lake response to climate drivers:

1. Meteorological data—due to limitations on available model-ready data, we applied meteorological data from Duluth, Minnesota, to lakes on Isle Royale National Park, two sites that are over 150 miles apart. Although the lake models performed reasonably well on Isle Royale lakes, it would be valuable to consider meteorological data from Thunder Bay, Ontario, and/or data taken directly at Isle Royale and compare their model results to those generated using Duluth meteorological data. Assembling and compiling meteorological data is a sizeable task in developing thermal models and should be considered a measureable outcome in any additional application or refinement of the MINLAKE models in NPS lakes.

2. Data analysis and model output—thermal model output in this preliminary modeling exercise was subjected to a straightforward test of differences between the first half and second half of a 50-year (1962–2011) time series using the Mann-Whitney U test. There are many other statistical approaches which could be applied to assess trends and differences within and among model output including seasonal Kendall or Mann-Kendall tests. Additional analyses should be considered in future applications of thermal modeling to NPS lakes.
3. A powerful application of lake thermal models is their use in forecasting lake response under future meteorological conditions and climate scenarios. The eight lake models developed in this project for VOYA and ISRO lakes are good starting points for developing lake forecasts and management response plans. The additional of more lake models is also appropriate as only eight lakes having been modeled did not allow patterns of lake susceptibility to climate drivers based on readily available lake data and distribution (e.g., lake area:watershed area or lake geometric ratio) to be fully explored.
4. Information from the initial modeling exercise suggests that some lake types or in-lake habitats in the boreal region may be more responsive to climate drivers. This includes warming of shallow reaches in all lake types and increased frequency and duration of thermal gradients equaling or exceeding 2 °C or 3 °C per meter in deeper lakes. Additional targeted monitoring is a reasonable response to these modeled trends. More regular sampling (or continuous data loggers), especially of lake thermal structure in deep water stations and nearshore stations might be coupled with some biological sampling to better understand species and community-level ecology of things, such as diatom communities, to climate drivers. Some of this sampling has been proposed recently in other NPS proposals. Lakes targeted for additional monitoring might include those identified in this study or that are similar, which are likely candidates for greater climate response.
5. Sediment cores studied in this project were initially analyzed as part of GLKN’s diatom monitoring program. Cores from GLKN index lakes were earlier collected, radiometrically dated, and subjected to paleolimnological analysis for geochemistry and diatom communities. However, the diatom communities were only analyzed at approximately decadal resolution for the last 150 years, so for the modeled thermal hindcasts from 1962–2011, we usually had only 4–6 diatom samples with which to evaluate coherence to thermal models. If additional studies are made that explore these relationships, higher resolution analysis of sediment cores is necessary to allow more rigorous comparison of historical biological changes with hindcasted lake thermal models. Current NPS proposals that have been submitted to work on ISRO lakes include this modified approach.
6. Additional approaches might also be considered in analyzing diatom community change. Here the DCA scores estimated species turnover. A better understanding of species-level ecology done through modern sampling and experimentation (see Saros et al. 2012) would provide a more mechanistic understanding of how diatom communities in GLKN boreal lakes respond to climate drivers. These data could then inform model development (e.g., Saros et al. 2012) to use specific taxa to as indicators of changing thermal structure.

Alternatively, focus or indicator species could also be tracked in sediment assemblages, both historical and as part of regular GLKN monitoring (Edlund et al. 2011), and with additional lakes more clear patterns of historical response may along broader patterns among lakes to be seen.

## Literature Cited

- Adrian, R., C. M. O'Reilly, H. Zagarese, S. B. Baines, D. O. Hessen, and W. Keller. 2009. Lakes as sentinels of climate change. *Limnology and Oceanography* 54(6):2283–2297.
- Anderson, N. J. 2000. Miniview: Diatoms, temperature and climatic change. *European Journal of Phycology* 35(4):307–314.
- Appleby, P. G., and F. Oldfield. 1978. The calculation of lead– 210 dates assuming a constant rate of supply of unsupported  $^{210}\text{Pb}$  to the sediment. *Catena* 5:1–8.
- Bauer, D. F. 1972. Constructing confidence sets using rank statistics. *Journal of the American Statistical Association* 67:687–690.
- Binford, M. W. 1990. Calculation and uncertainty analysis of 210-Pb dates for PIRLA project lake sediment cores. *Journal of Paleolimnology* 3:253–267.
- Camburn, K. E., and D. F. Charles. 2000. Diatoms of Low-Alkalinity Lakes in the Northeastern United States. Academy of Natural Sciences of Philadelphia, Special Publication 18. Academy of Natural Sciences of Philadelphia, Philadelphia, Pennsylvania.
- Camburn, K. E., J. C. Kingston, and D. F. Charles, editors. 1984–1986. PIRLA diatom iconograph. PIRLA Unpublished Report Series, Report 3. Electric Power Research Institute, Palo Alto, California.
- Camburn, K. E., R. L. Lowe, and D. L. Stoneburner. 1978. The haptobenthic diatom flora of Long Branch Creek, South Carolina. *Nova Hedwigia* 30:149–279.
- Carlson, R. E. 1977. A trophic state index for lakes. *Limnology and Oceanography* 22:361–369.
- Cleveland, W. S. 1979. Robust locally weighted regression and smoothing scatterplots. *Journal of the American Statistical Association* 74:829–836.
- Cleveland, W. S. 1981. LOWESS: A program for smoothing scatterplots by robust locally weighted regression. *The American Statistician* 35: 54.
- Collins, G. B., and R. G. Kalinsky. 1977. Studies on Ohio diatoms: I. Diatoms of the Scioto River Basin. II. Referenced checklist of diatoms from Ohio. *Bulletin of the Ohio Biological Survey—new series* 5(3):1–76.
- Conley, D. J., and C. L. Schelske. 2001. 14. Biogenic silica. Pages 281–293 in J. P. Smol, H. J. B. Birks, and W. M. Last, editors. *Tracking Environmental Change Using Lake Sediments. Volume 3: Terrestrial, Algal, and Siliceous Indicators*. Kluwer Academic Publishers, Dordrecht, The Netherlands.

- Cumming, B. F., S. E. Wilson, R. I. Hall, and J. P. Smol. 1995. Diatoms from British Columbia (Canada) lakes and their relationship to salinity, nutrients and other limnological variables. *Bibliotheca Diatomologica* 31:1–207.
- Dean, W. E. 1974. Determination of carbonate and organic matter in calcareous sediments and sedimentary rocks by loss on ignition: Comparison with other methods. *Journal of Sedimentary Petrology* 44:242–248.
- DeMaster, D. J. 1979. The marine budgets of silica and  $^{32}\text{Si}$ . Dissertation, Yale University, New Haven, Connecticut.
- DeMaster, D. J. 1981. The supply and accumulation of silica in the marine environment. *Geochim. Cosmochim. Acta* 45:1715–1732.
- Desai, A. R., J. A. Austin, V. Bennington, and G. A. McKinley. 2009. Stronger winds over a large lake in response to weakening air-to-lake temperature gradient. *Nature Geoscience* 2:855–858.
- Edlund, M. B., J. M. Ramstack, J. Elias, P. Leavitt, and D. R. Engstrom. 2010. Unprecedented change in national park lakes: ISRO's Lake Richie. Page 32 *in* Eighth Annual Western Great Lakes Research Conference. Available at: [www.cesu.umn.edu/prod/groups/cfans/@pub/@cfans/@cesu/documents/asset/cfans\\_asset\\_367484.pdf](http://www.cesu.umn.edu/prod/groups/cfans/@pub/@cfans/@cesu/documents/asset/cfans_asset_367484.pdf).
- Edlund, M. B., J. M. Ramstack, D. R. Engstrom, J. E. Elias, and B. Moraska Lafrancois. 2011. Biomonitoring using diatoms and paleolimnology in the western Great Lakes national parks. Natural Resource Technical Report NPS/GLKN/NRTR—2011/447. National Park Service, Fort Collins, Colorado.
- Edlund, M. B., J. Ramstack Hobbs, and D. R. Engstrom. 2013. Biomonitoring using diatoms and paleolimnology in the western Great Lakes national parks: 2011/2012 summary. Natural Resource Technical Report NPS/GLKN/NRTR—2013/814. National Park Service, Fort Collins, Colorado.
- Engstrom, D., B. A. Monson, S. J. Balogh, E. B. Swain, and K. R. Parson. 2012. Resolving the cause of the recent rise of fish-mercury levels in the western Great Lakes region. Final Research Report of the 2009 Great Lakes Air Deposition Program, Great Lakes Commission, Final Version 1.1.
- Fallu, M.-A., N. Allaire, and R. Peinitz. 2000. Freshwater diatoms from northern Québec and Labrador (Canada). Species-environment relationships in lakes of boreal forest, forest-tundra and tundra regions. *Bibliotheca Diatomologica* 45:1–200.
- Fang, X., and H. G. Stefan. 1996. Development and validation of the water quality model MINLAKE96 with winter data. Project Report 390 (unpublished). St. Anthony Falls Laboratory, University of Minnesota, St. Paul, Minnesota.

- Fang, X., and H. G. Stefan. 1997. Simulated climate change effects on dissolved oxygen characteristics in ice-covered lakes. *Ecological Modelling* 103:209–229.
- Fang, X., S. R. Alam, P. Jacobson, D. Pereira, and H. Stefan. 2010. Simulations of water quality in cisco lakes in Minnesota. Unpublished report prepared for the Minnesota Department of Natural Resources, Minneapolis, Minnesota.
- Ford, D. E., and H. G. Stefan. 1980. Thermal predictions using integral energy model, *Journal of the Hydraulics Division* 106:39–55.
- Gorham, E., and Boyce, F. M. 1989. Influence of lake surface area and depth upon thermal stratification and the depth of the summer thermocline. *Journal of Great Lakes Research* 15(2): 233–245.
- Gu, R., and H. G. Stefan. 1990. Year-round temperature simulation of cold climate lakes. *Cold Regions Science and Technology*. 18:147–160.
- Hadley, K. R., A. M. Paterson, E. A. Stainsby, N. Michelutti, H. Yao, J. A. Rusak, R. Ingram, C. McConnell, and J. P. Smol. 2013. Climate warming alters thermal stability but not stratification phenology in a small north-temperate lake. *Hydrological Processes* DOI: 10.1002/hyp.10120.
- Heiskary, S. A., and C. B. Wilson. 1988. Minnesota lake water quality assessment report. Minnesota Pollution Control Agency, St. Paul, Minnesota.
- Hill, M. O., and H. G. Gauch. 1980. Detrended correspondence-analysis: An improved ordination technique. *Vegetatio* 42:47–58.
- Hollander, M., and D. A. Wolfe. 1973. *Nonparametric Statistical Methods*. John Wiley and Sons, New York, New York.
- Hondzo, M., and H. G. Stefan. 1992. Water temperature characteristics of lakes subjected to climate change. Unpublished Project Report No. 329. St. Anthony Falls Hydrologic Laboratory, University of Minnesota, Minneapolis, Minnesota.
- Hondzo, M., and H. G. Stefan. 1993. Lake water temperature simulation model. *Journal of Hydraulic Engineering* 119:1251–1273.
- Hustedt, F. 1927–1966. Die Kieselalgen Deutschlands, Österreichs und der Schweiz mit Berücksichtigung der übrigen Länder Europas sowie der angrenzenden Meeresgebiete. In Dr. L. Rabenhorst's *Kryptogrammen-Flora von Deutschland, Österreich und der Schweiz*. Akademische Verlagsgesellschaft Geest und Portig K.-G., Leipzig.
- Hustedt, F. 1930. Die Süßwasserflora Mitteleuropas. Heft 10. 2nd edition. Bacillariophyta (Diatomeae). A. Pascher, editor. Verlag von Gustav Fischer, Germany.

- Jensen, O. P., B. J. Benson, J. J. Magnuson, V. M. Card, M. N. Futter, P. A. Soranno, and K. M. Stewart. 2007. Spatial analysis of ice phenology trends across the Laurentian Great Lakes region during a recent warming period. *Limnology and Oceanography* 52:2013–2026.
- Johnson, S. L., and H. G. Stefan. 2006. Indicators of climate warming in Minnesota: Lake ice covers and snowmelt runoff. *Climatic Change* 75:421–453.
- Koppen, J. D. 1975. A morphological and taxonomic consideration of Tabellaria (Bacillariophyceae) from the northcentral United States. *Journal of Phycology* 11:236–244.
- Krammer, K., and H. Lange-Bertalot. 1986–1991. Bacillariophyceae. *In* H. Ettl, J. Gerloff, H. Heynig, and D. Mollenhauer, editors. *Süßwasser flora von Mitteleuropa, Band 2/1–4*. Gustav Fischer Verlag: Stuttgart, Germany and New York.
- Leavitt, P. R., S. C. Fritz, N. J. Anderson, and 14 others. (2009). Paleolimnological evidence of the effects on lakes of energy and mass transfer from climate and humans. *Limnology and Oceanography* 54:2330–2348
- McKnight, R. 1991. QuikChem method 10-114-27-1-A. Determination of silica in waters by flow injection analysis, 0.2 to 20.0 mg SiO<sub>2</sub>/L. Lachat Instruments, 6645 West Mill Road, Milwaukee, Wisconsin 53218.
- Megard, R. O., W. S. Combs Jr., P. D. Smith, and A. S. Knoll. 1979. Attenuation of light and daily integral rates of photosynthesis attained by planktonic algae. *Limnology and Oceanography* 24:1038–1050.
- Monteith, D. T., J. L. Stoddard, C. D. Evans, and 10 others. 2007. Dissolved organic carbon trends resulting from changes in atmospheric deposition chemistry. *Nature* 450:537–541.
- Moriasi, D. N., J. G. Arnold, M. W. Van Liew, R. L. Bingner, R. D. Harmel, and T. L. Veith. 2007. Model evaluation guidelines for systematic quantification of accuracy in watershed simulations. *Transactions of the ASABE (American Society of Agricultural and Biological Engineers)* 50(3):885–900.
- Patrick, R., and C. W. Reimer. 1966. The diatoms of the United States, exclusive of Alaska and Hawaii, Volume 1–Fragilariaceae, Eunotiaceae, Achnanthaceae, Naviculaceae. Academy of Natural Sciences of Philadelphia Monograph No. 13. Academy of Natural Sciences of Philadelphia, Philadelphia, Pennsylvania.
- Patrick, R., and C. W. Reimer. 1975. The diatoms of the United States, exclusive of Alaska and Hawaii, Volume 2, Part 1–Entomoneidaceae, Cymbellaceae, Gomphonemaceae, Epithemaceae. Academy of Natural Sciences of Philadelphia Monograph No. 13. Academy of Natural Sciences of Philadelphia, Philadelphia, Pennsylvania.
- R Core Development Team. 2013. R: A language and environment for statistical computing. R Foundation for Statistical Computing, Vienna, Austria. Available at: [www.R-project.org](http://www.R-project.org).

- Ramstack, J., M. Edlund, D. Engstrom, B. Moraska Lafrancois, and J. Elias. 2008. Diatom monitoring protocol, version 1.0. National Park Service, Great Lakes Inventory and Monitoring Network. Natural Resource Report NPS/GLKN/NRR—2008/068. National Park Service, Fort Collins, Colorado.
- Reavie, E. D., and J. P. Smol. 1998. Freshwater diatoms from the St. Lawrence River. *Bibliotheca Diatomologica* 41:1–137.
- Riley, M., and H. G. Stefan. 1988. MINLAKE: A dynamic lake water quality simulation model. *Ecol. Model.* 43:155–182.
- Rühland, K., A. M. Paterson, and J. P. Smol. 2008. Hemispheric-scale patterns of climate-related shifts in planktonic diatoms from North America and European lakes. *Global Change Biology* 14:1–15.
- Saros, J. E., J. R. Stone, G. Pederson, K. E. H. Slemmons, T. Spanbauer, A. Schliep, D. Cahl, C. E. Williamson, and D. E. Engstrom. 2012. Climate-induced changes in lake ecosystem structure inferred from coupled neo- and paleo-ecological approaches. *Ecology* 93:2155–2164. Available at: <http://dx.doi.org/10.1890/11-2218.1>.
- Serieyssol, C. A., M. B. Edlund, and L. W. Kallemeyn. 2009. Impacts of settlement, damming, and hydromanagement in two boreal lakes: A comparative paleolimnological study. *Journal of Paleolimnology* 42:497–513.
- Smol, J. P., A. P. Wolfe, H. H. Birks, and 23 others. 2005. Climate-driven regime shifts in the biological communities of arctic lakes. *Proceedings of the National Academy of Sciences of the United States of America*. 102:4397–4402. Available at: <http://www.pnas.org/content/102/12/4397.full>.
- Stefan, H. G., and X. Fang. 1994. Dissolved oxygen model for regional lake analysis. *Ecological Modelling* 71:37–68.
- Stefan, H. G., M. Hondzo, X. Fang, J. G. Eaton, and J. H. McCormick. 1996. Simulated long-term temperature and dissolved oxygen characteristics of lakes in the north-central United States and associated fish habitat limits. *Limnology and Oceanography* 41(5):1124–1135.
- Wagner, C., and R. Adrian. 2009. Cyanobacteria dominance: Quantifying the effects of climate change. *Limnology and Oceanography* 54:2460–2468.
- Wetzel, R.G. 1975. *Limnology*. W. B. Saunders Company, Philadelphia, Pennsylvania.
- Wright, H. E. 1991. Coring tips. *Journal of Paleolimnology* 6:37–49.



## **Appendix A. Thermal model output for study lakes.**

Lakes are arranged alphabetically. Within the set for each lake, figures are arranged in the following order:

- Observed and modeled temperature profiles
- Modeled mean summer temperatures
- Modeled temperature gradients
- Modeled ice-covered and open-water seasons

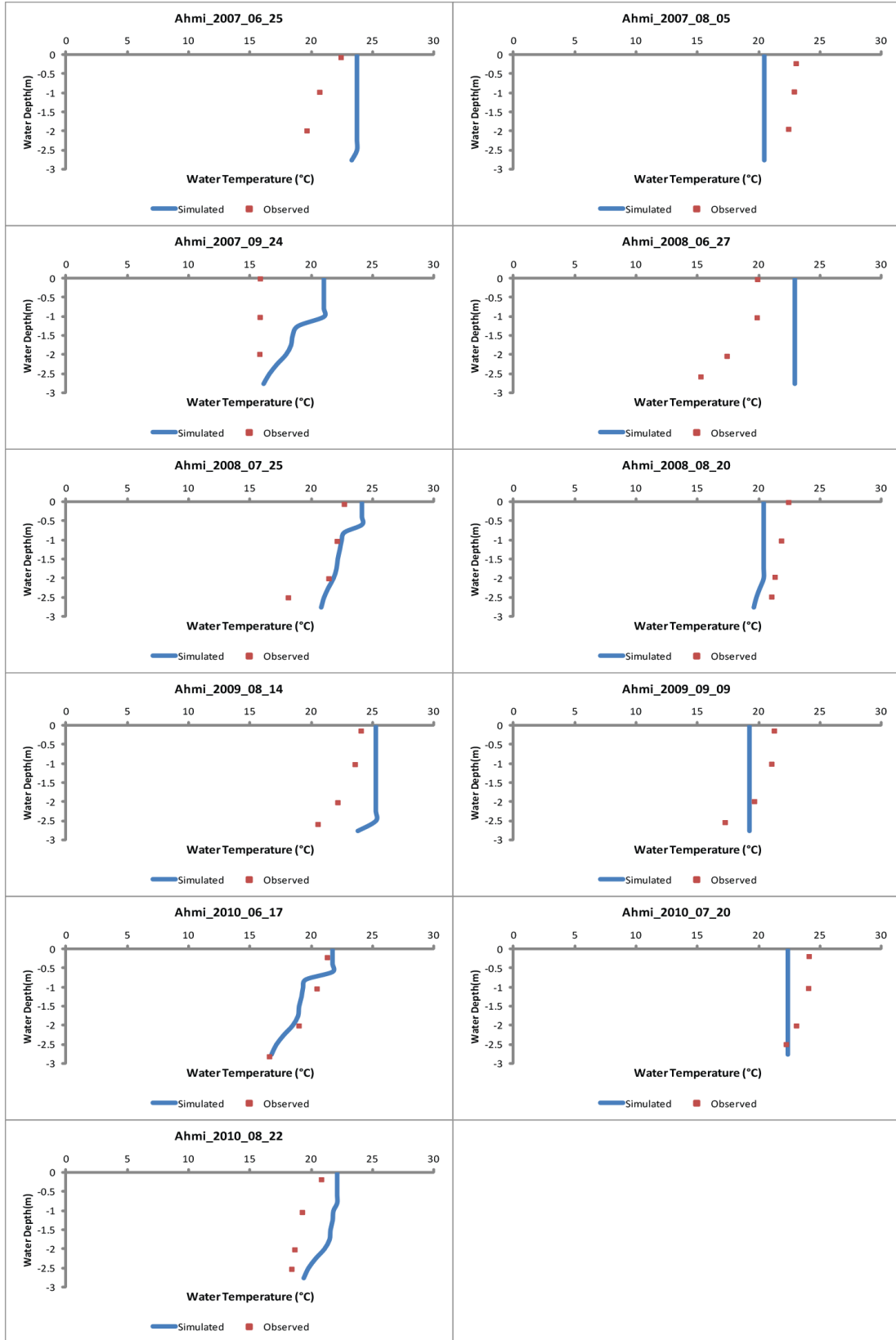
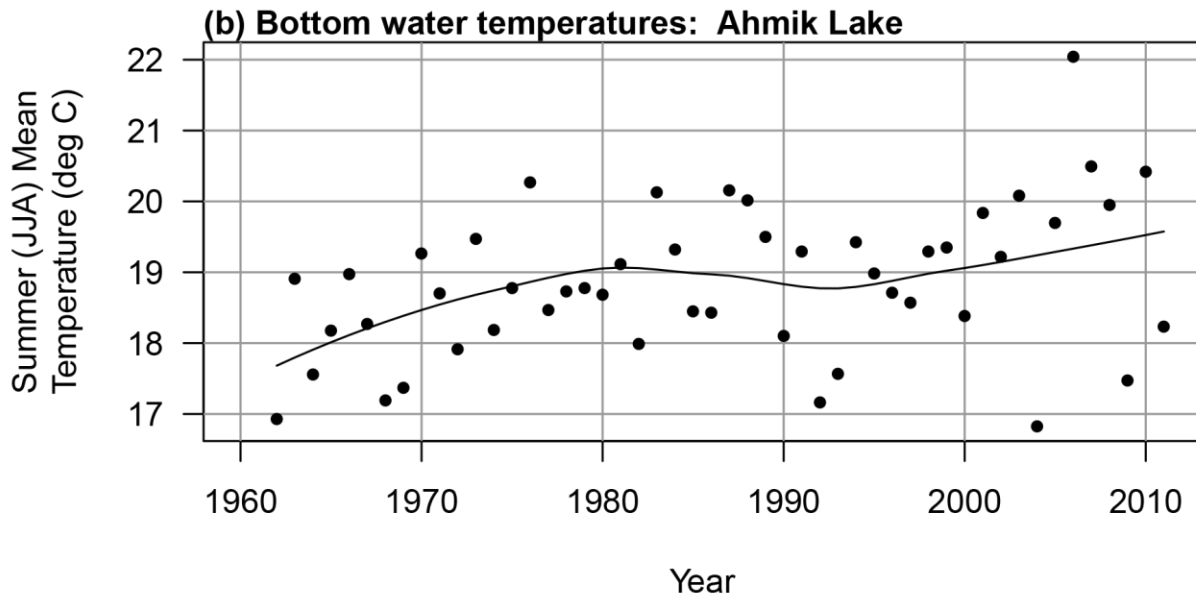
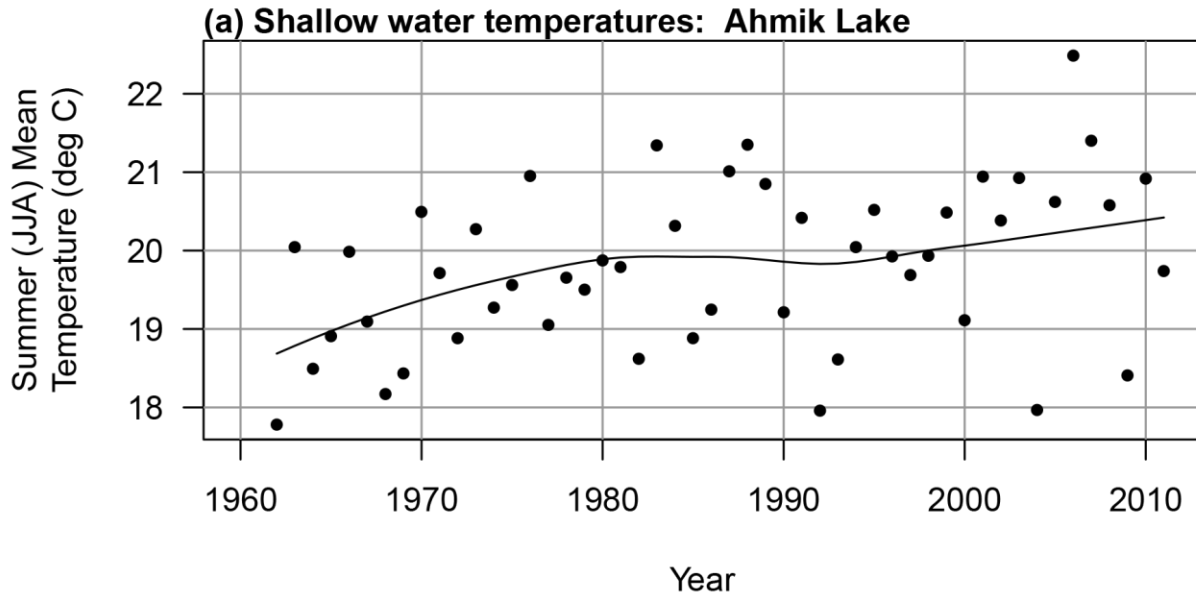
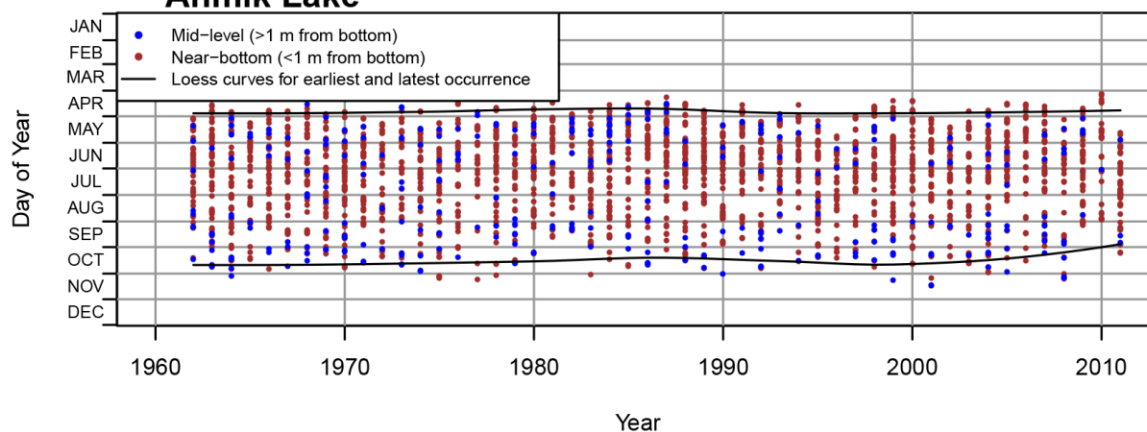


Figure A1. Ahmik Lake (Isle Royale): Observed and modeled temperature profiles, 2007–2010.

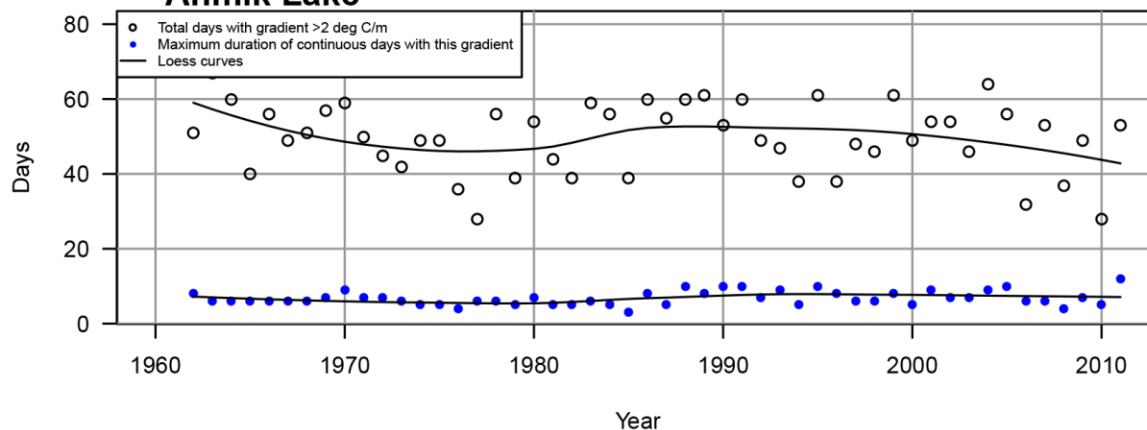


**Figure A2.** Ahmik Lake (Isle Royale): Modeled mean summer temperatures for (a) shallow and (b) bottom waters, 1962–2011.

**(a) Days of year with thermal gradient >2 deg C/m:  
Ahmik Lake**



**(b) Number of days with thermal gradient >2 deg C/m:  
Ahmik Lake**



**(c) Mean depth of gradient >2 deg C/m in summer (JJA):  
Ahmik Lake**

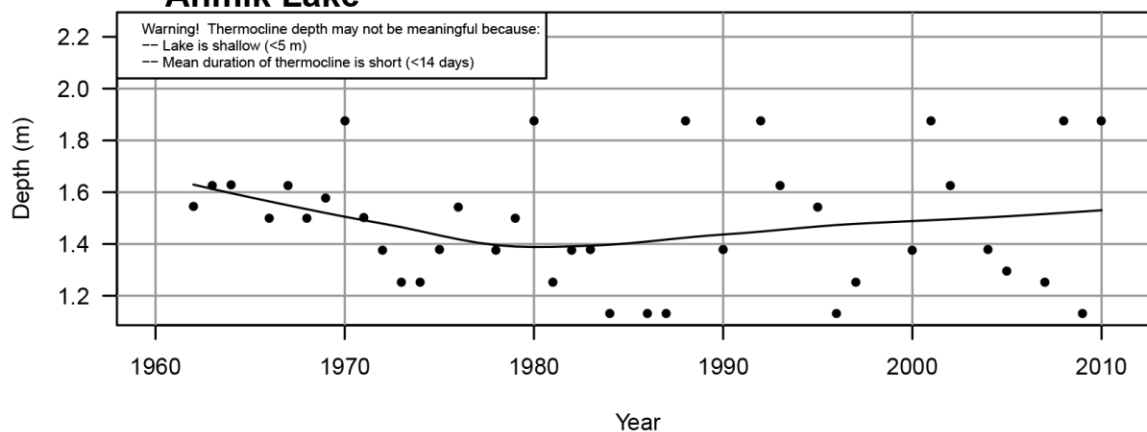
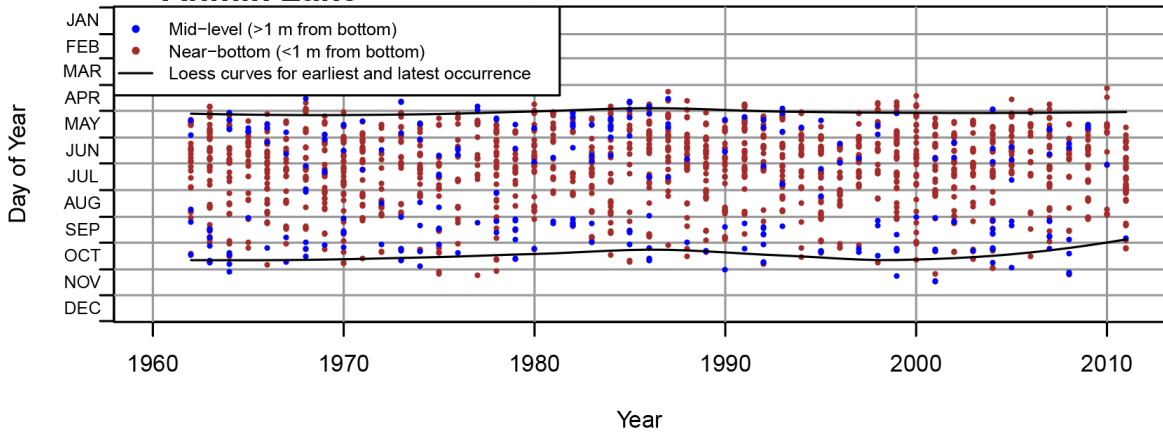
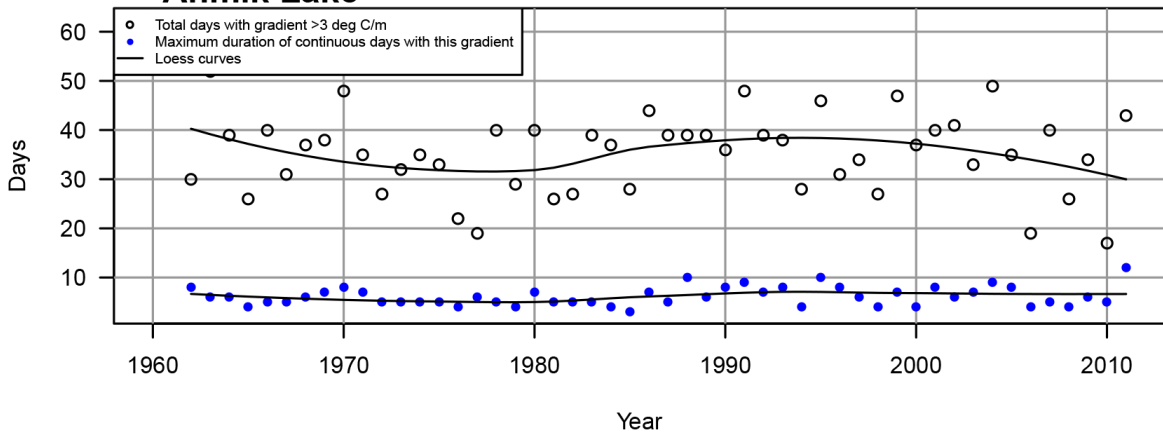


**Figure A3.** Ahmik Lake (Isle Royale): Modeled (a) dates, (b) duration, and (c) mean summer depth of thermal gradients  $\geq 2^\circ\text{C}$  per meter, 1962–2011.

**(a) Days of year with thermal gradient >3 deg C/m:  
Ahmik Lake**



**(b) Number of days with thermal gradient >3 deg C/m:  
Ahmik Lake**



**(c) Mean depth of gradient >3 deg C/m in summer (JJA):  
Ahmik Lake**

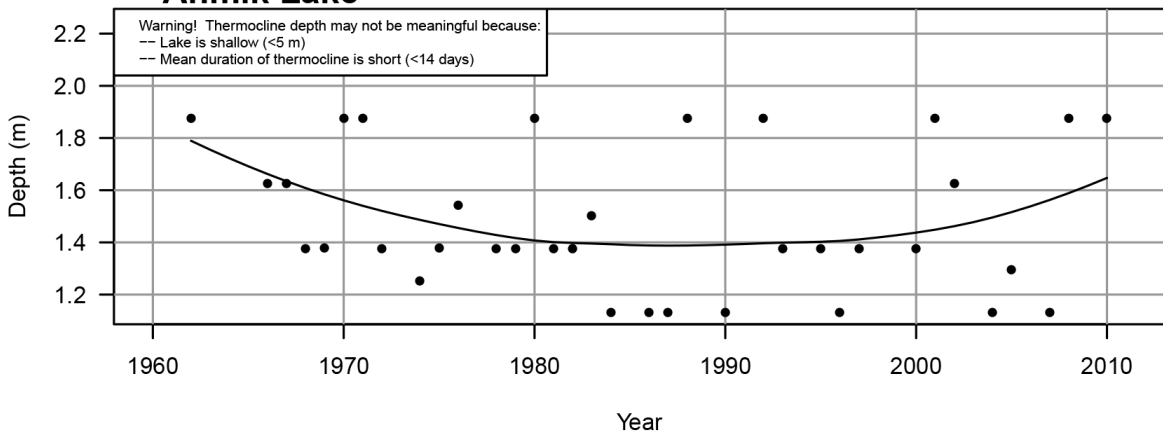


**Figure A4.** Ahmik Lake (Isle Royale): Modeled (a) dates, (b) duration, and (c) mean summer depth of thermal gradients  $\geq 3^{\circ}\text{C}$  per meter, 1962–2011.

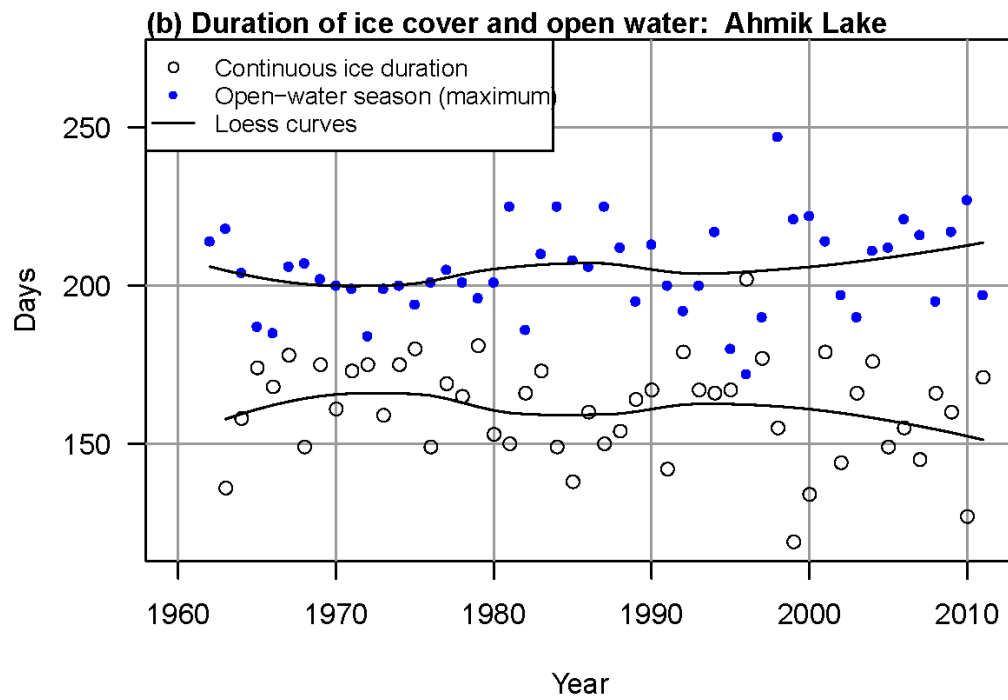
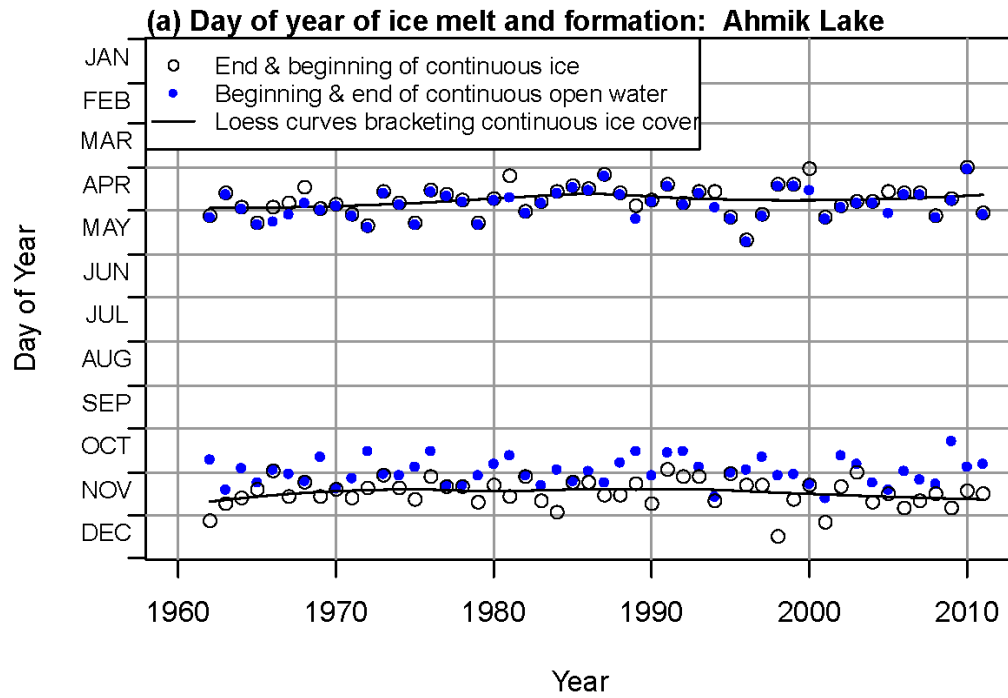


**Figure A5.** Ahmik Lake (Isle Royale): Modeled (a) dates and (b) duration of ice-covered and open-water seasons, 1962–2011.

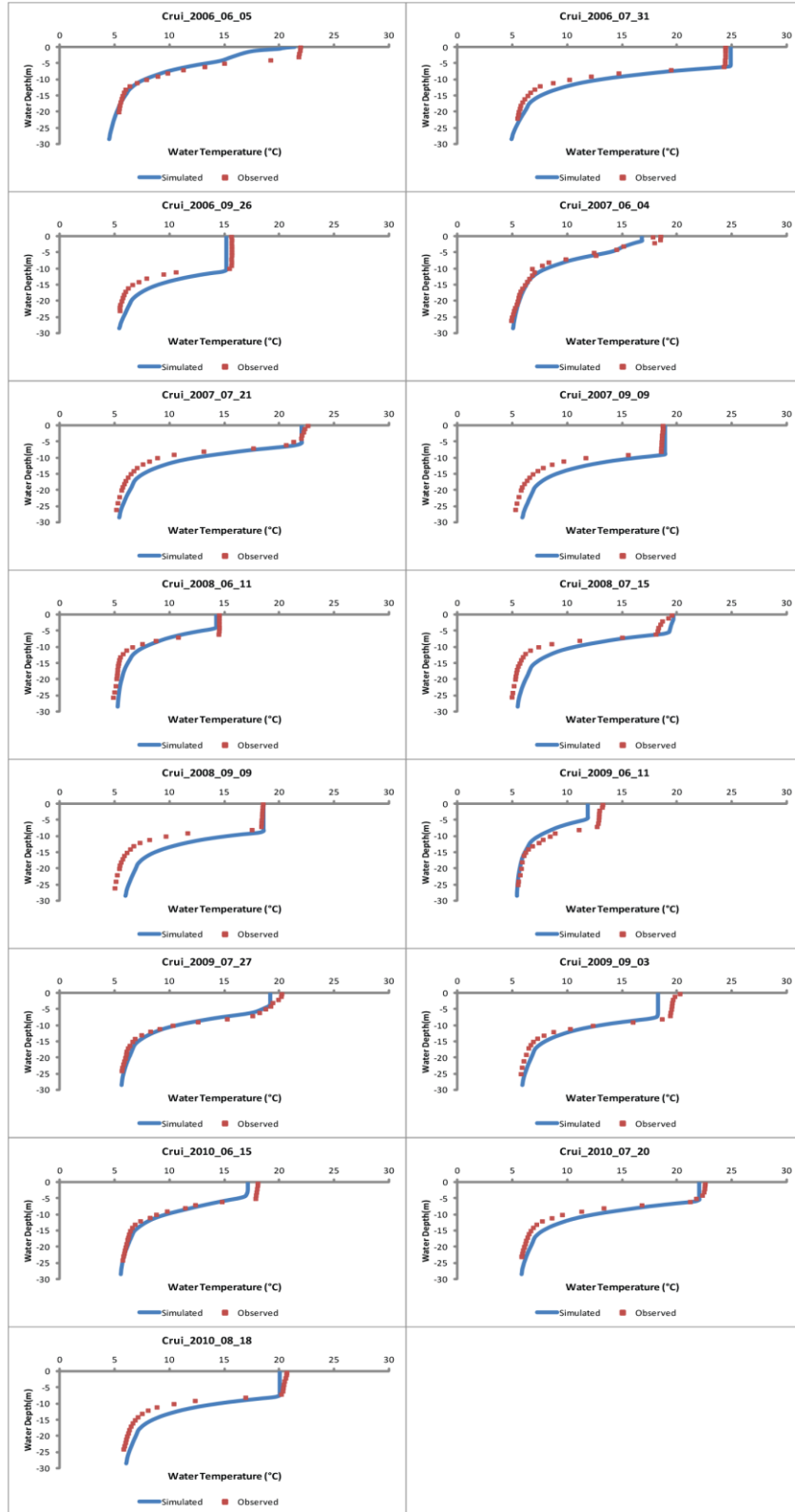
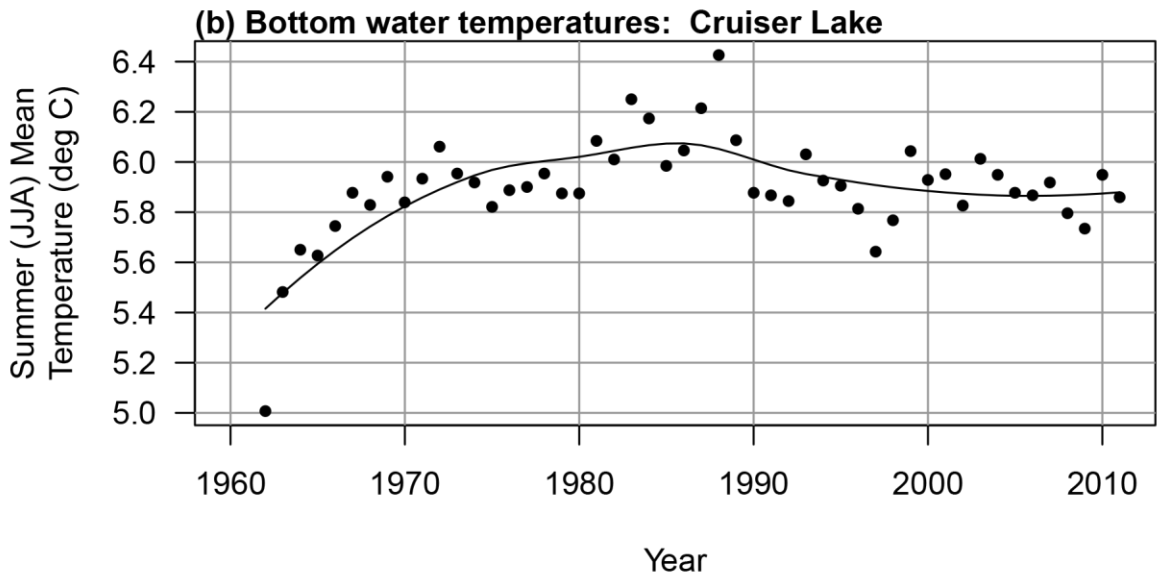
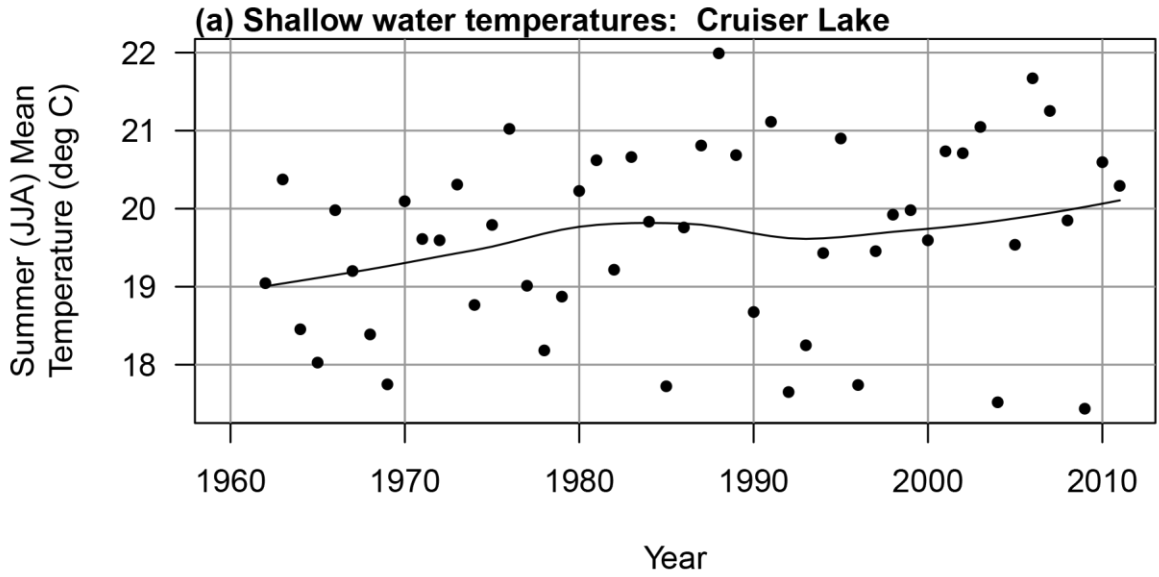
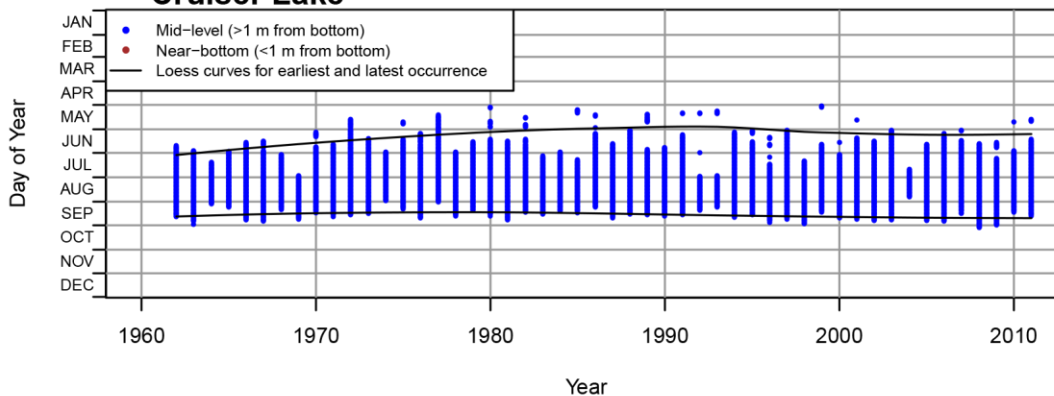


Figure A6. Cruiser Lake (Voyageurs): Observed and modeled temperature profiles, 2006–2010.

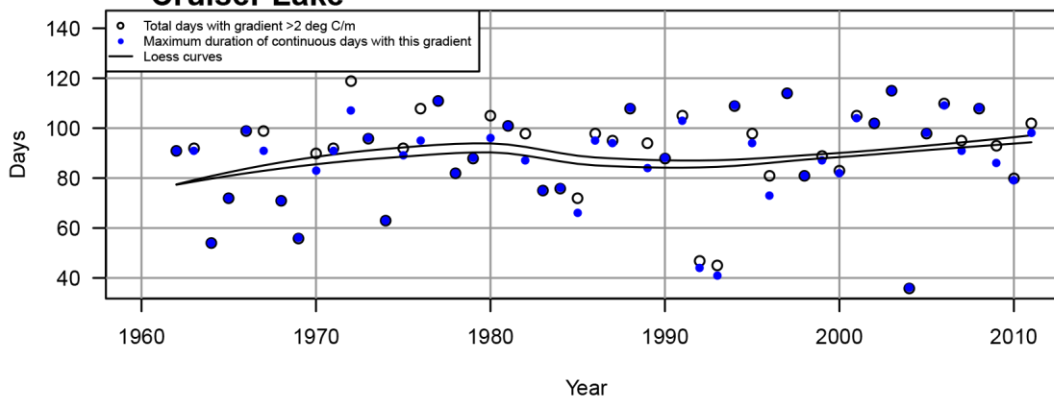


**Figure A7.** Cruiser Lake (Voyageurs): Modeled mean summer temperatures for (a) shallow and (b) bottom waters, 1962–2011.

**(a) Days of year with thermal gradient >2 deg C/m:  
Cruiser Lake**



**(b) Number of days with thermal gradient >2 deg C/m:  
Cruiser Lake**



**(c) Mean depth of gradient >2 deg C/m in summer (JJA):  
Cruiser Lake**

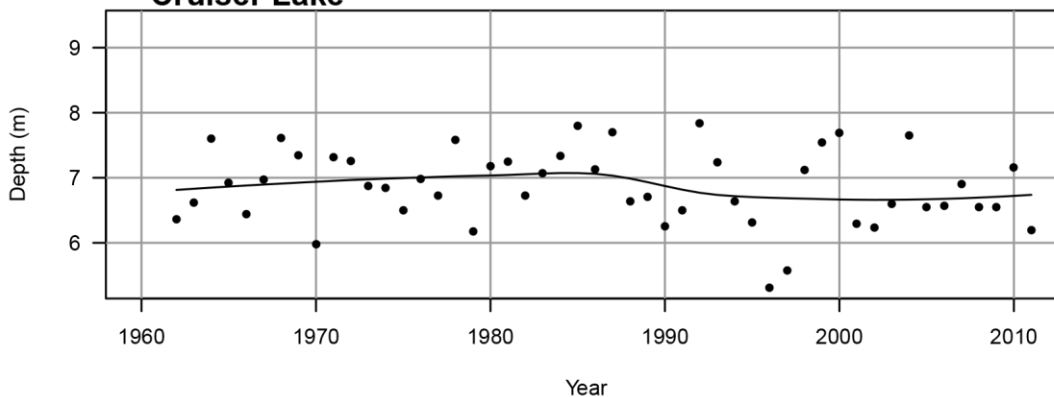
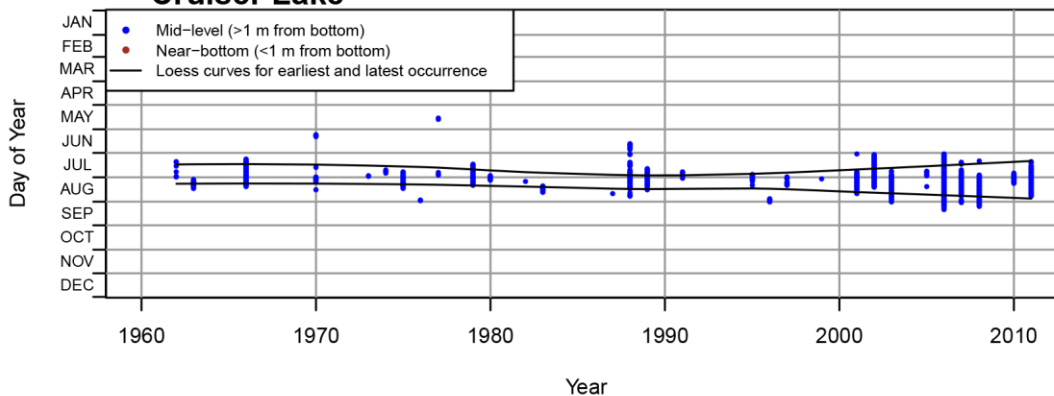
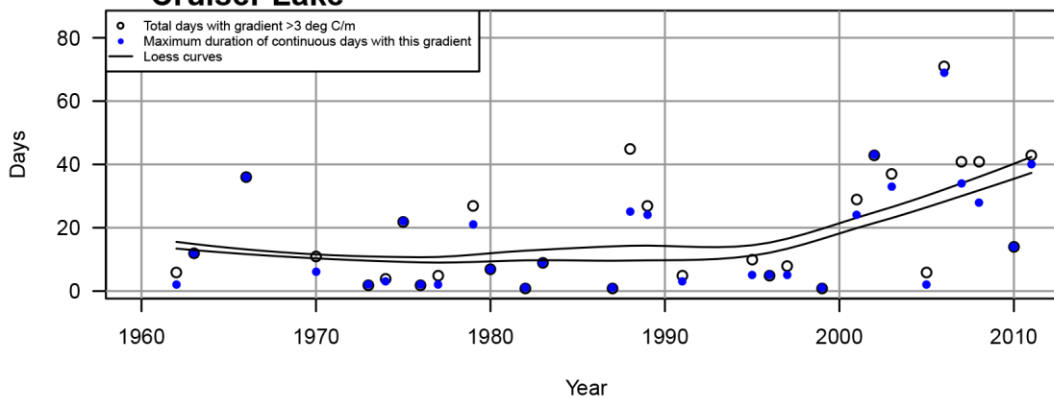


**Figure A8.** Cruiser Lake (Voyageurs): Modeled (a) dates, (b) duration, and (c) mean summer depth of thermal gradients  $\geq 2^{\circ}\text{C}$  per meter, 1962–2011.

**(a) Days of year with thermal gradient >3 deg C/m:  
Cruiser Lake**



**(b) Number of days with thermal gradient >3 deg C/m:  
Cruiser Lake**



**(c) Mean depth of gradient >3 deg C/m in summer (JJA):  
Cruiser Lake**

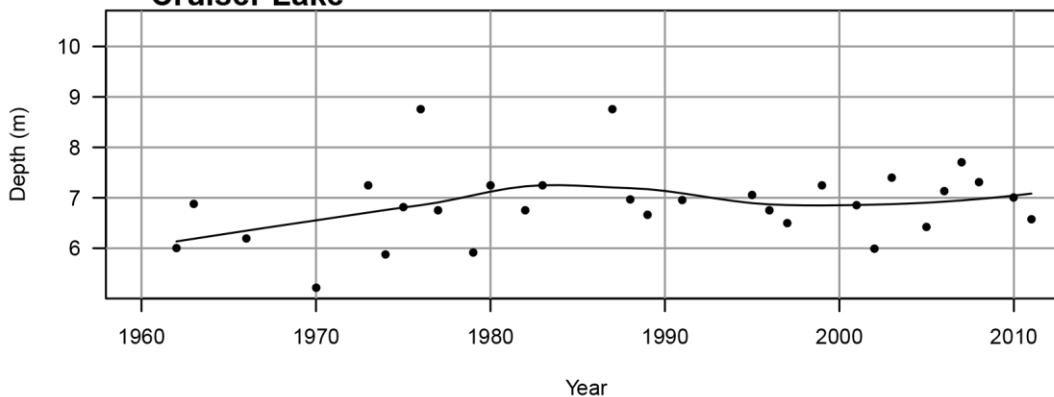


**Figure A9.** Cruiser Lake (Voyageurs): Modeled (a) dates, (b) duration, and (c) mean summer depth of thermal gradients  $\geq 3^{\circ}\text{C}$  per meter, 1962–2011.

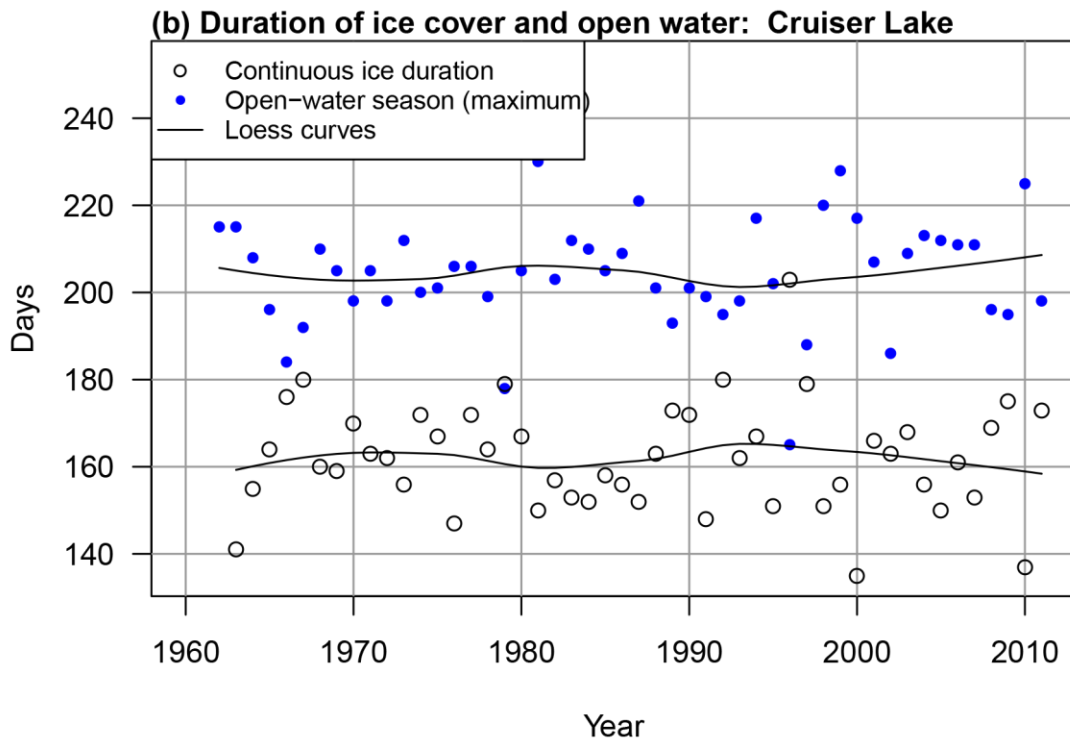
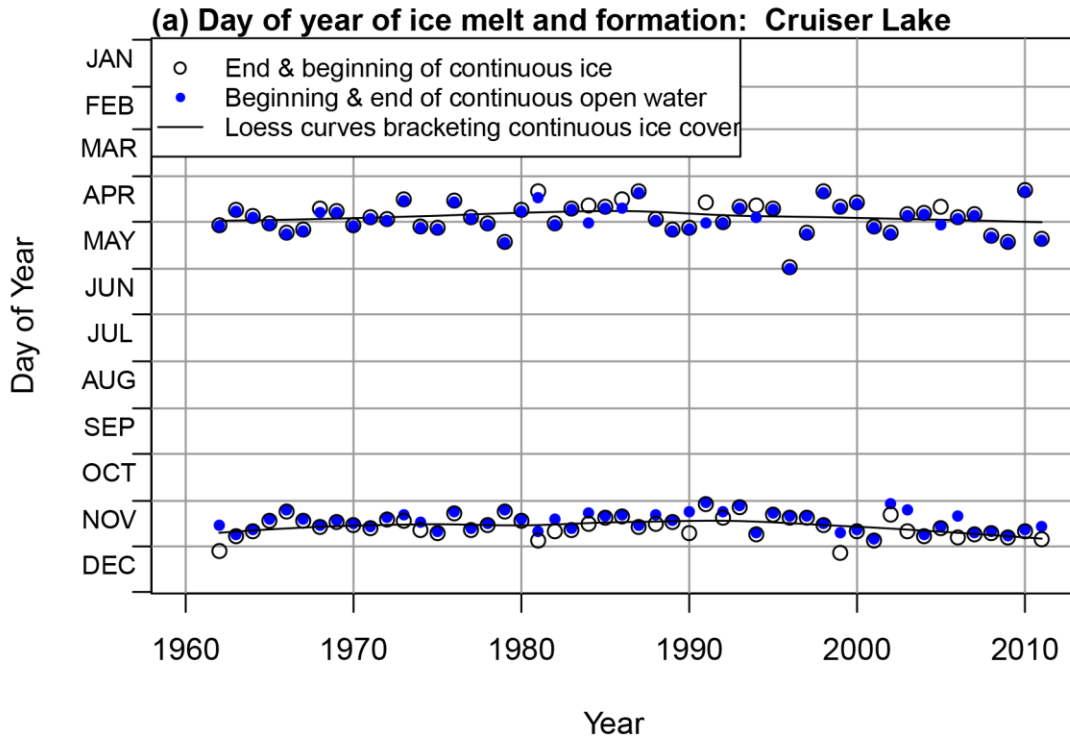


**Figure A10.** Cruiser Lake (Voyageurs): Modeled (a) dates and (b) duration of ice-covered and open-water seasons, 1962–2011.

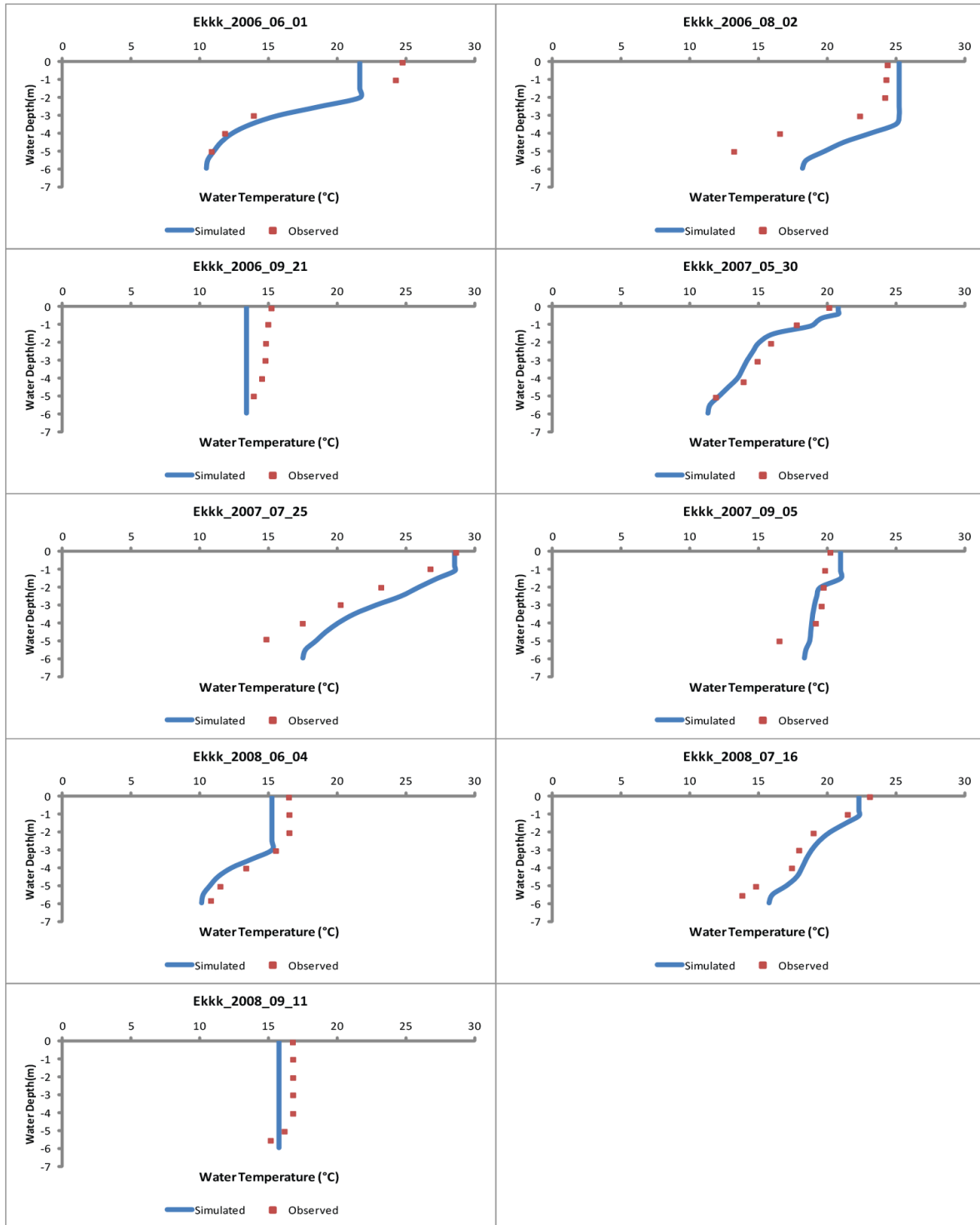


**Figure A11.** Ek Lake (Voyageurs): Observed and modeled temperature profiles, 2006–2008.

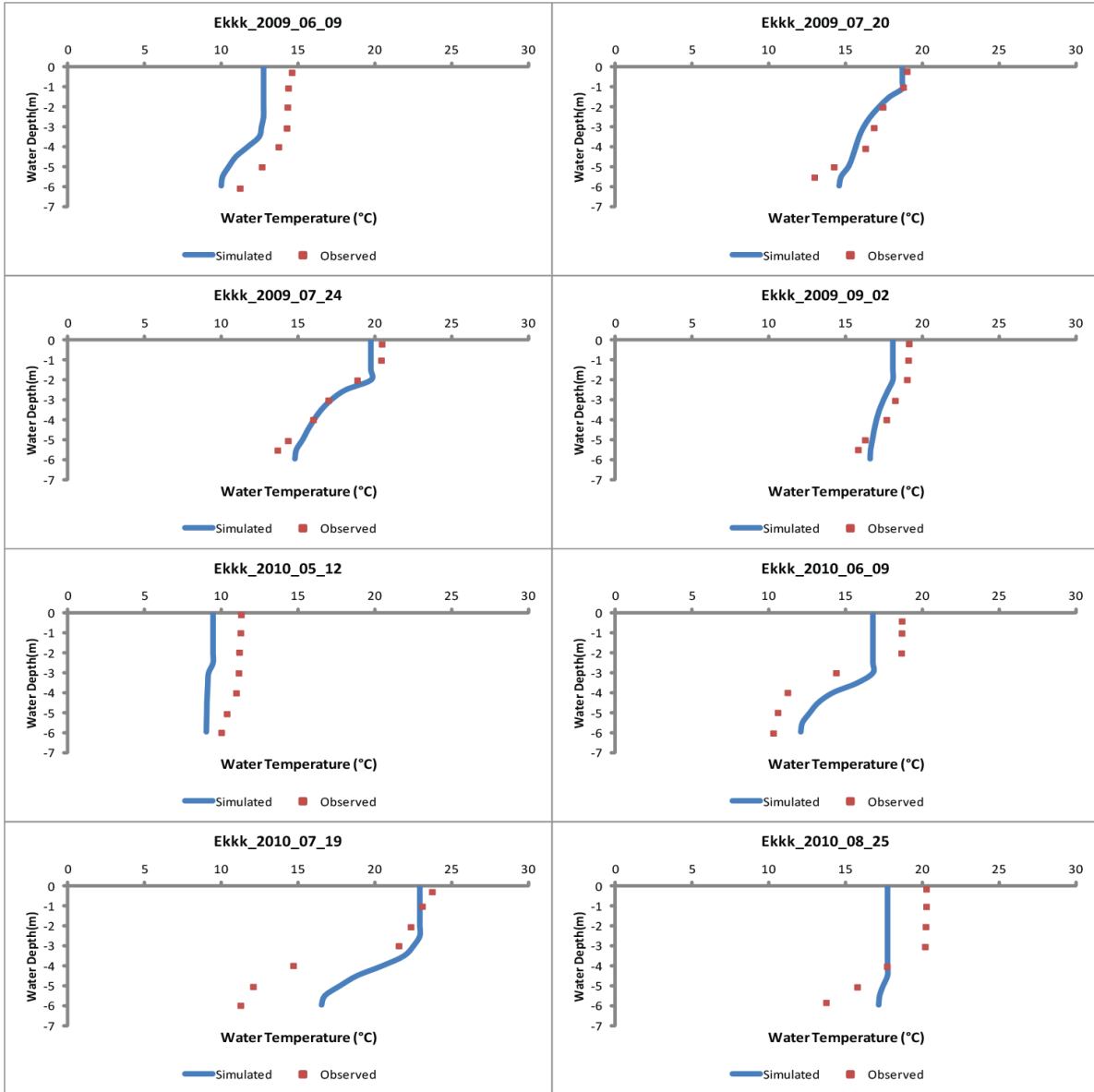
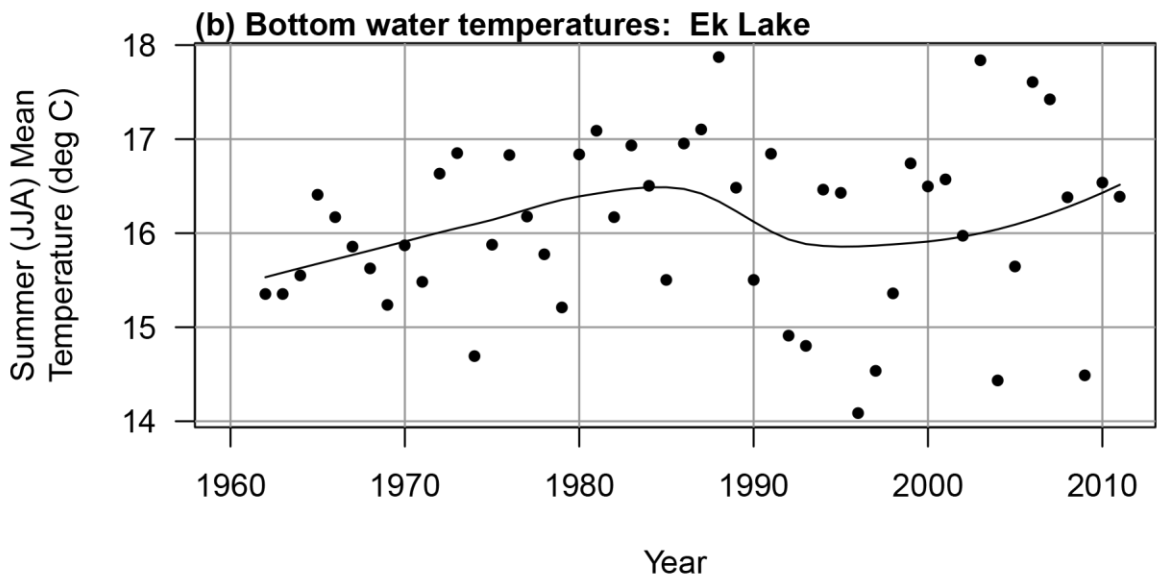
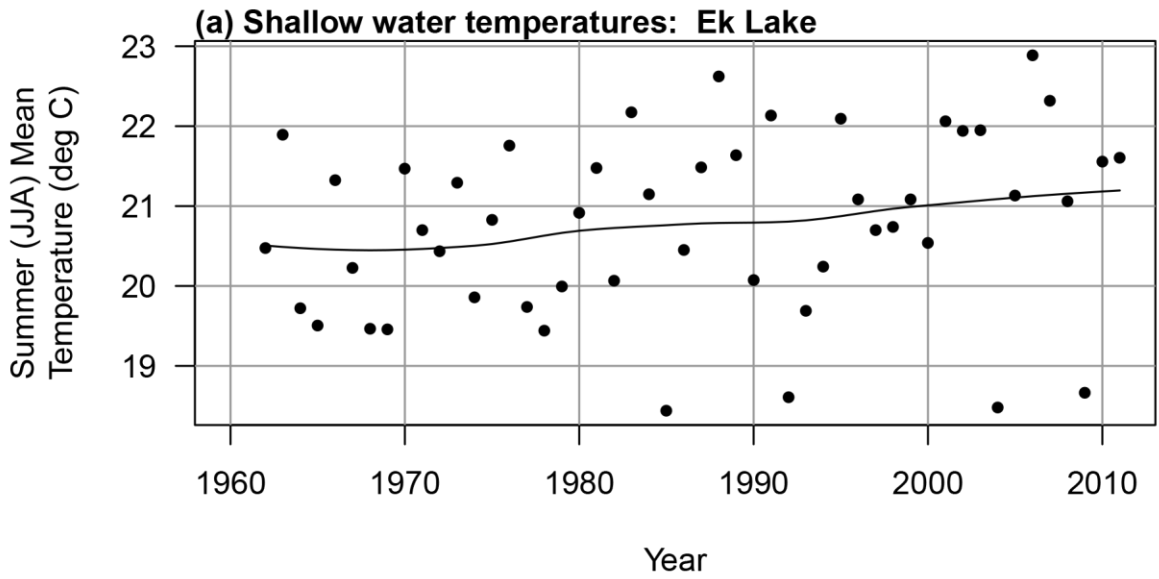
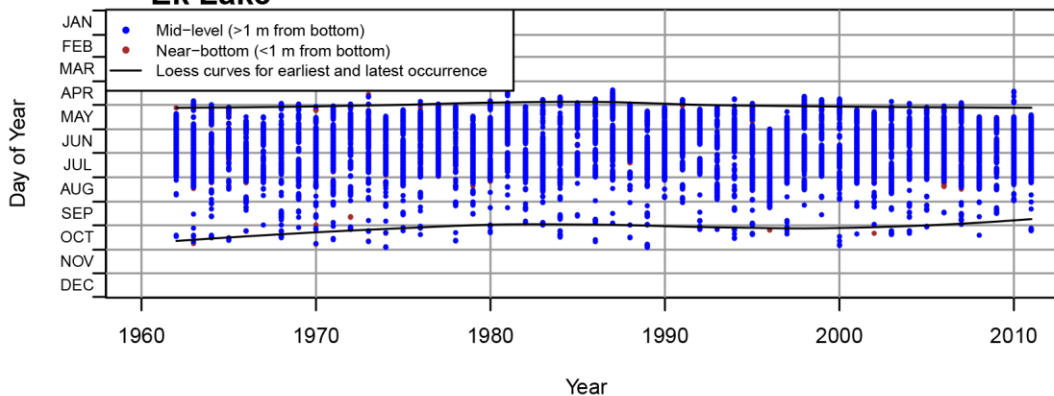


Figure A12. Ek Lake (Voyageurs): Observed and modeled temperature profiles, 2009–2010.

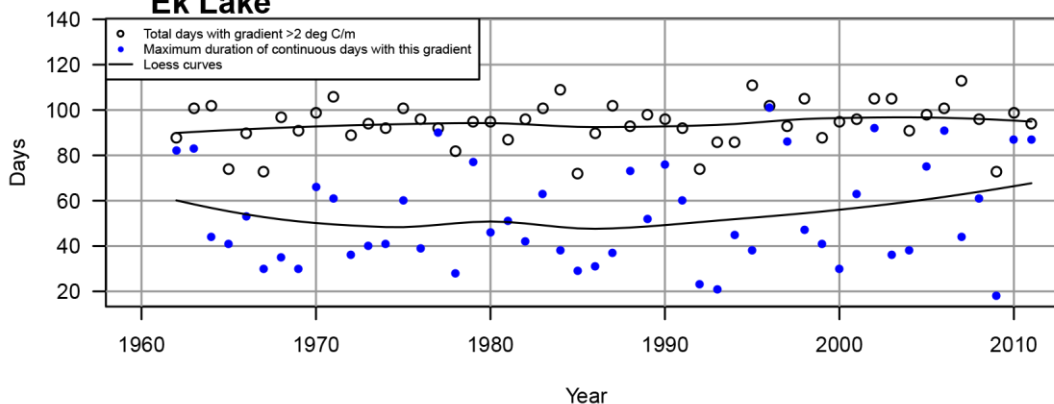


**Figure A13.** Ek Lake (Voyageurs): Modeled mean summer temperatures for (a) shallow and (b) bottom waters, 1962–2011.

**(a) Days of year with thermal gradient >2 deg C/m:  
Ek Lake**



**(b) Number of days with thermal gradient >2 deg C/m:  
Ek Lake**



**(c) Mean depth of gradient >2 deg C/m in summer (JJA):  
Ek Lake**

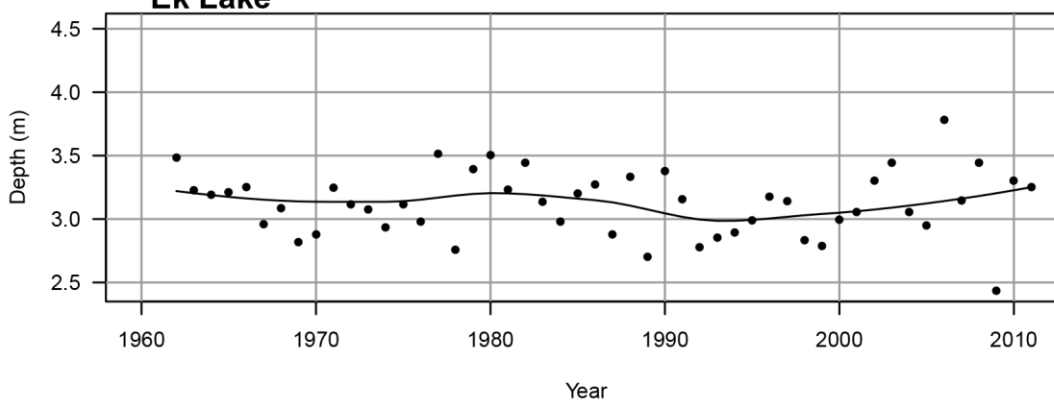
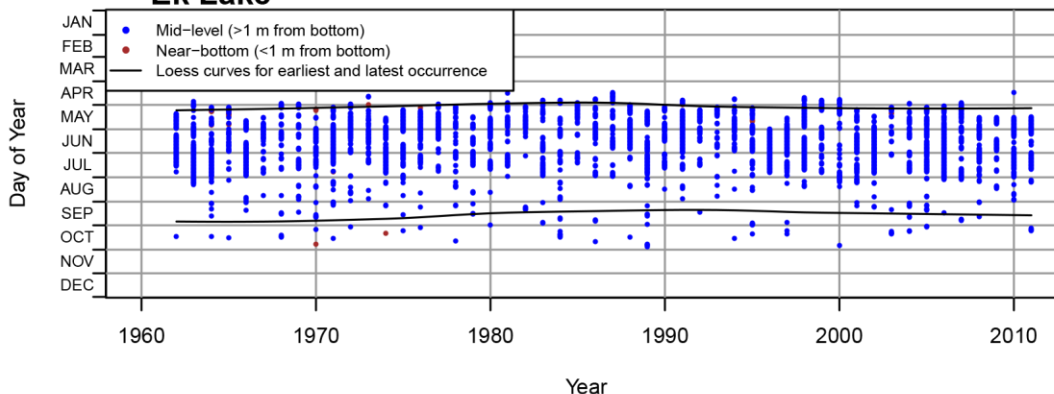
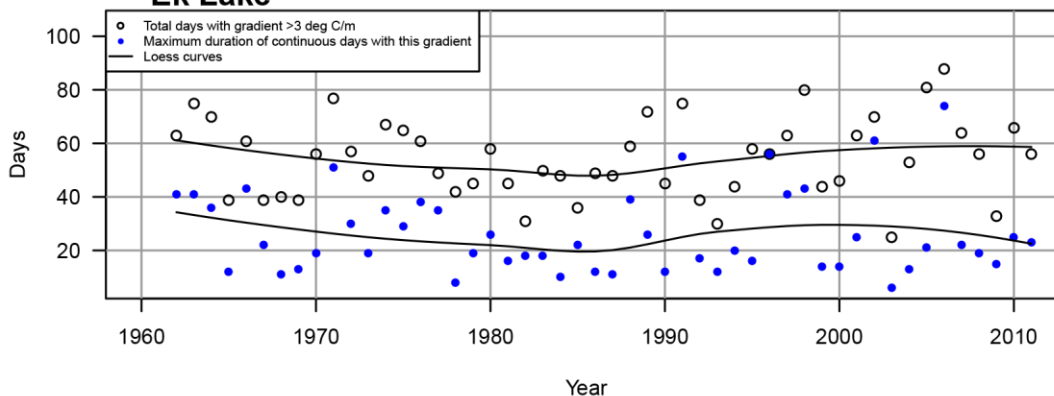


**Figure A14.** Ek Lake (Voyageurs): Modeled (a) dates, (b) duration, and (c) mean summer depth of thermal gradients  $\geq 2^{\circ}\text{C}$  per meter, 1962–2011.

**(a) Days of year with thermal gradient >3 deg C/m:  
Ek Lake**



**(b) Number of days with thermal gradient >3 deg C/m:  
Ek Lake**



**(c) Mean depth of gradient >3 deg C/m in summer (JJA):  
Ek Lake**

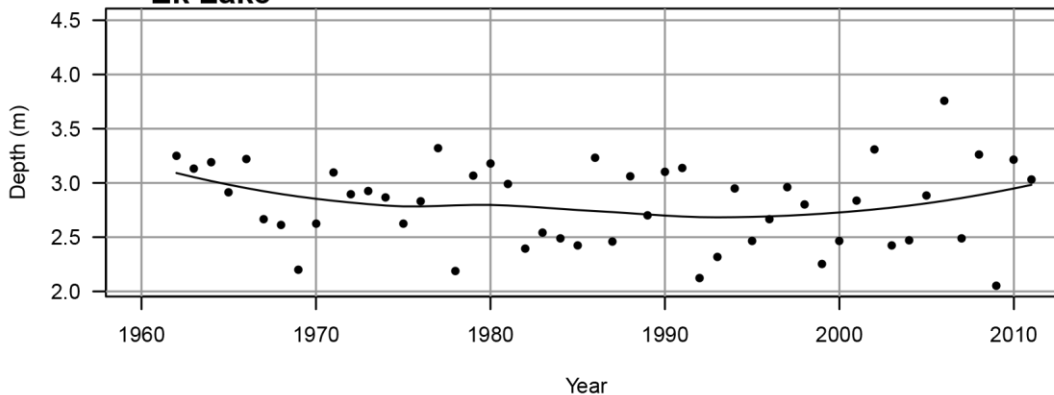


**Figure A15.** Ek Lake (Voyageurs): Modeled (a) dates, (b) duration, and (c) mean summer depth of thermal gradients  $\geq 3^{\circ}\text{C}$  per meter, 1962–2011.

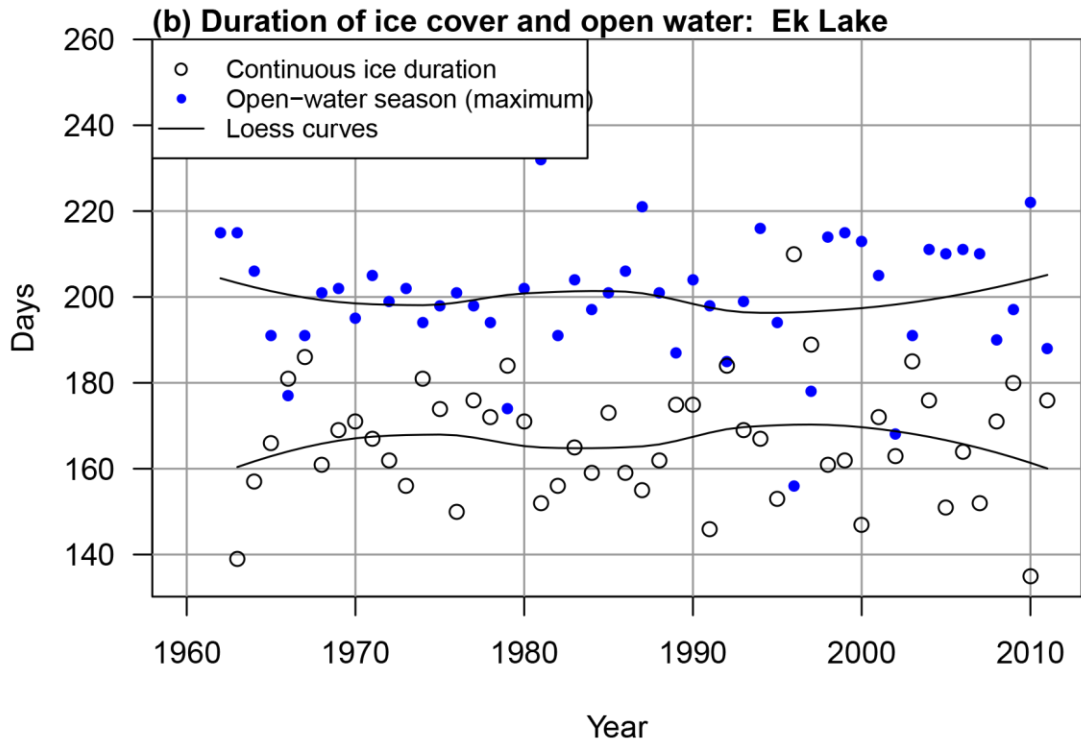
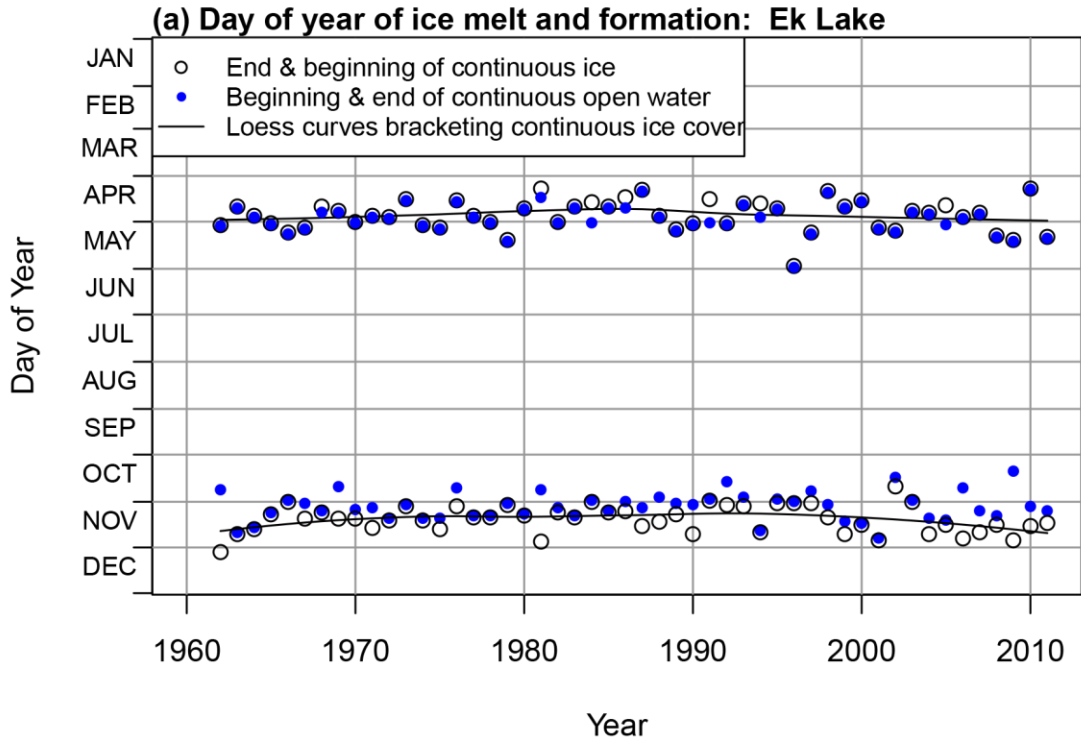


**Figure A16.** Ek Lake (Voyageurs): Modeled (a) dates and (b) duration of ice-covered and open-water seasons, 1962–2011.

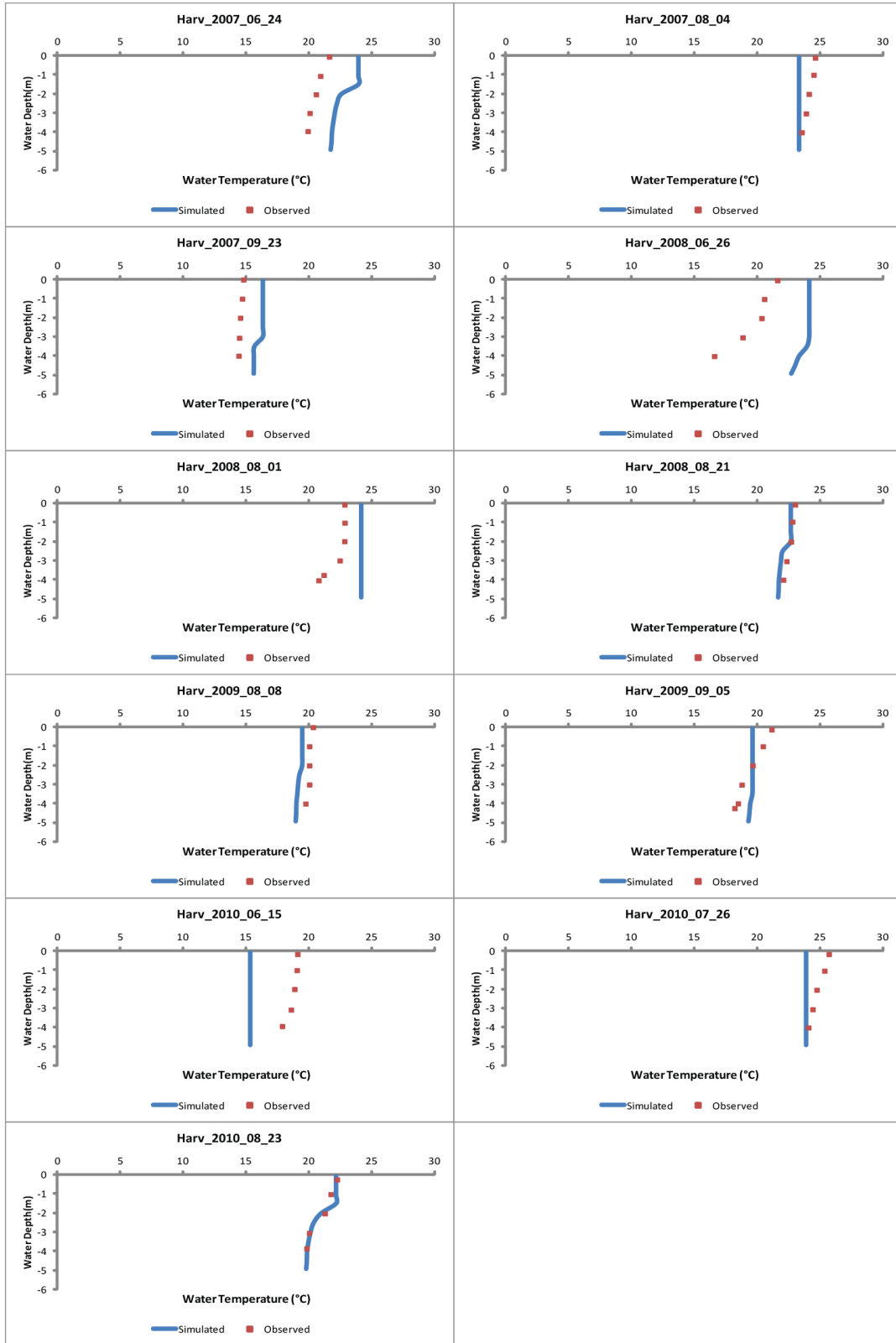
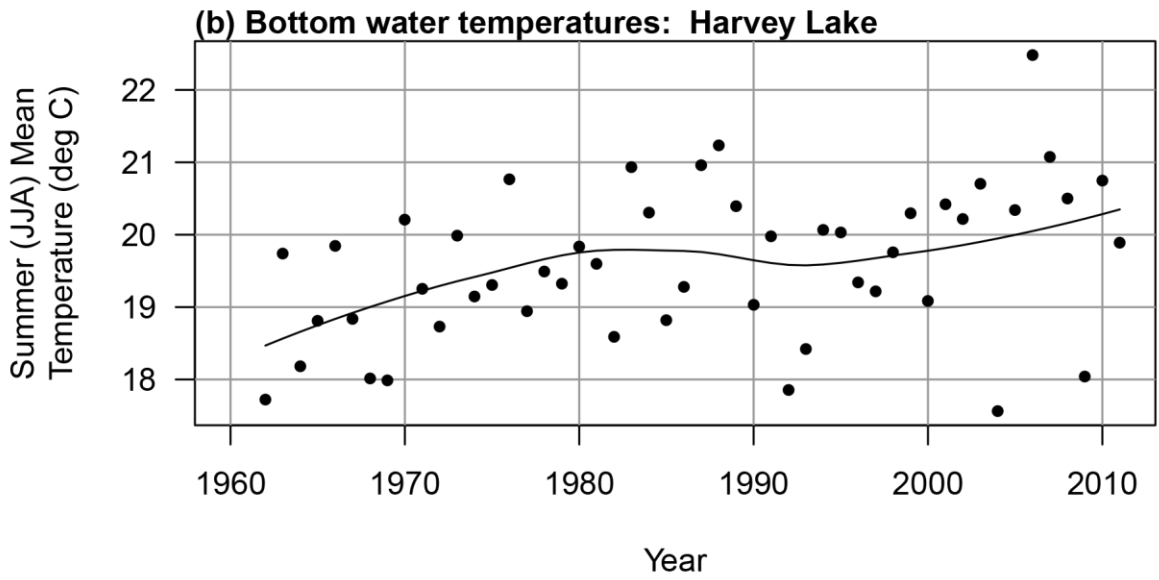
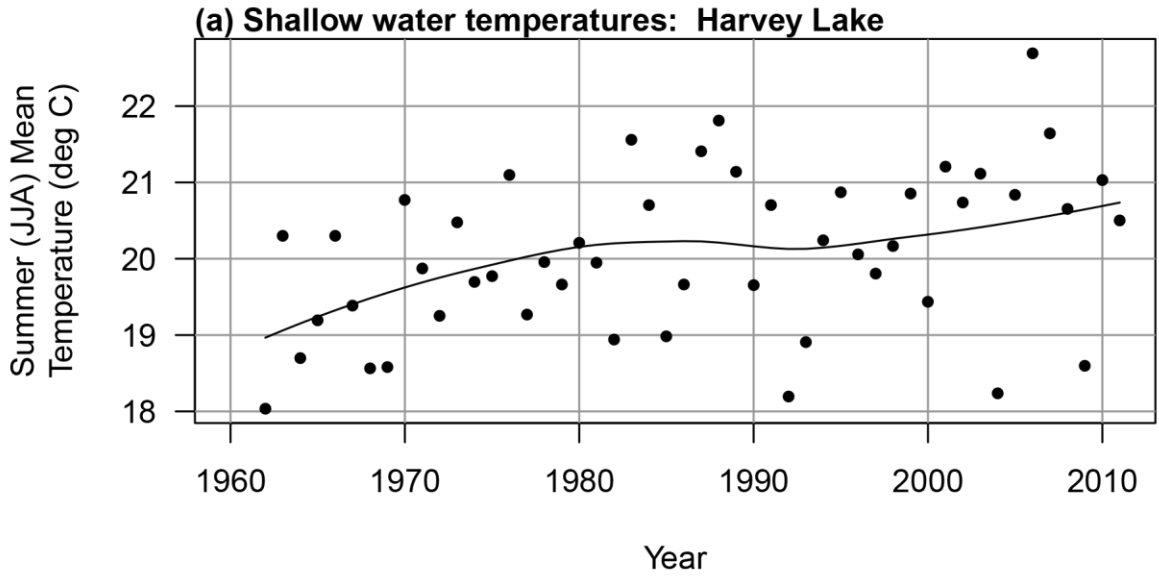
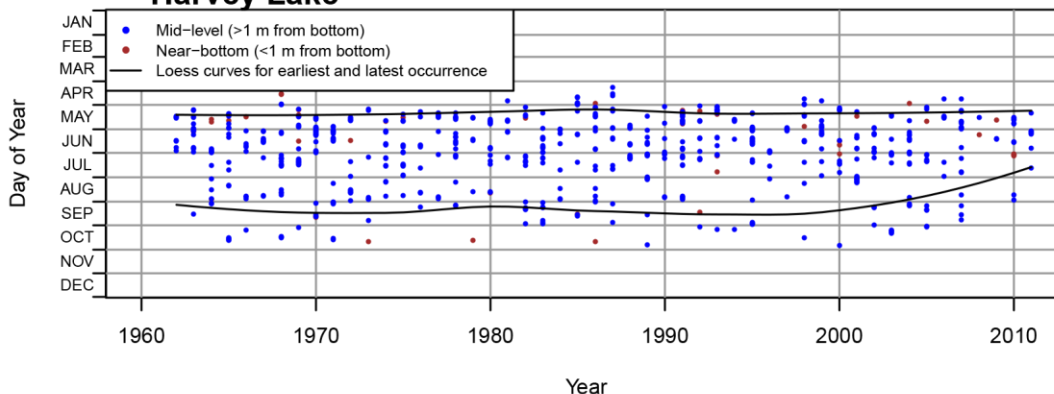


Figure A17. Lake Harvey (Isle Royale): Observed and modeled temperature profiles, 2007–2010.

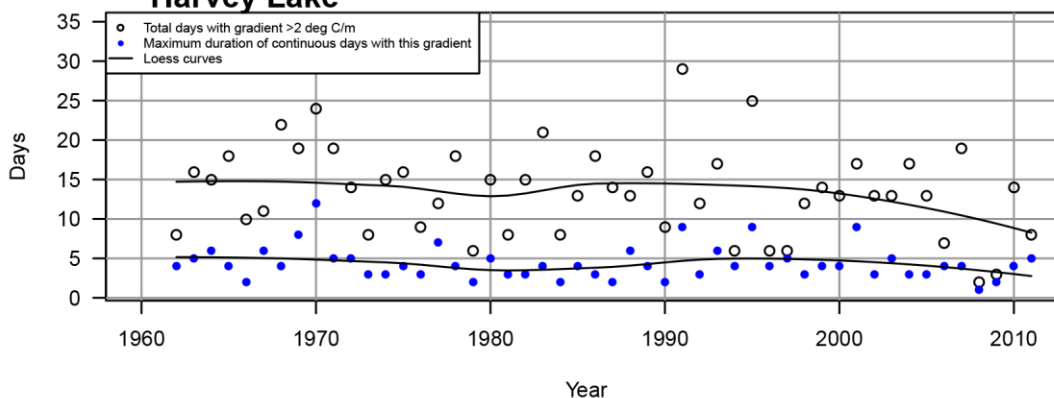


**Figure A18.** Lake Harvey (Isle Royale): Modeled mean summer temperatures for (a) shallow and (b) bottom waters, 1962–2011.

**(a) Days of year with thermal gradient >2 deg C/m:  
Harvey Lake**



**(b) Number of days with thermal gradient >2 deg C/m:  
Harvey Lake**



**(c) Mean depth of gradient >2 deg C/m in summer (JJA):  
Harvey Lake**

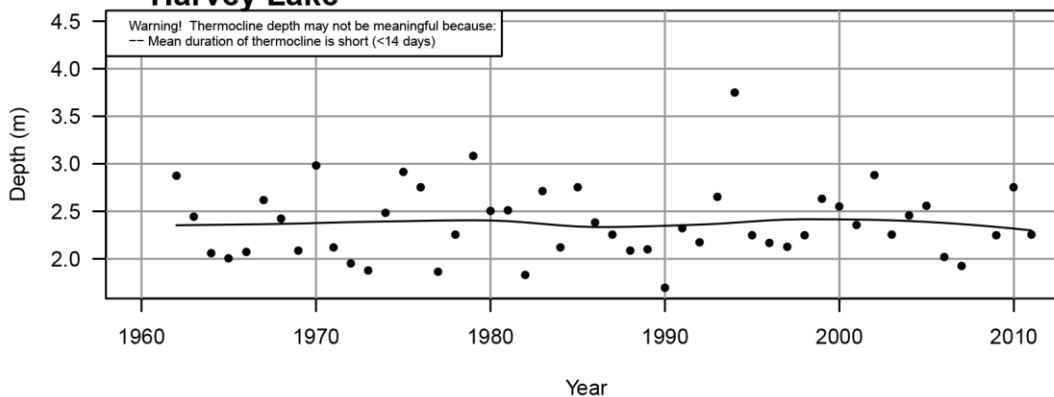
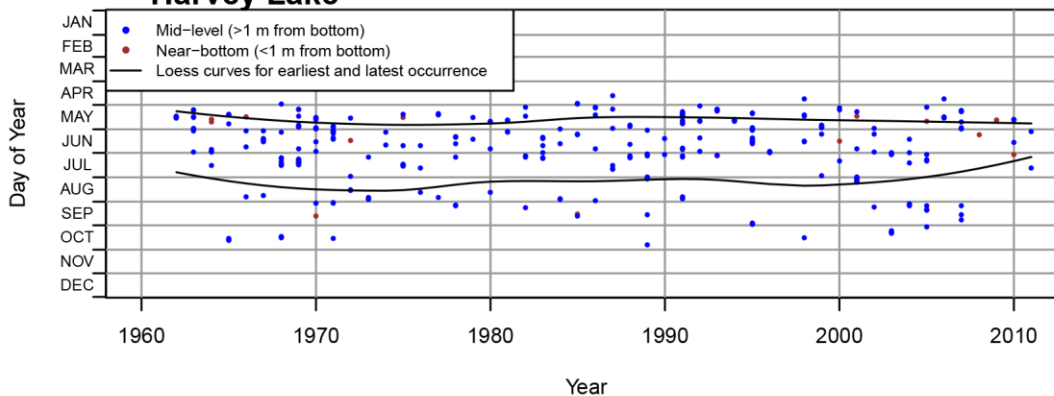
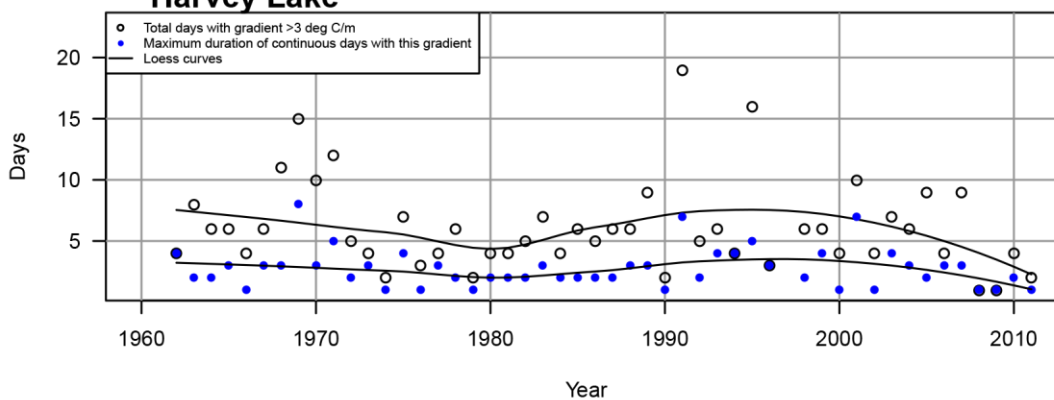


**Figure A19.** Lake Harvey (Isle Royale): Modeled (a) dates, (b) duration, and (c) mean summer depth of thermal gradients  $\geq 2^\circ\text{C}$  per meter, 1962–2011.

**(a) Days of year with thermal gradient >3 deg C/m:  
Harvey Lake**



**(b) Number of days with thermal gradient >3 deg C/m:  
Harvey Lake**



**(c) Mean depth of gradient >3 deg C/m in summer (JJA):  
Harvey Lake**

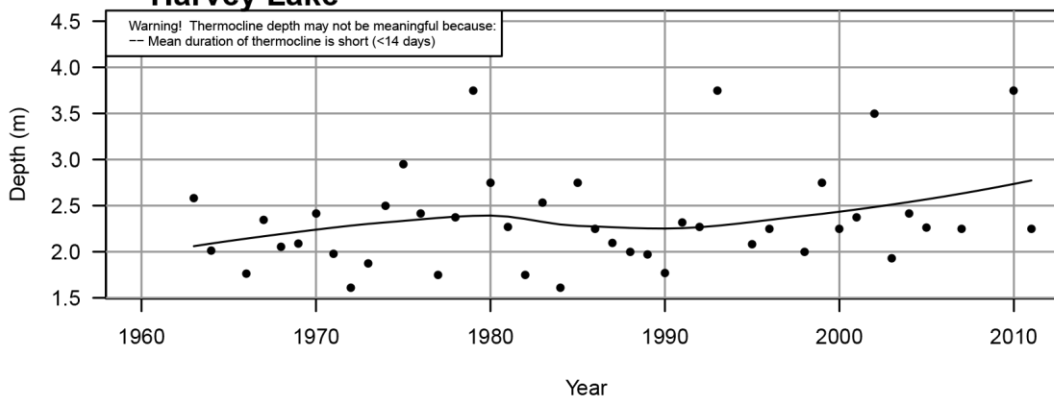


**Figure A20.** Lake Harvey (Isle Royale): Modeled (a) dates, (b) duration, and (c) mean summer depth of thermal gradients  $\geq 3^{\circ}\text{C}$  per meter, 1962–2011.

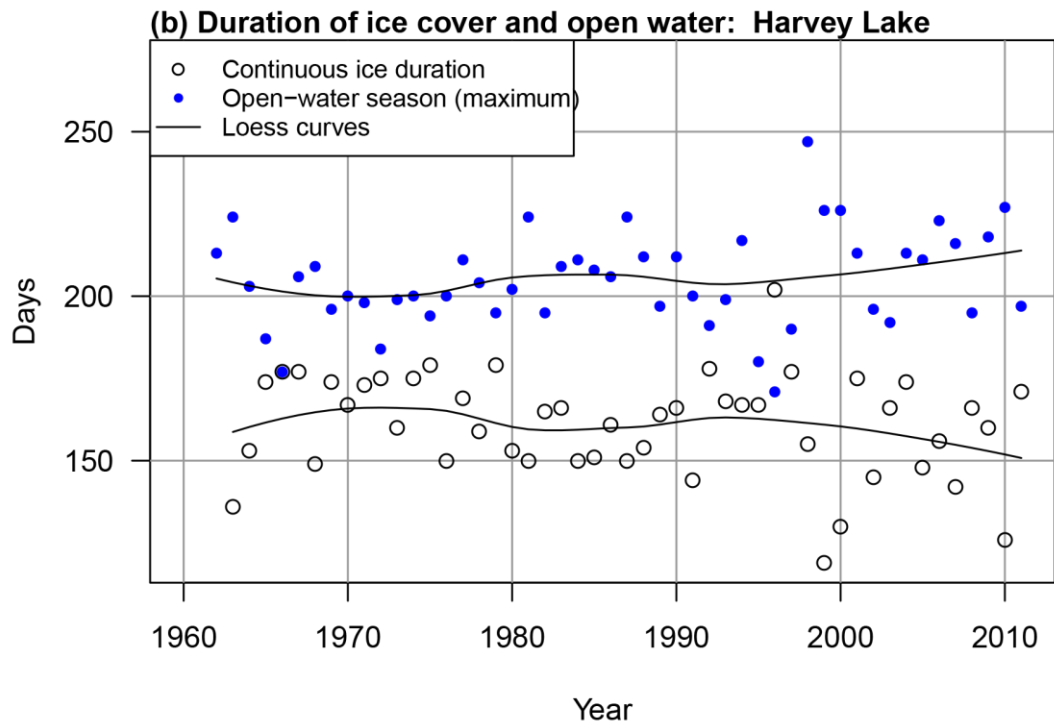
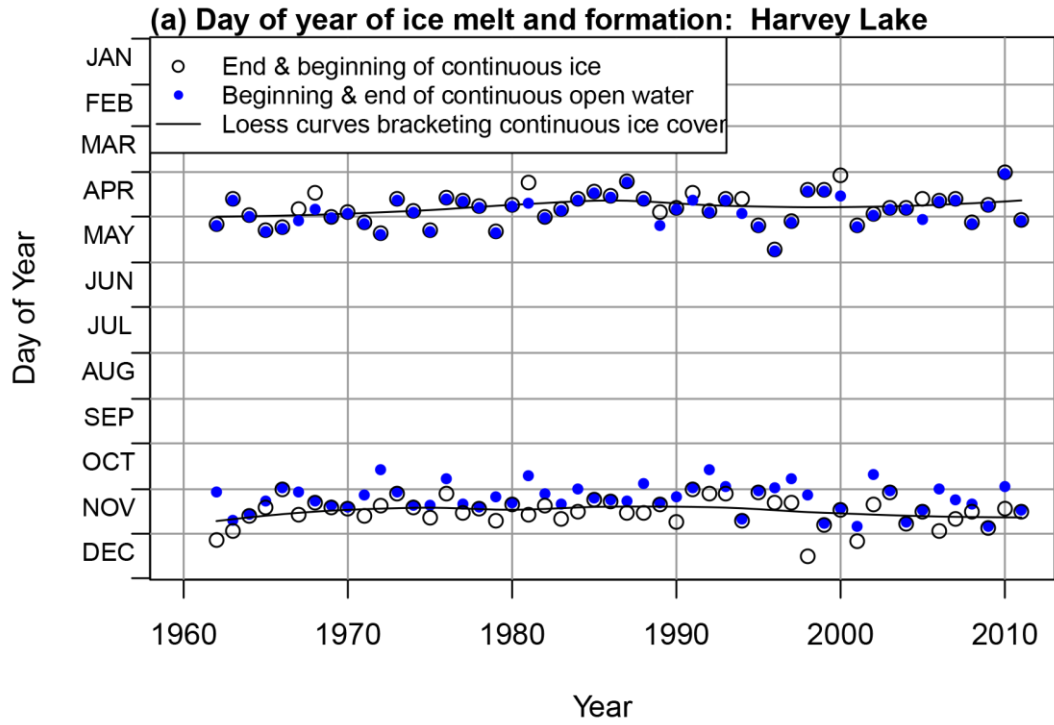


**Figure A21.** Lake Harvey (Isle Royale): Modeled (a) dates and (b) duration of ice-covered and open-water seasons, 1962–2011.

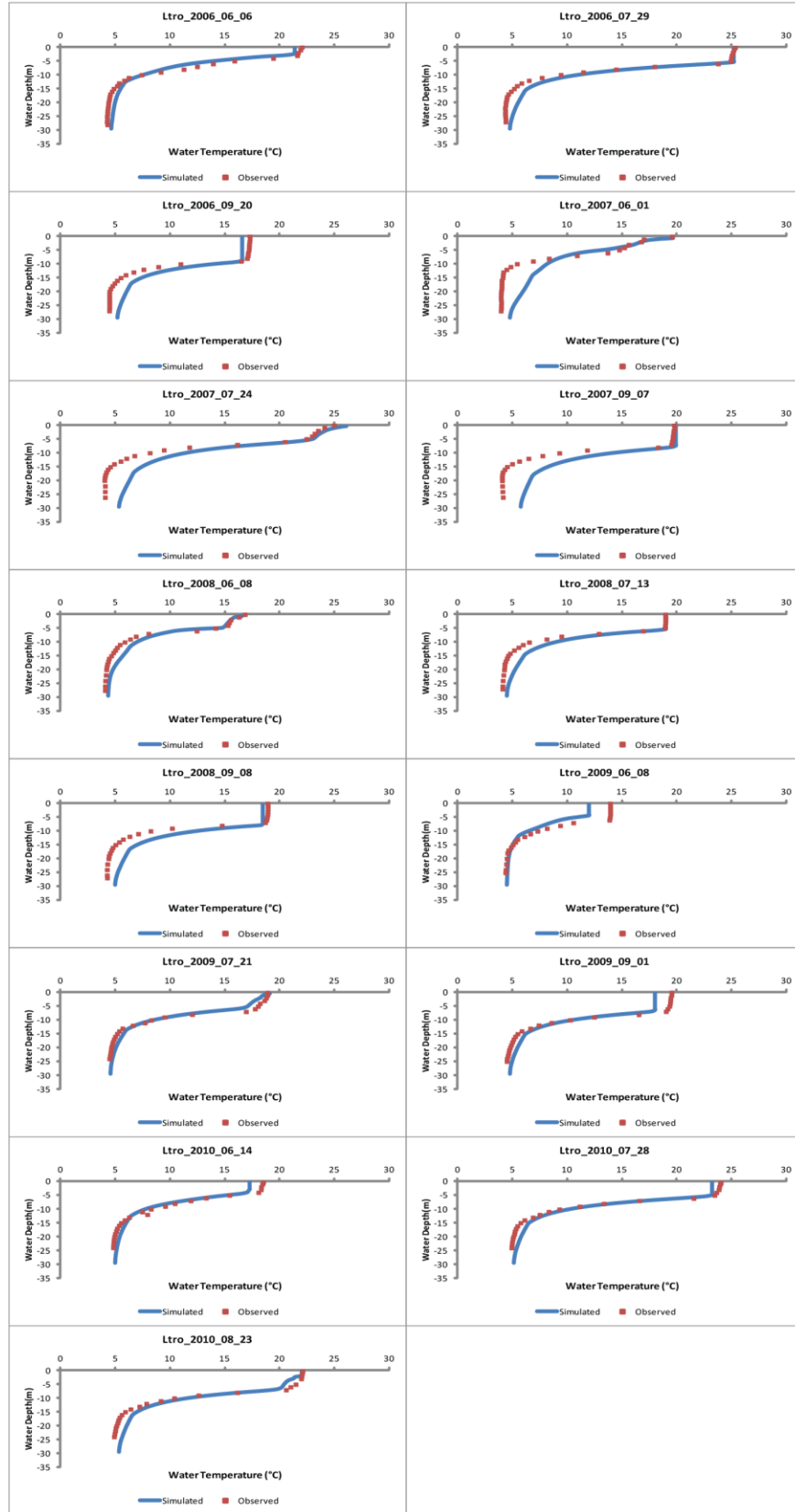
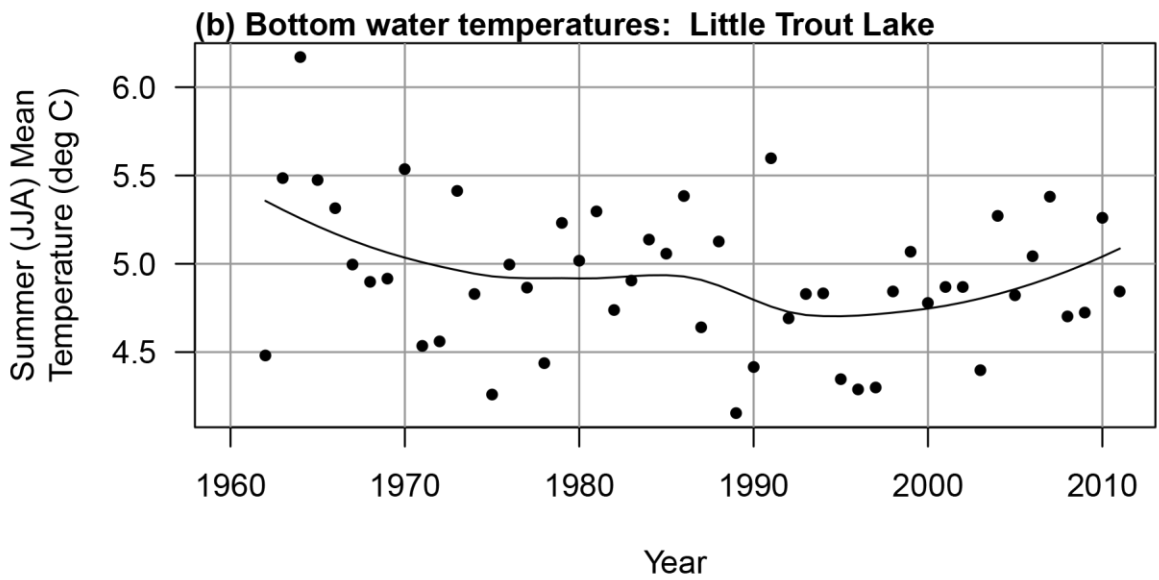
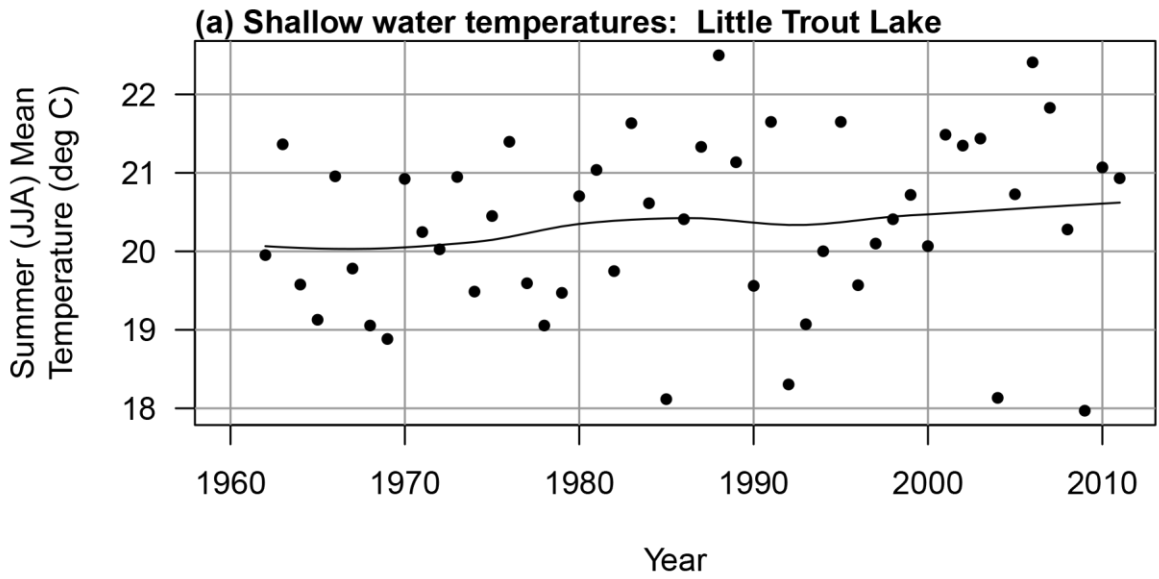
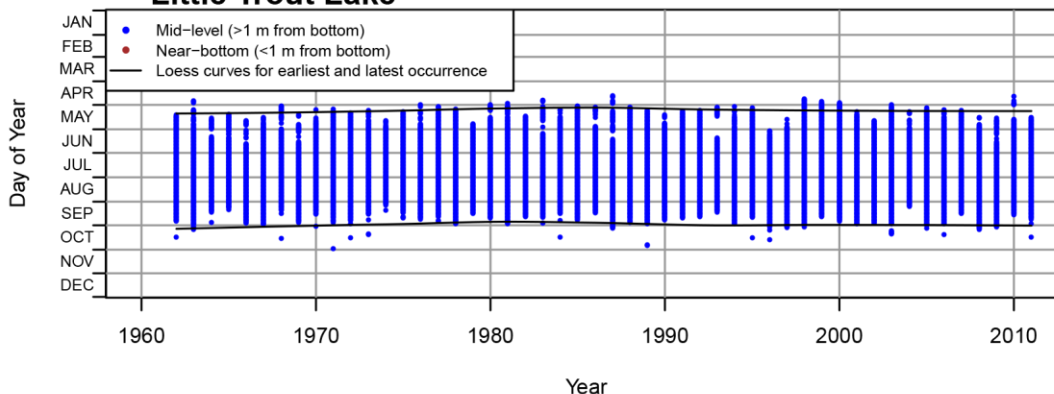


Figure A22. Little Trout Lake (Voyageurs): Observed and modeled temperature profiles, 2006–2010.

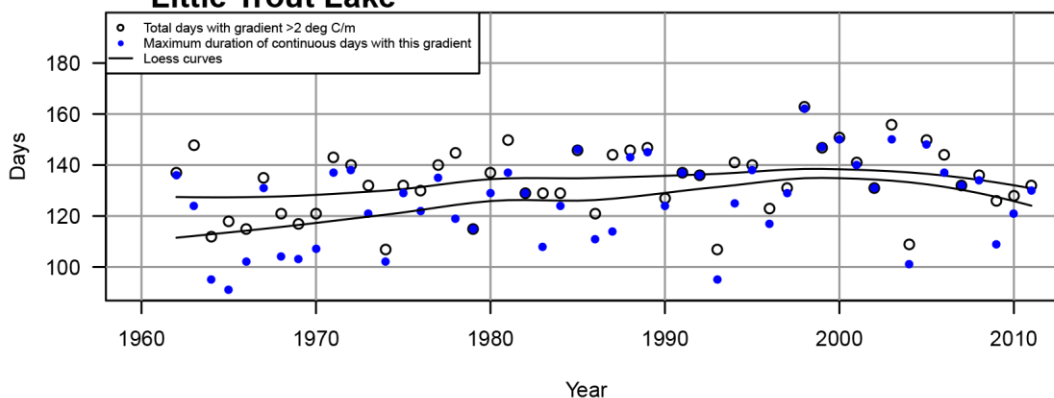


**Figure A23.** Little Trout Lake (Voyageurs): Modeled mean summer temperatures for (a) shallow and (b) bottom waters, 1962–2011.

**(a) Days of year with thermal gradient >2 deg C/m:  
Little Trout Lake**



**(b) Number of days with thermal gradient >2 deg C/m:  
Little Trout Lake**



**(c) Mean depth of gradient >2 deg C/m in summer (JJA):  
Little Trout Lake**

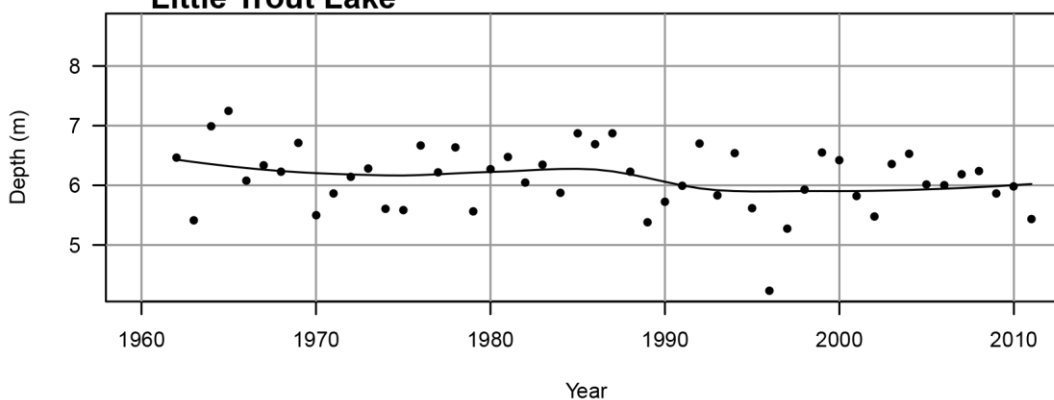
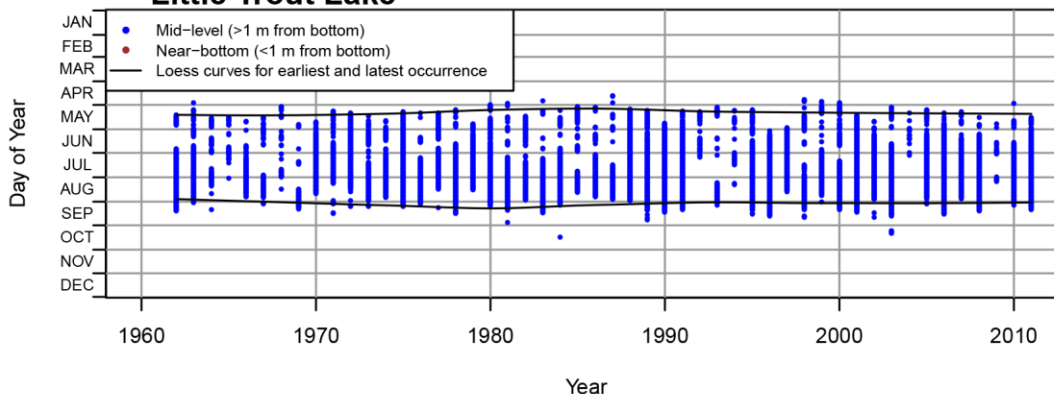
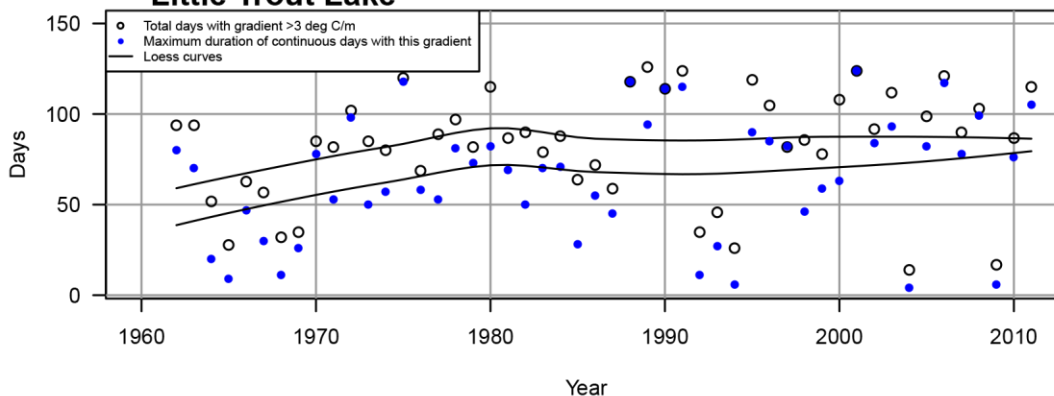


**Figure A24.** Little Trout Lake (Voyageurs): Modeled (a) dates, (b) duration, and (c) mean summer depth of thermal gradients  $\geq 2^{\circ}\text{C}$  per meter, 1962–2011.

**(a) Days of year with thermal gradient >3 deg C/m:  
Little Trout Lake**



**(b) Number of days with thermal gradient >3 deg C/m:  
Little Trout Lake**



**(c) Mean depth of gradient >3 deg C/m in summer (JJA):  
Little Trout Lake**

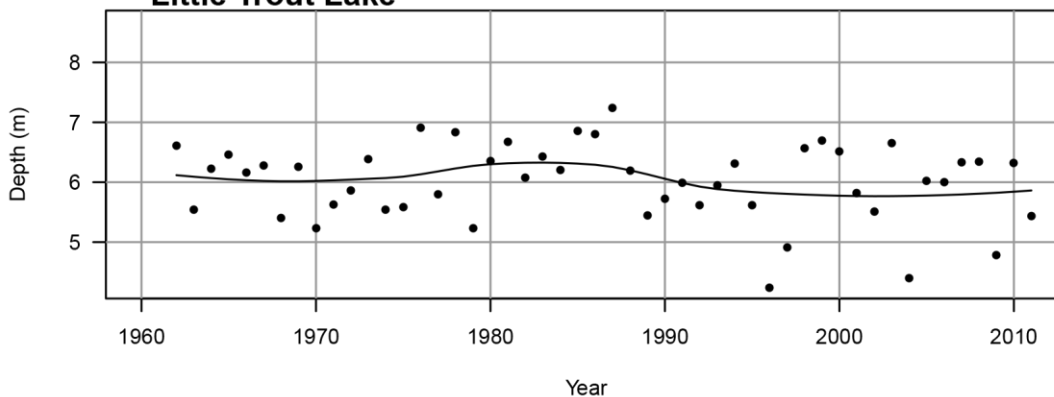


**Figure A25.** Little Trout Lake (Voyageurs): Modeled (a) dates, (b) duration, and (c) mean summer depth of thermal gradients  $\geq 3^{\circ}\text{C}$  per meter, 1962–2011.

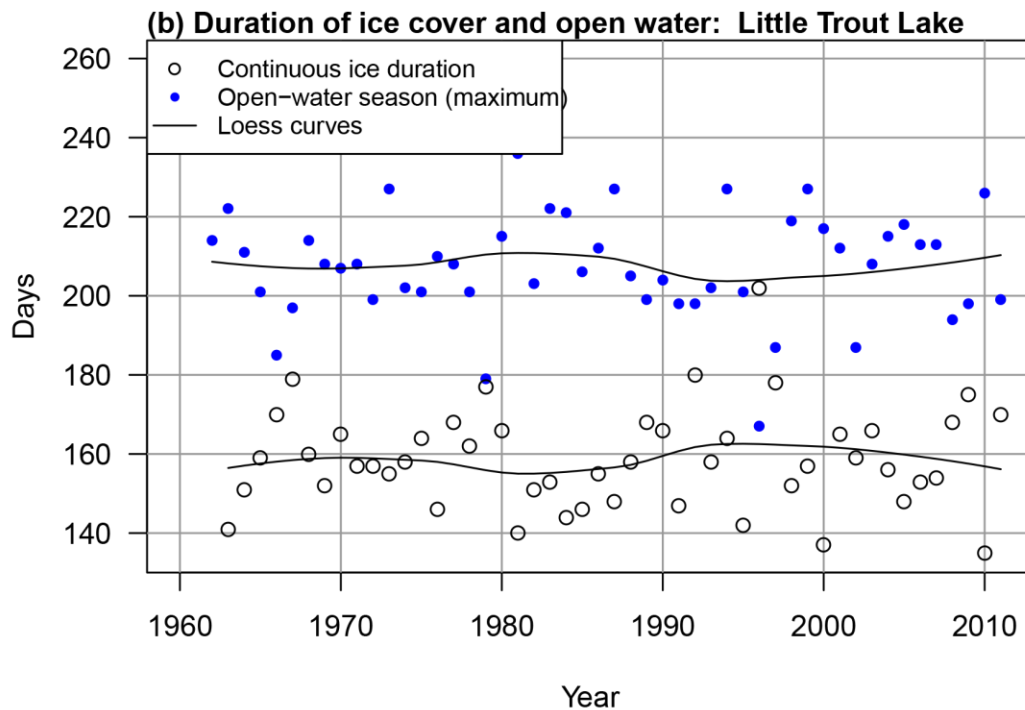
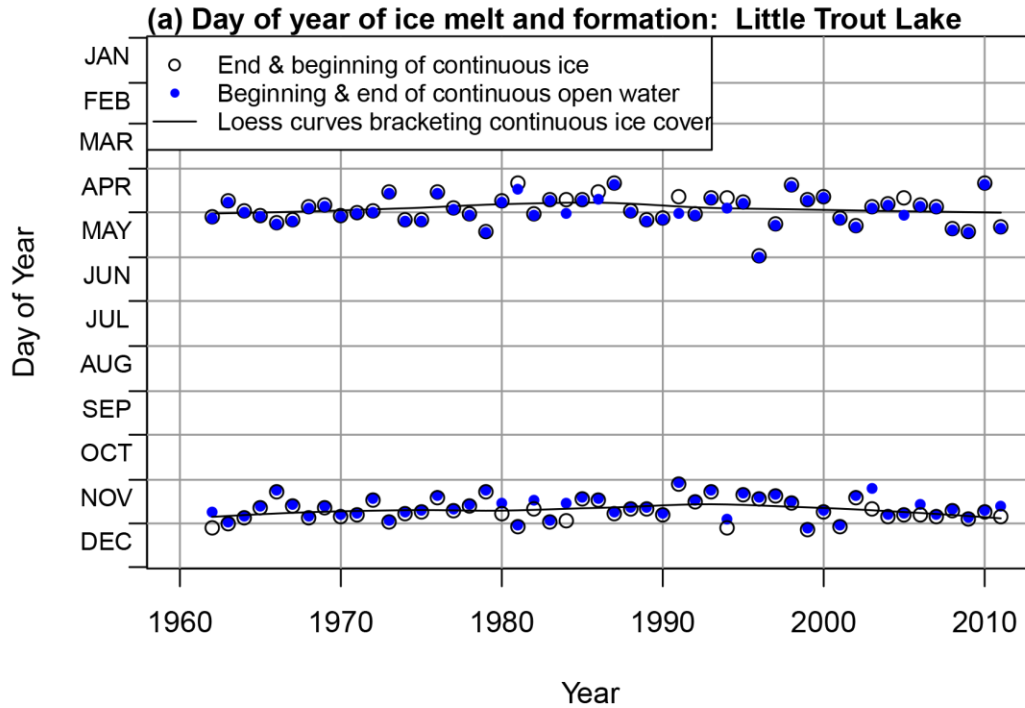


**Figure A26.** Little Trout Lake (Voyageurs): Modeled (a) dates and (b) duration of ice-covered and open-water seasons, 1962–2011.

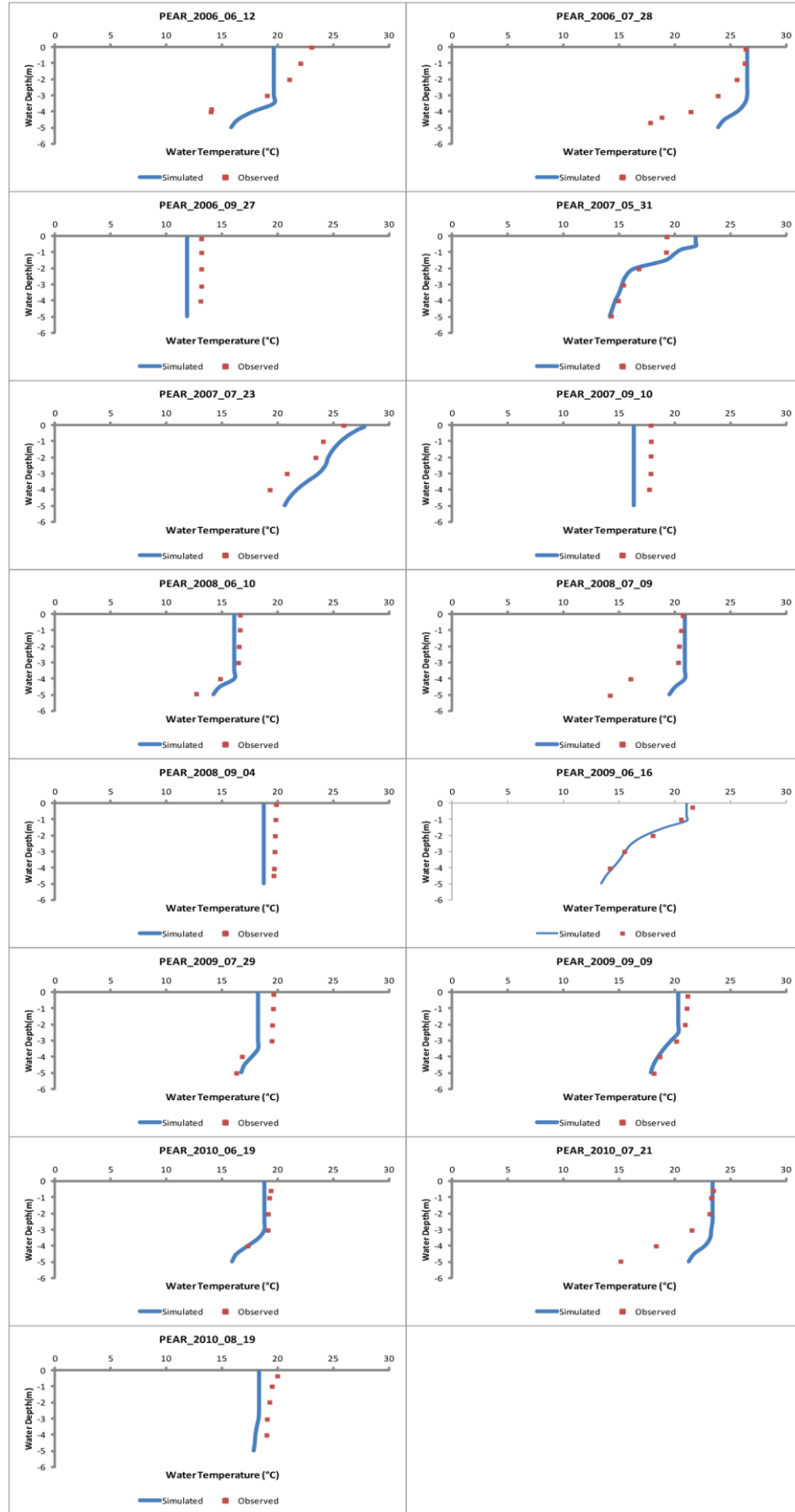
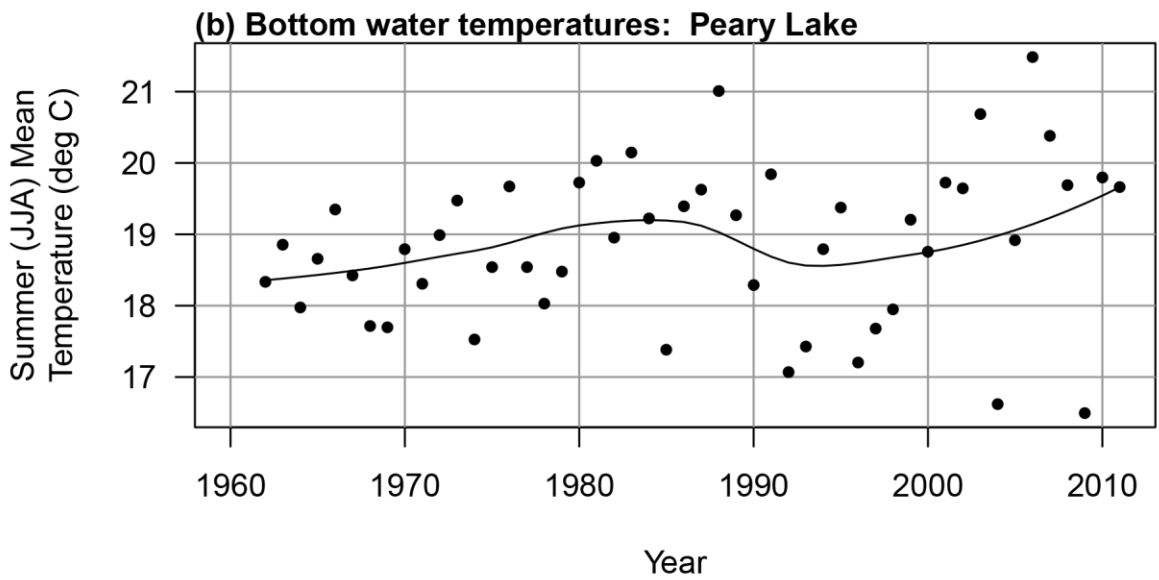
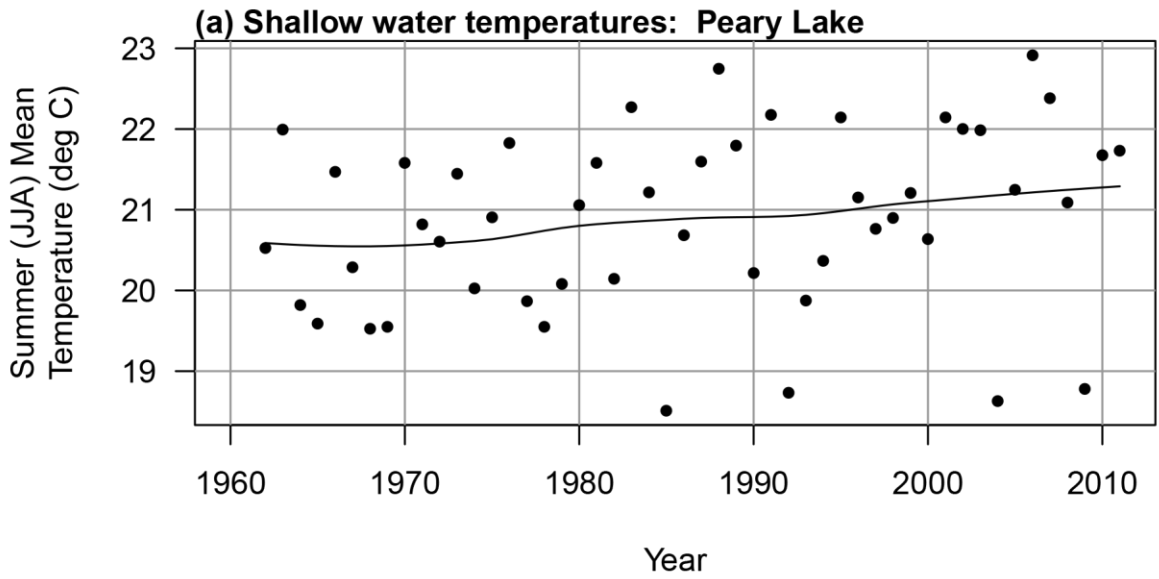
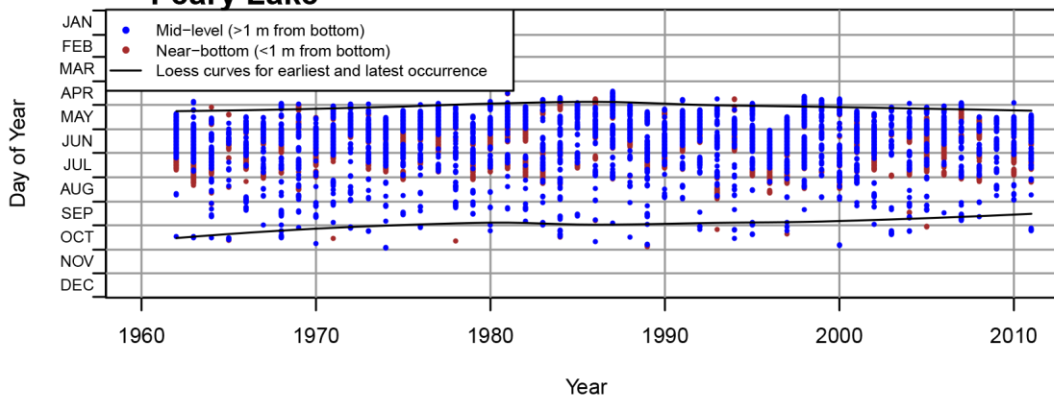


Figure A27. Peary Lake (Voyageurs): Observed and modeled temperature profiles, 2006–2010.

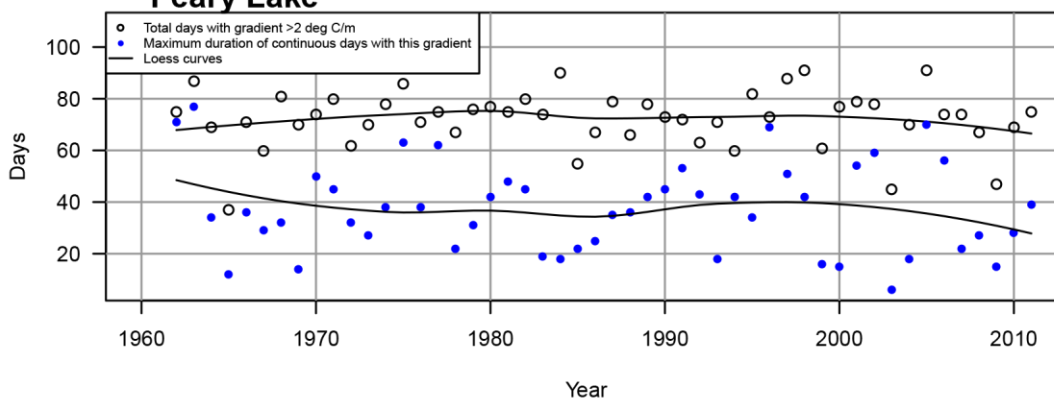


**Figure A28.** Peary Lake (Voyageurs): Modeled mean summer temperatures for (a) shallow and (b) bottom waters, 1962–2011.

**(a) Days of year with thermal gradient >2 deg C/m:  
Peary Lake**



**(b) Number of days with thermal gradient >2 deg C/m:  
Peary Lake**



**(c) Mean depth of gradient >2 deg C/m in summer (JJA):  
Peary Lake**

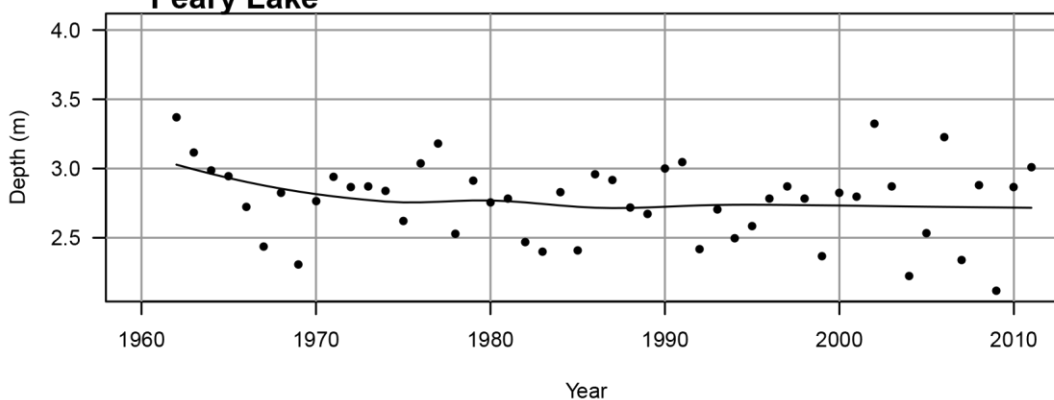
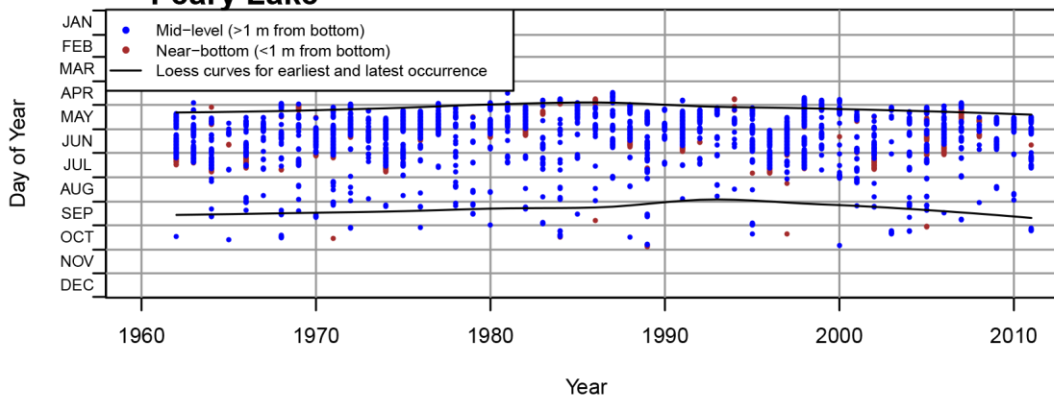
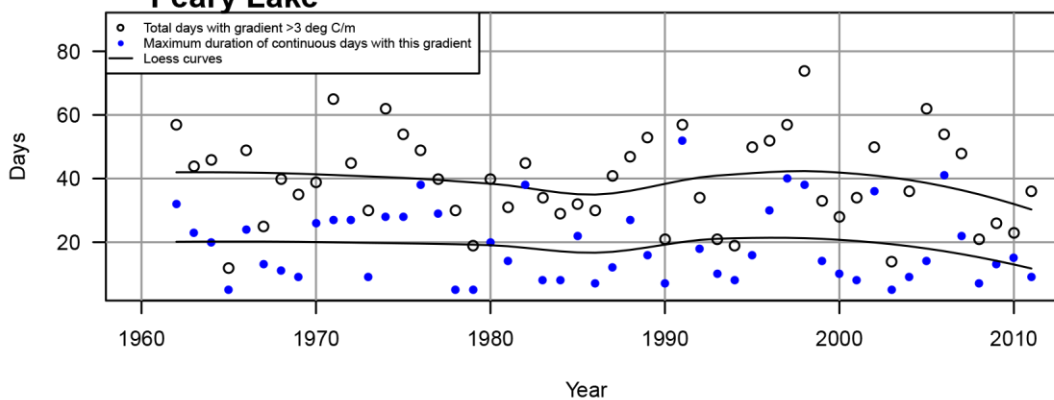


**Figure A29.** Peary Lake (Voyageurs): Modeled (a) dates, (b) duration, and (c) mean summer depth of thermal gradients  $\geq 2^\circ\text{C}$  per meter, 1962–2011.

**(a) Days of year with thermal gradient >3 deg C/m:  
Peary Lake**



**(b) Number of days with thermal gradient >3 deg C/m:  
Peary Lake**



**(c) Mean depth of gradient >3 deg C/m in summer (JJA):  
Peary Lake**

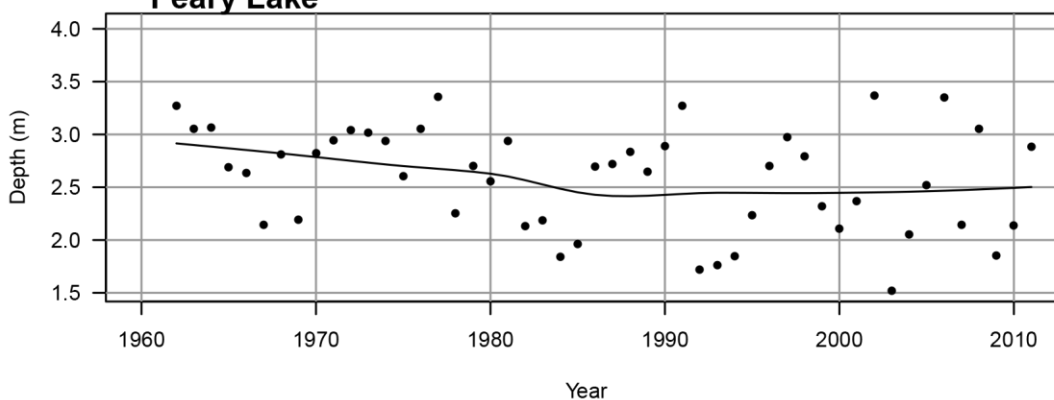


**Figure A30.** Peary Lake (Voyageurs): Modeled (a) dates, (b) duration, and (c) mean summer depth of thermal gradients  $\geq 3^{\circ}\text{C}$  per meter, 1962–2011.

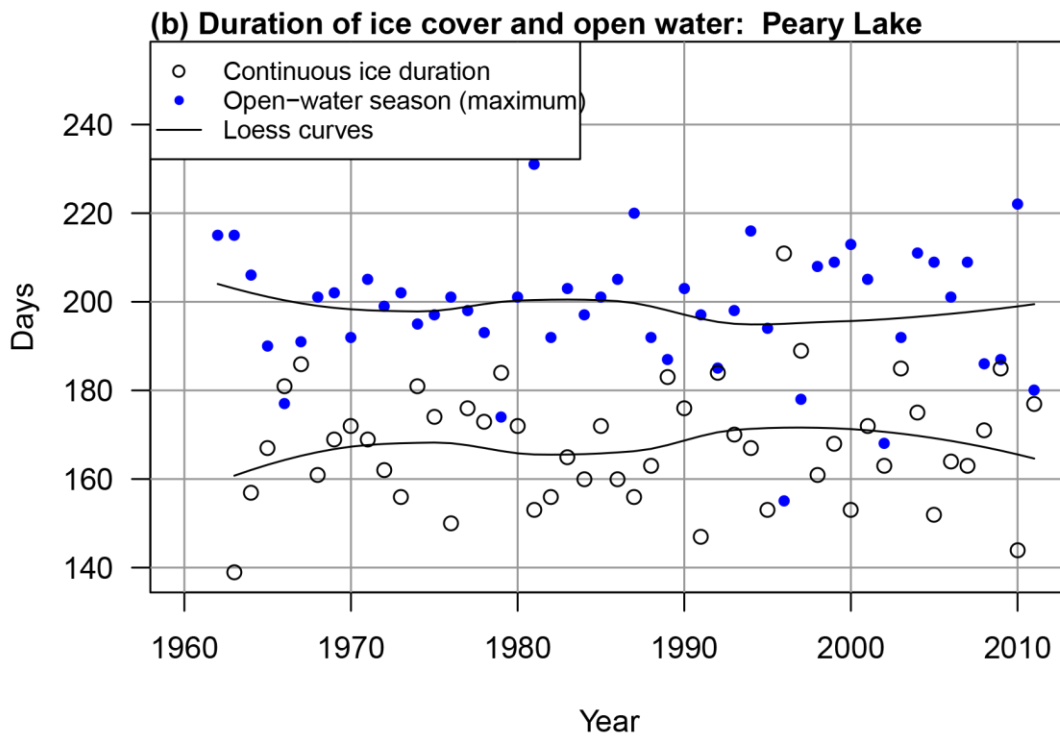
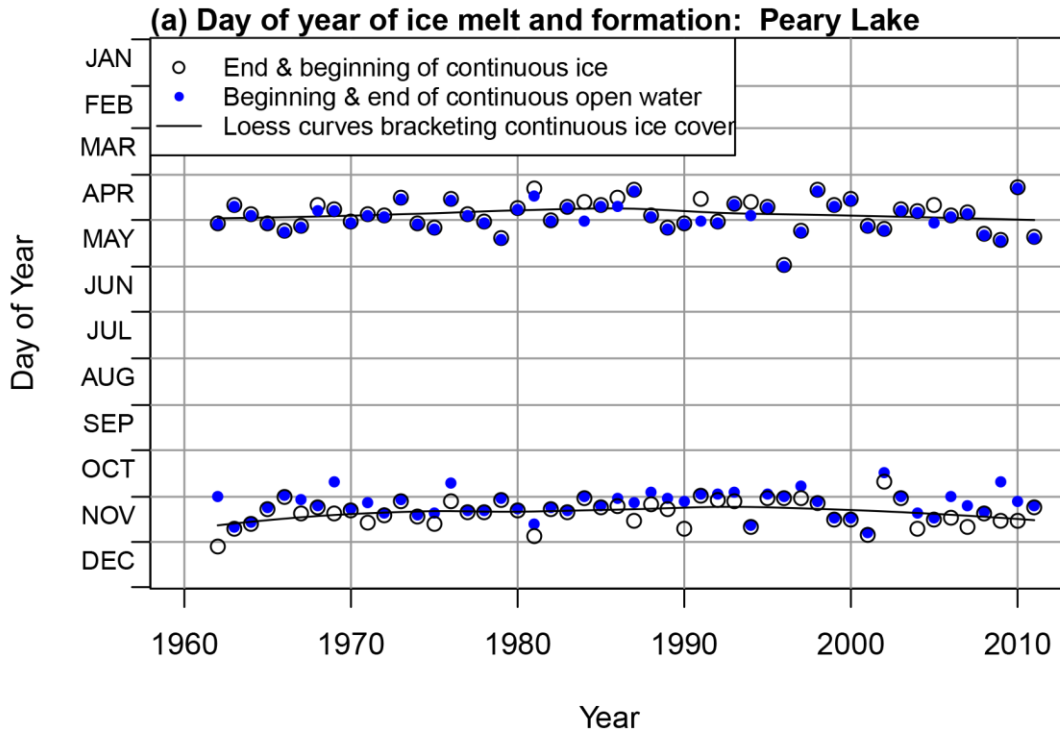


**Figure A31.** Peary Lake (Voyageurs): Modeled (a) dates and (b) duration of ice-covered and open-water seasons, 1962–2011.

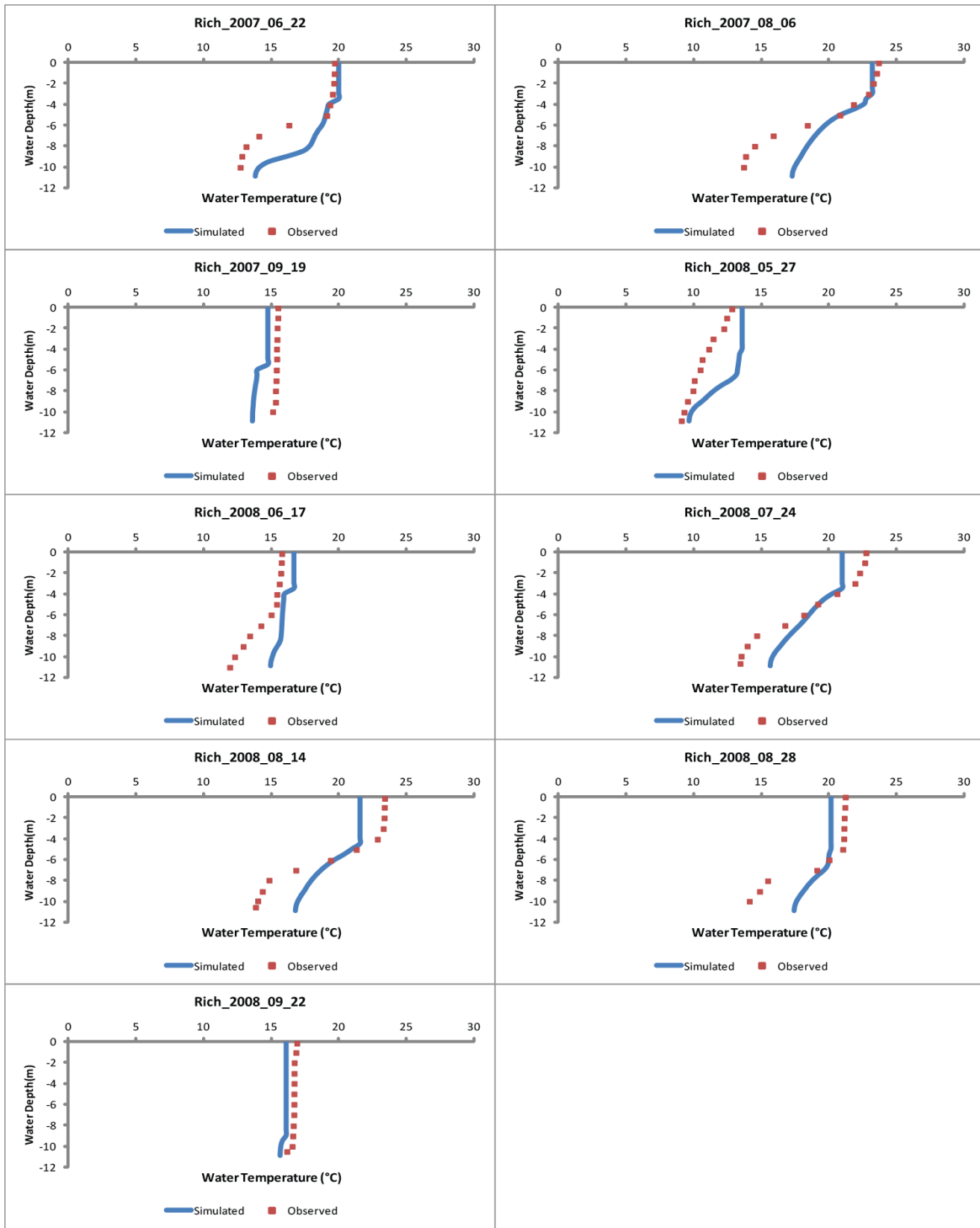


Figure A32. Lake Richie (Isle Royale): Observed and modeled temperature profiles, 2007–2008.

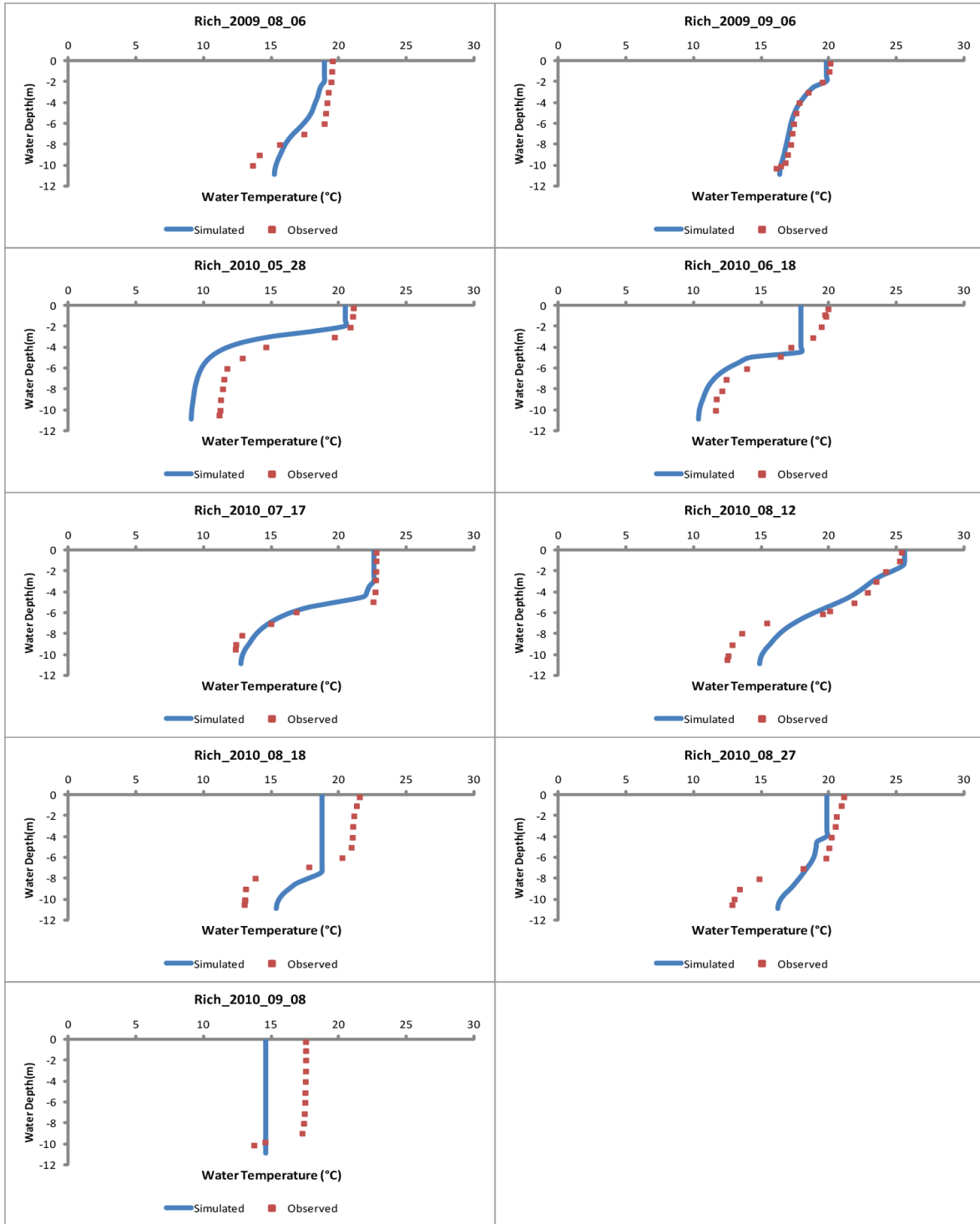
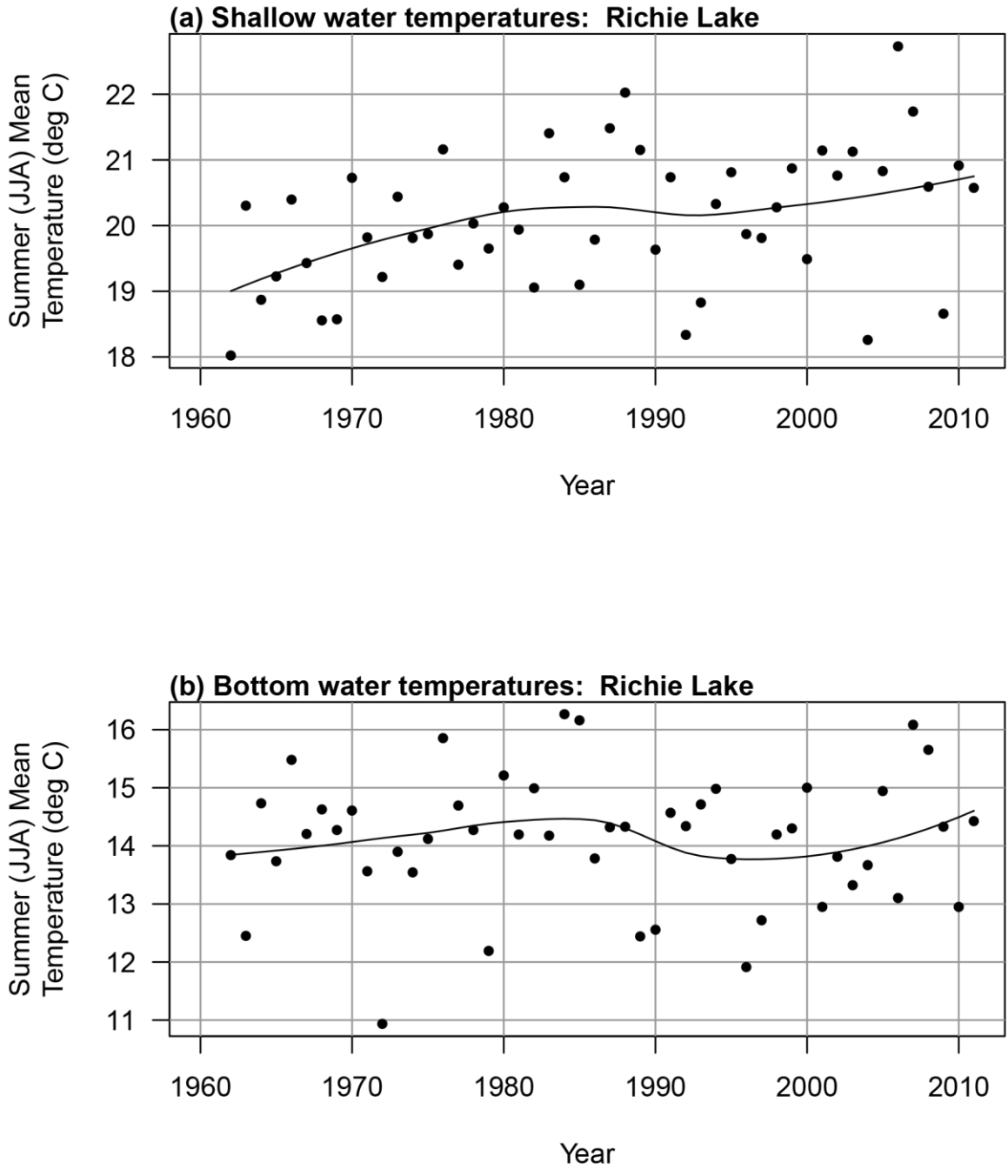
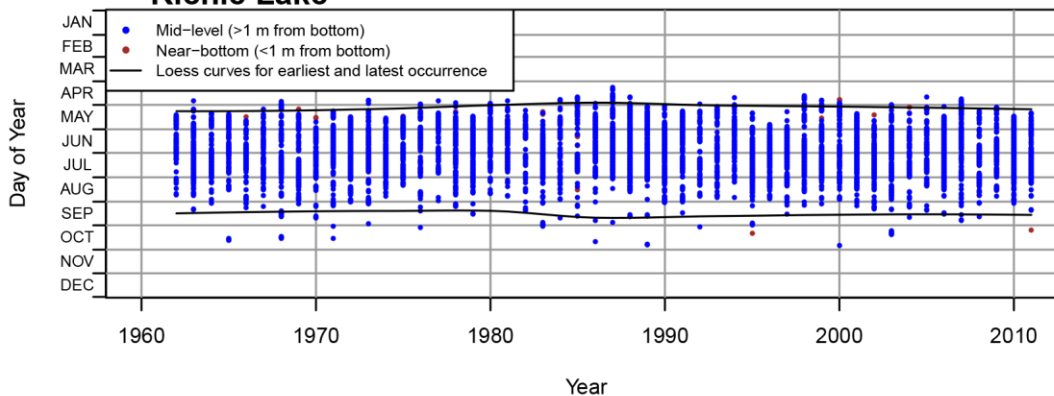


Figure A33. Lake Richie (Isle Royale): Observed and modeled temperature profiles, 2009–2010.

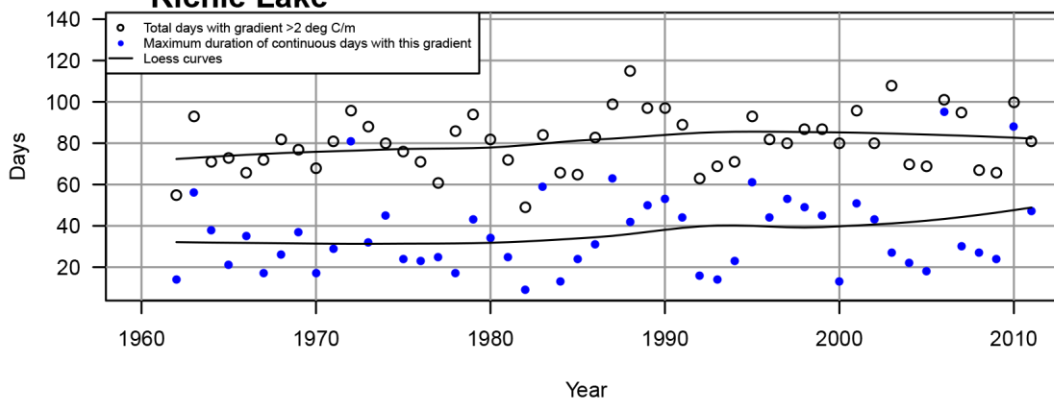


**Figure A34.** Lake Richie (Isle Royale): Modeled mean summer temperatures for (a) shallow and (b) bottom waters, 1962–2011.

**(a) Days of year with thermal gradient >2 deg C/m:  
Richie Lake**



**(b) Number of days with thermal gradient >2 deg C/m:  
Richie Lake**



**(c) Mean depth of gradient >2 deg C/m in summer (JJA):  
Richie Lake**

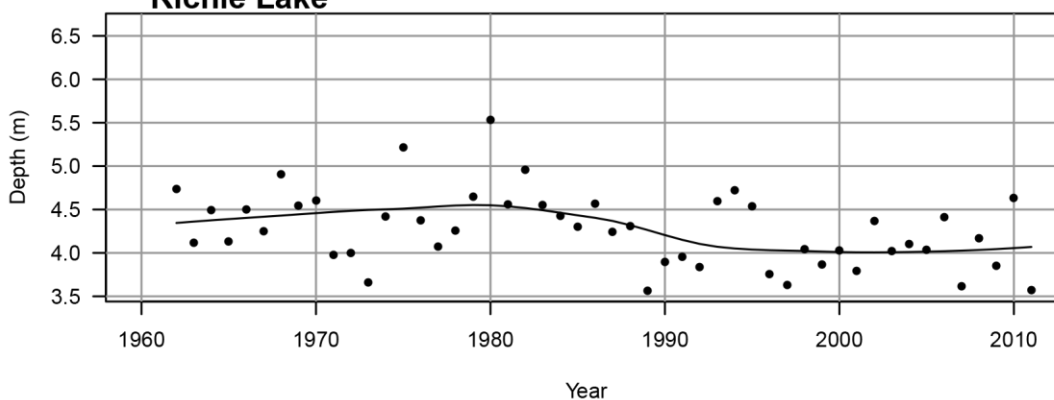
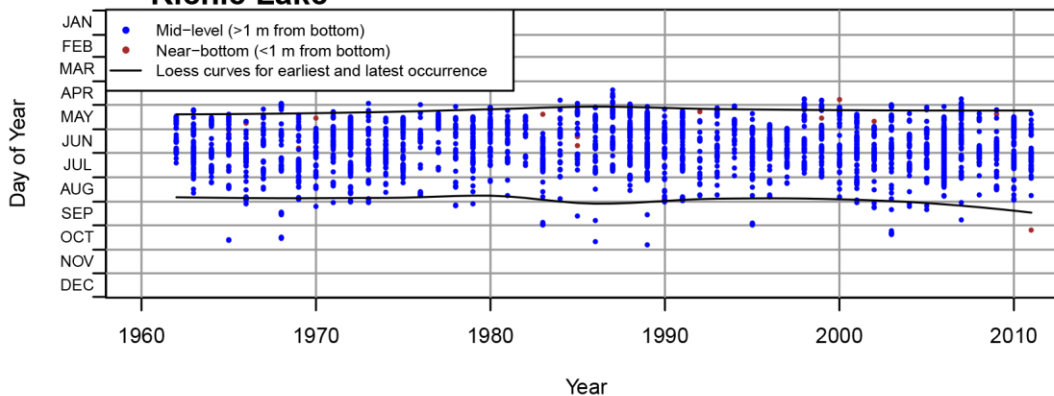
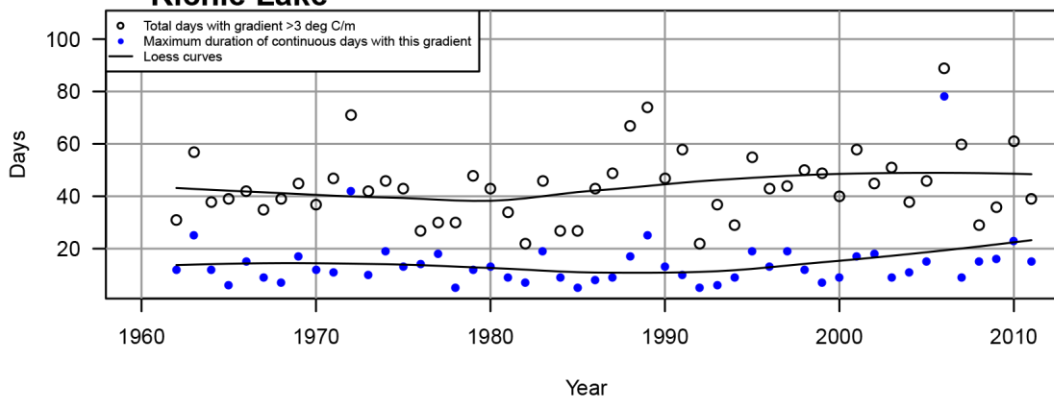


**Figure A35.** Lake Richie (Isle Royale): Modeled (a) dates, (b) duration, and (c) mean summer depth of thermal gradients  $\geq 2^{\circ}\text{C}$  per meter, 1962–2011.

**(a) Days of year with thermal gradient >3 deg C/m:  
Richie Lake**



**(b) Number of days with thermal gradient >3 deg C/m:  
Richie Lake**



**(c) Mean depth of gradient >3 deg C/m in summer (JJA):  
Richie Lake**

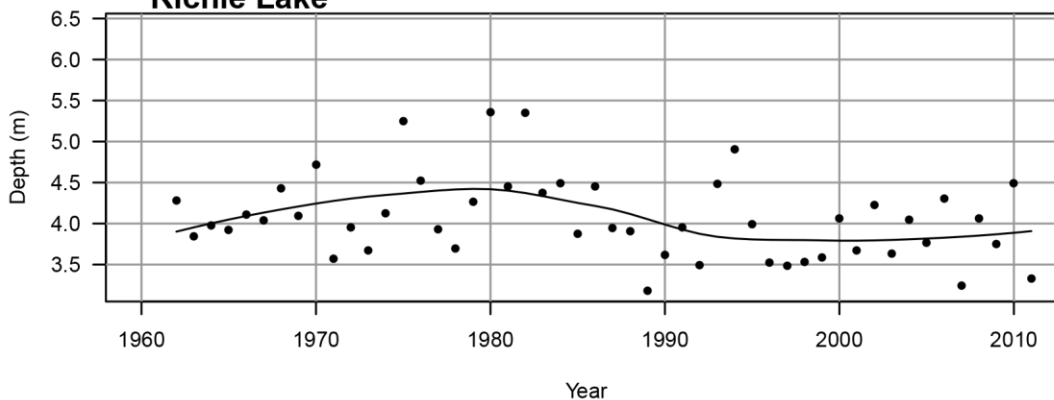


**Figure A36.** Lake Richie (Isle Royale): Modeled (a) dates, (b) duration, and (c) mean summer depth of thermal gradients  $\geq 3^{\circ}\text{C}$  per meter, 1962–2011.

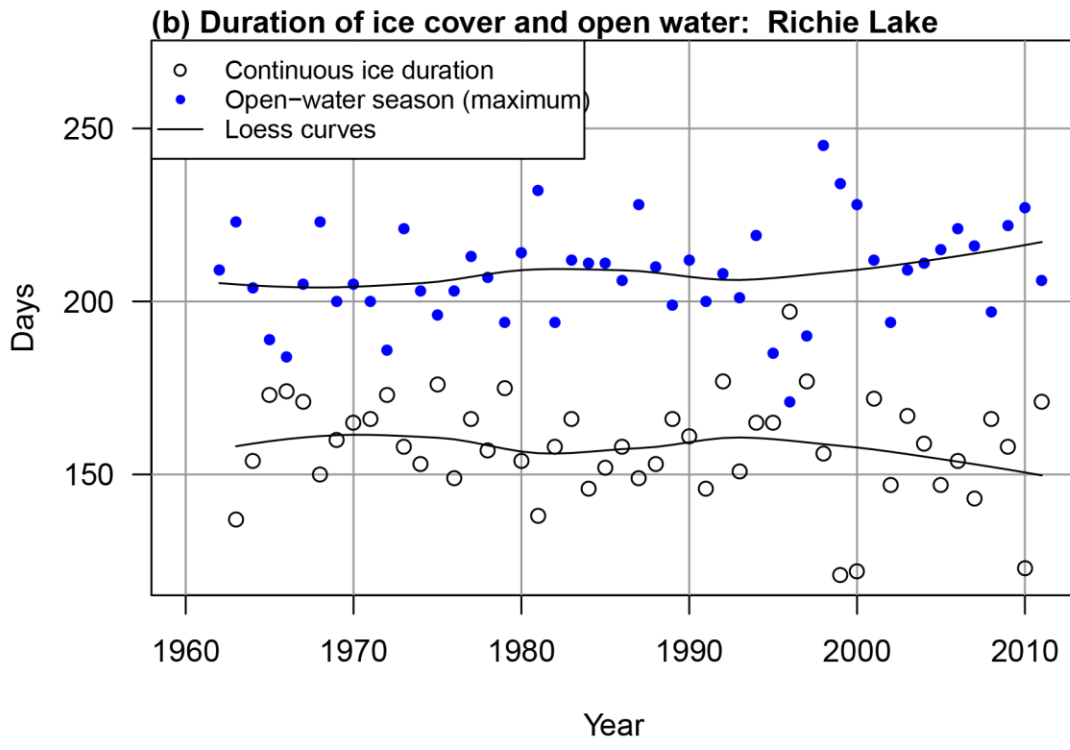
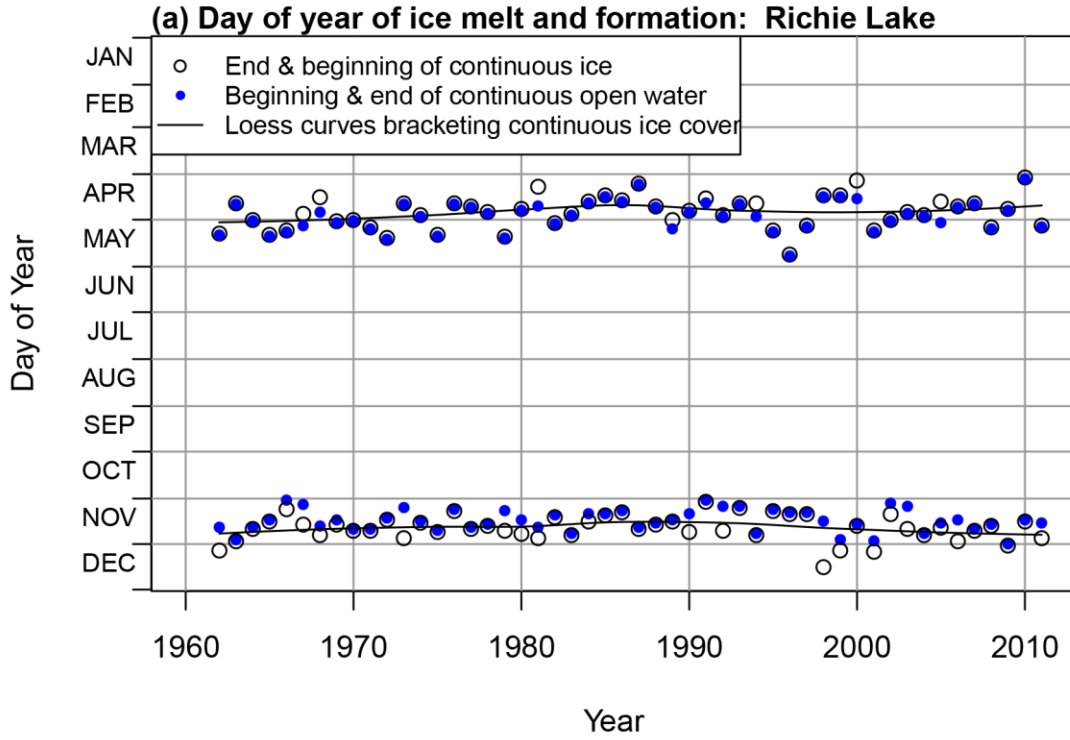


**Figure A37.** Lake Richie (Isle Royale): Modeled (a) dates and (b) duration of ice-covered and open-water seasons, 1962–2011.

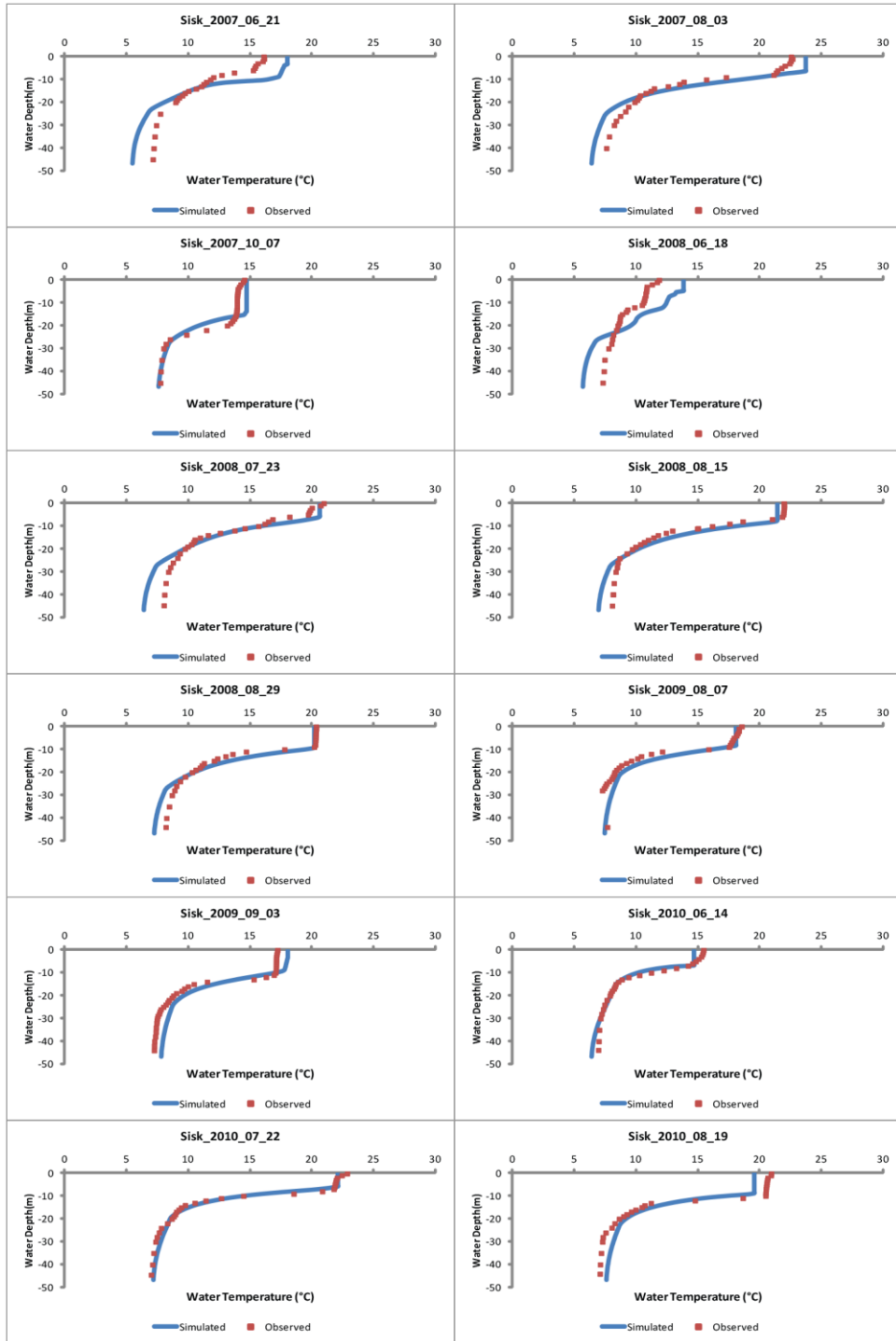
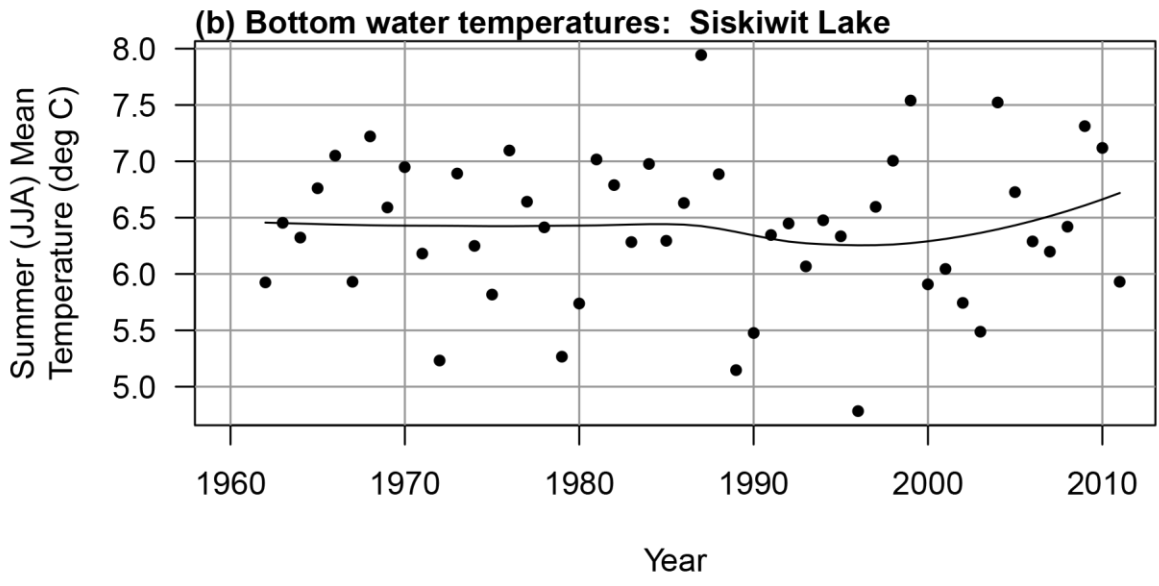
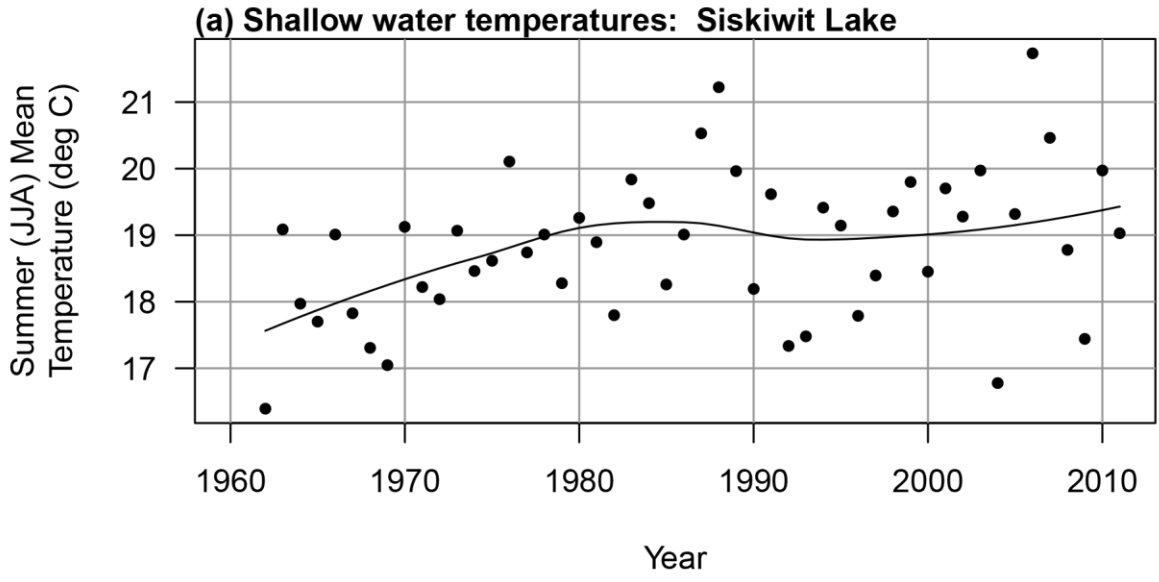
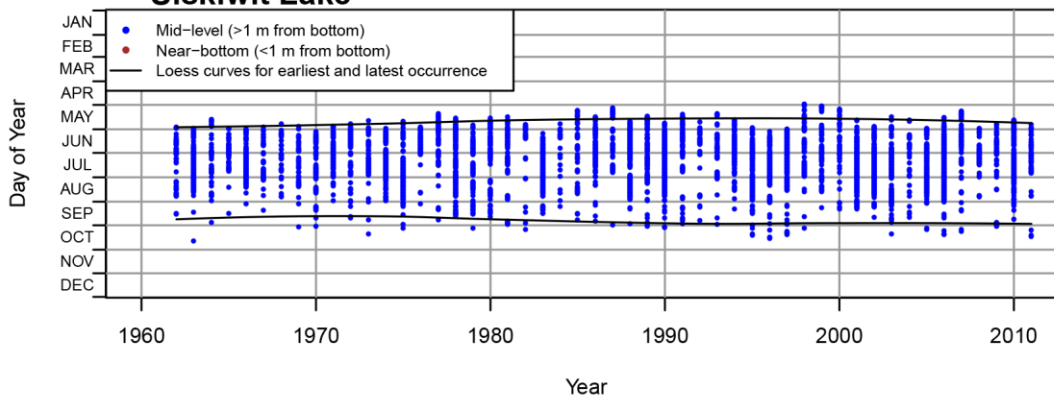


Figure A38. Siskiwit Lake (Isle Royale): Observed and modeled temperature profiles, 2007–2010.

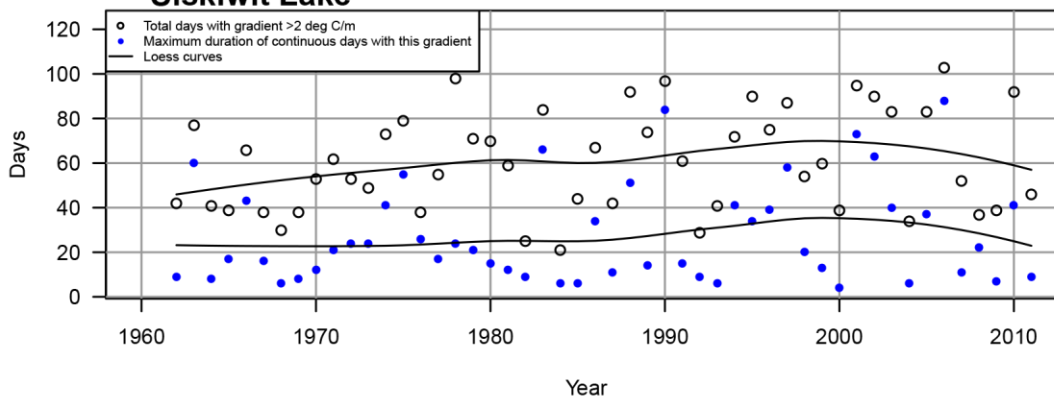


**Figure A39.** Siskiwit Lake (Isle Royale): Modeled mean summer temperatures for (a) shallow and (b) bottom waters, 1962–2011.

**(a) Days of year with thermal gradient >2 deg C/m:  
Siskiwit Lake**



**(b) Number of days with thermal gradient >2 deg C/m:  
Siskiwit Lake**



**(c) Mean depth of gradient >2 deg C/m in summer (JJA):  
Siskiwit Lake**

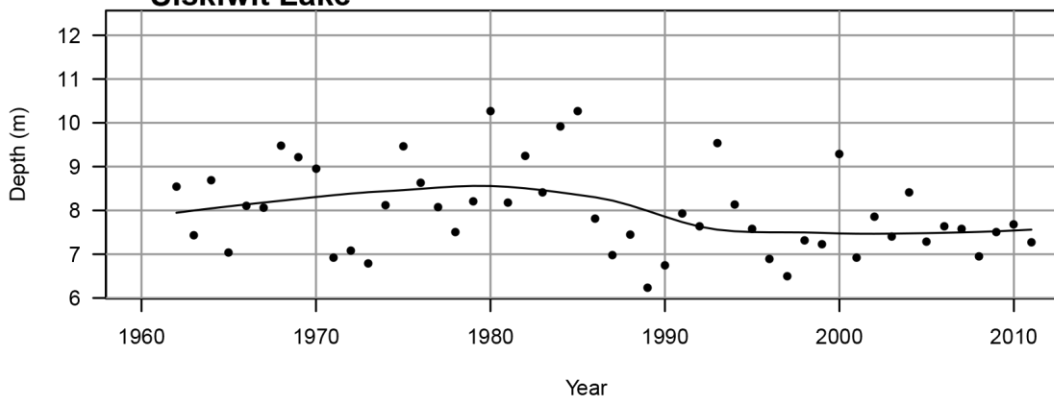
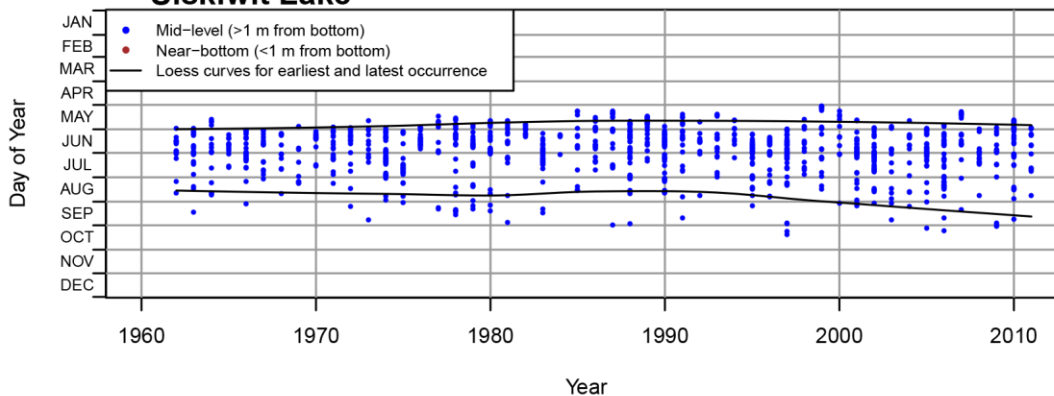
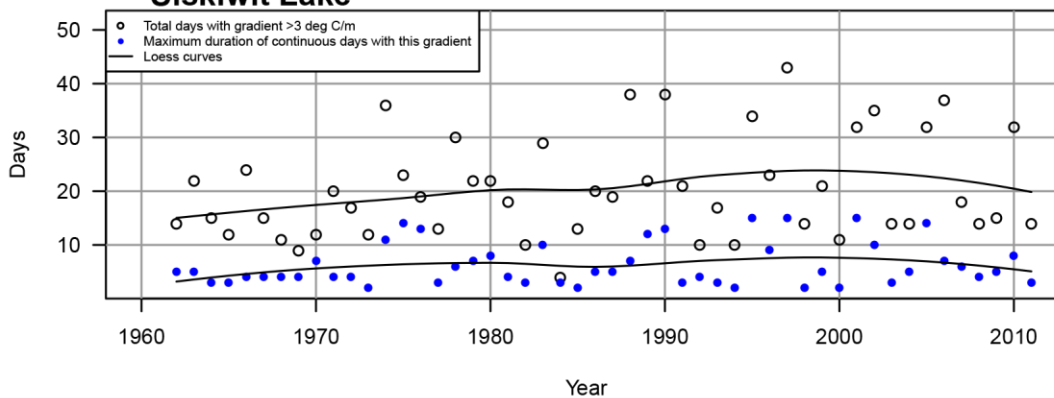


**Figure A40.** Siskiwit Lake (Isle Royale): Modeled (a) dates, (b) duration, and (c) mean summer depth of thermal gradients  $\geq 2^\circ\text{C}$  per meter, 1962–2011.

**(a) Days of year with thermal gradient >3 deg C/m:  
Siskiwit Lake**



**(b) Number of days with thermal gradient >3 deg C/m:  
Siskiwit Lake**



**(c) Mean depth of gradient >3 deg C/m in summer (JJA):  
Siskiwit Lake**

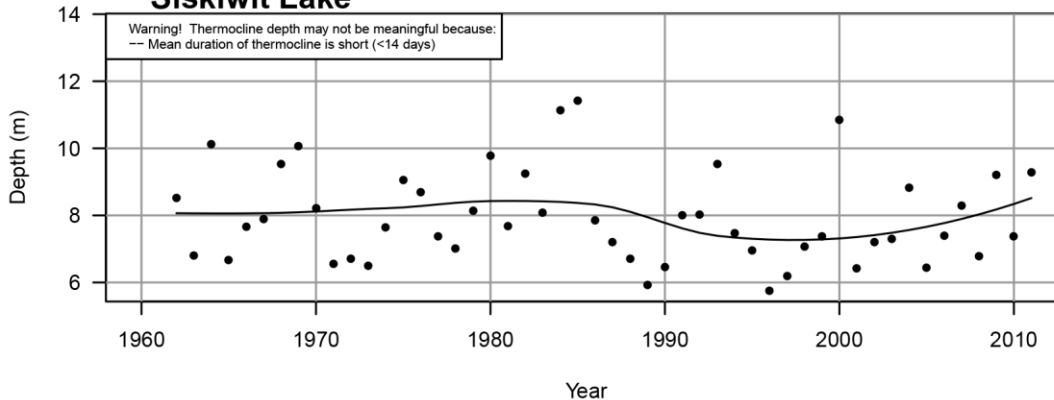


**Figure A41.** Siskiwit Lake (Isle Royale): Modeled (a) dates, (b) duration, and (c) mean summer depth of thermal gradients  $\geq 3^{\circ}\text{C}$  per meter, 1962–2011.

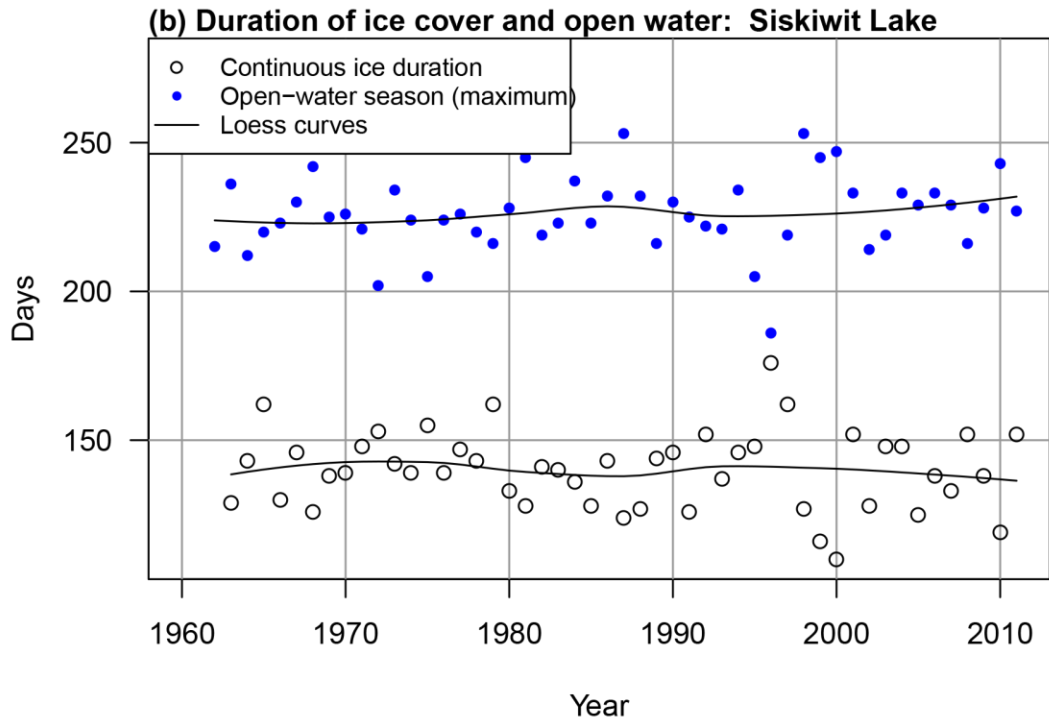
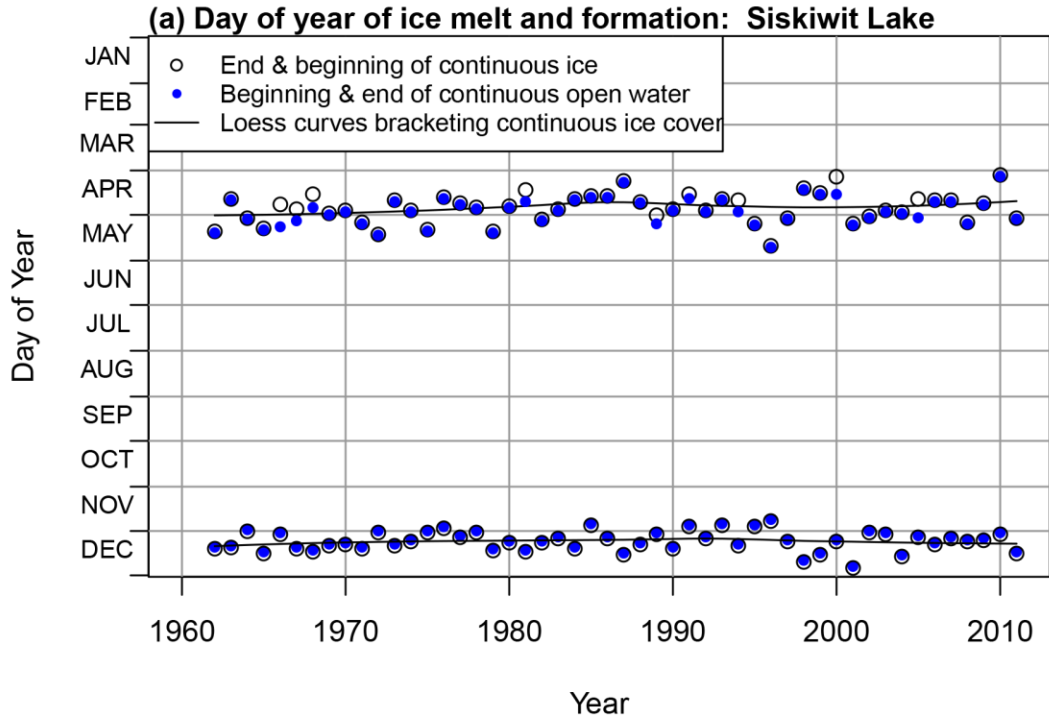


**Figure A42.** Siskiwit Lake (Isle Royale): Modeled (a) dates and (b) duration of ice-covered and open-water seasons, 1962–2011.



The Department of the Interior protects and manages the nation's natural resources and cultural heritage; provides scientific and other information about those resources; and honors its special responsibilities to American Indians, Alaska Natives, and affiliated Island Communities.

NPS 139/126558, 172/126558, September 2014

**National Park Service**  
**U.S. Department of the Interior**



---

**Natural Resource Stewardship and Science**  
1201 Oakridge Drive, Suite 150  
Fort Collins, CO 80525

[www.nature.nps.gov](http://www.nature.nps.gov)

**EXPERIENCE YOUR AMERICA™**